SYNAPTIC AND NON-SYNAPTIC ACTIONS OF BARBITURATES ON NEURONS OF THE CORTICO-THALAMCORTICAL SYSTEM

by

XIANG WAN

Bachelor of Medicine, Hunan Medical University, 1997
M.Sc. Sun Yat-sen University of Medical Sciences, 2000

A THESIS SUBMITTED IN PARTIAL FULFILLMENT

OF THE REQUIREMENTS FOR THE DEGREE OF

DOCTOR OF PHILOSOPHY

in

THE FACULTY OF GRADUATE STUDIES

Department of Pharmacology & Therapeutics
Faculty of Medicine

We accept this thesis as conforming
to the required standard

THE UNIVERSITY OF BRITISH COLUMBIA

June 2004

Abstract

The cortico-thalamocortical (CTC) system plays an essential role in maintaining consciousness. In this thesis, I examined the interactions of barbiturates with neurons in the CTC system to determine potential mechanisms by which barbiturates generate general anesthetic, anti-epileptic and possible analgesic effects.

The thesis addressed four questions: (1) does pentobarbital, at clinically relevant concentrations, modulate intrinsic membrane properties of neurons in the CTC system? (2) how does pentobarbital modulate intrinsic ion channels and synaptic properties in the CTC neurons? (3) how amobaribital and phenobarbital alter neuronal excitation and synaptic transmission? (4) what are the concentration-response relationships for the effects of the barbiturates on neurons of the CTC system?

The investigations were carried out on pyramidal neurons in layer IV of neocortex, nucleus reticularis thalami (nRT) and thalamocortical neurons. Differential interference contrast (DIC-IR) videomicroscopy-guided whole-cell patch clamp techniques were used to record from rat brain slice preparation. Outside-out single channel recording techniques were applied to record from acute dissociated thalamic neurons. Pentobarbital, an anesthetic barbiturate, decreased neuronal excitability in thalamocortical neurons by multiple mechanisms: (1) decreased glutamatergic excitatory neurotransmission; (2) potentiated GABAergic inhibitory neurotransmission; (3) increased resting membrane conductance by activating leak and voltage-dependent K^+ channels; and (4) decreased a

hyperpolarization-activated Na^+/K^+ inward current (I_h). These actions occurred at different EC_{50}s or IC_{50}s. All these actions contributed to pentobarbital-induced inhibition *in vitro* and may account for pentobarbital's effects *in vivo*.

Pentobarbital decreased neuronal excitability in neocortical and nRT neurons by mechanisms similar to those in thalamocortical neurons, but with higher EC_{50}s. Hence, the lower EC_{50} in thalamocortical neurons indicated that these neurons, compared to nRT and neocortical neurons, may be more susceptible to pentobarbital-induced inhibition. This implies that different neurons in the CTC system may have different roles in pentobarbital-induced depression *in vivo*.

Amobarbital is an isomer of pentobarbital with lower potency as an anesthetic and with newly found analgesic properties. Compared with pentobarbital, amobarbital exerted distinct actions on neurons of the CTC system. The most distinguishing actions of amobarbital were that it activated and potentiated $GABA_A$ receptor, increased both the amplitude and duration of inhibitory postsynaptic currents (IPSCs), and did not alter intrinsic ion channels in all the types of neurons that we examined. Therefore, amobarbital may induce anesthesia by selective actions on $GABA_A$ receptors. Amobarbital preferentially suppressed firing in dorsal thalamic neurons which receive nociceptive inputs. This may relate to amobarbital's utility as an analgesic agent.

Phenobarbital, which has anti-epileptic properties, selectively inhibited neuronal excitability by inhibiting repetitive neuronal firing and potentiating GABAergic synaptic

transmission in neocortical neurons. These findings may provide a possible mechanism for phenobarbital's efficacy in the treatment of generalized tonic-clonic and partial seizures. On the other hand, phenobarbital did not have pronounced effects on thalamocortical neurons, which may account for clinical observations that phenobarbital lacks efficacy or even aggravates absence seizures attributable to CTC mechanism (Mattson, 1995).

These investigations showed that synaptic and non-synaptic actions of barbiturates have different but overlapping concentration-dependence. This study is the first investigation to compare three barbiturates in three major types of neurons in the CTC system. The different actions of the barbiturates on neurons in this system may account for their differences in ability to cause CNS depression and to modulate excitability in pathophysiological concentrations.

Table of Contents

List of Figures

List of Tables

Acknowledgements and Dedication

I would like to acknowledge with gratitude the supervision of Dr. Ernie Puil, and the support from the members of my supervisory committee: Dr. David A. Mathers, Dr. Michael. J.A. Walker, and Dr. Bernard A. Macleod.

The development of the research presented in this thesis was a concerted effort between my supervisor and me, and would not have been possible as an isolated undertaking. Fruitful discussion with many other people helped the research along, most outstanding with Dr. David. A. Mathers.

This work was supported financially by research grants from the Canadian Institutes for Health Research, Graduate Fellowship and Cordula and Gunter Paetzold Fellowship from the University of British Columbia.

I want to express my gratitude to Dr. Hee-Soo Kim for her great work on amobarbital effects on single channel currents. I thank Ms. Viktoriya Dobrovinska for preparation of slices and dispersed cultures and Mr. Christian Caritey for technical support. I am grateful to Dr. Richard S. Neuman for a supply of ZD-7288, and Dr. Juhn Wada for a supply of amobarbital. I thank Mr. Douglas Brown for his assistance with photography of brain slices.

My gratitude for invaluable emotional, physical and intellectual support goes to my family and many friends and colleagues. I would like to thank my lab mates Amer Ghavanini, Israeli Ran, Stefan Reinker, Stephan Schwarz for providing help and interesting discussion, sharing with solutions and slice preparations.

Chapter 1
INTRODUCTION

1.1. Scope of the thesis

This thesis addresses the effects and mechanisms of the actions of barbiturates in the central nervous system (CNS). Barbiturates have varying degrees of sedative-hypnotic, anesthetic, anti-epileptic and, recently reported, analgesic properties. However, there are no hypotheses that adequately explain the neuronal mechanisms by which these agents alter consciousness. There are two main reasons for this. First, barbiturate actions have not been thoroughly studied in a system which is closely involved in wakefulness and arousal. Although almost all of the CNS and spinal cord contribute to consciousness, the cortico-thalamocortical (CTC) system is essential for producing and maintaining consciousness, as compared to other regions. Barbiturates may alter the activities of neurons in this system. Secondly, it is hard to assess the relationship between *in vitro* mechanisms with their anesthetic, analgesic and anticonvulsant effects. A pharmacological way to achieve this aim is to determine whether the EC_{50}s of *in vitro* effects of barbiturates correlate with *in vivo* clinical doses. Thus, the general hypothesis of this thesis is that barbiturates depress neuron excitability by interacting with the synaptic and non-synaptic membrane functions of neurons in the CTC system, to decrease neuronal excitability, which may contribute to alteration of consciousness. These *in vitro* studies are relevant to understanding barbiturate effects in general anesthesia, pain and epilepsy.

1.2. Background

1.2.1. The consciousness system in the brain

The current theory concerning the neural substrates of consciousness tend to fall into two broad classes: (1) those that hypothesize that the discharge activities of particular subpopulations of neurons are sufficient to support conscious awareness and to modulate experiential contents and (2) those that hypothesize that some coherent organization of neural signaling processes (Singer, 1995; Grossberg, 1995; Cariani, 2000).

In everyday neurology, consciousness is generally equated with the waking state and the abilities to perceive, interact and communicate with the environment and with others in the integrated manner, which wakefulness normally implies. Awareness is sometimes called 'core consciousness' and without it, total consciousness is impossible (Evens 2003). However, awareness and wakefulness are not the same thing, and in brain damaged patients, wakefulness can occur without awareness (Evens, 2003).

The state of "conscious awareness" is likely an emergent property of distributed neural networks involving the thalamus and cerebral cortex, as well as brainstem (Crick and Koch, 1995; Llinas et al., 1998; Tononi and Edelman, 1998). It is hypothesized that the loss of consciousness induced by general anesthetics may result, in part, from a disruption of functional interactions, as well as depression of neuronal excitability within the cortico-thalamocortical system (Angel 1993; Ries and Puil 1999a and Alkire et al., 2000). This idea is supported by a variety of evidence from work in animals (Angel 1991; Angel and LeBeau 1992; Angel 1993; Ries and Puil 1999a, 1999b and Steriade 2001) to functional neuroimaging studies in humans (Alkire et al., 1999; Fiset et al., 1999; Bonhomme et al., 2001 ; Kaisti et al., 2002).

1.2.1.1. Role of neocortex in consciousness

A functioning consciousness system is characterized by a steady-state level of cortical excitation (Matsumura et al., 1988), which is prerequisite to the fast, 'phasic' transfer of information bidirectional in the attention system. Neocortical activation results from subcortical as well as intracortical (horizontal or vertical) excitatory transmission (Enzure and Oshima, 1981; Giuffrida and Rustioni, 1989). Drugs that alter this activation system may induce unconsciousness.

1.2.1.2. Roles of thalamus in consciousness

The roles of the thalamus in information processing and attention have been dramatized by the study of the brain of Karen Ann Quinlan (Kinney et al., 1994). In a persistent vegetative state, Quinlan had initially intact sleep-wake cycles without signs of awareness or cognition. Surprisingly her autopsy revealed major injury to her thalamus, and not to her cerebral cortex. This finding leads to the reassessment of the role of thalamus during arousal in the recent years.

The arousal system evokes waking behavior from sleep in response to sensory stimuli. Information from external stimuli reaches the thalamus during sleep, although, compared to wakefulness, the amount of information is reduced. The process controlling this reduction is called 'sensory' gating, which takes place in the thalamus. Thalamic function is now known to be modulated by the brainstem reticular formation. This ascending activation system, which was called reticular activating system (RAS), are located in the upper brainstem, posterior hypothalamus, and basal forebrain and the transmitters include acetycholine, norepinephrine, serotonin, histamine and glutamate (Marrocco, 1994).

During arousal, the transmitters modulate thalamic relay by inducing a prolonged depolarization (McCormick, 1992). A descending corticothalamic system involving excitatory amino acid receptors reinforces the activation (McCormick and van Krosigk, 1992). Thalamic neuronal firing modes during wakefulness and sleep arise from intrinsic membrane properties that are voltage-dependent (Steriade, 2001). Onset of sleep switches thalamic neurons from a predominantly tonic-firing pattern to a predominantly burst-firing pattern due to a lack of depolarizing drive from RAS (Steriade, 1993). However, the cerebral cortex can be directly activated by cholinergic, serotonergic, noradrenergic and histaminergic arousal systems that originate in the brain stem, basal forebrain or hypothalamus and do not project through the thalamus (Foote and Morrison, 1987; McCormick, 1992; Steriade, et al., 1993). This means that the arousal may have resulted from a combination of extrathalamic and residual thalamic activation.

Based on the roles of the thalamus and the cortex in maintaining consciousness, Figure 1.1 illustrates the key components that form a triangular network of neocortical, thalamocortical and nRT neurons, comprising both positive and negative feedback loops. Drugs, e.g. general anesthetics may alter the synaptic transmission or intrinsic ion channels in this network, to reduce excitability.

1.2.2. Concept of anesthesia

Anesthesia can be interpreted by "insensitiveness". During anesthesia, auditory, visual and tactile stimuli still reach the CNS, but further information processing is disturbed without significant alteration in peripheral nerve conduction and neuromuscular transmission. General anesthetics induce unconsciousness predominantly within the CNS, especially the

CTC system (Antkowiak, 2001). General anesthesia is therefore characterized by amnesia, analgesics, depression of motor reflexes and unconsciousness. To explain how anesthetics alter consciousness in the CNS, many theories have been proposed, which can be categorized into non-specific and specific theories.

1.2.2.1. Non-specific theories

The potency of a large range of anesthetic compounds correlates well with their partition coefficient between water and oil. This discovery by Meyer and Overton leads to the proposal that anesthetics produce their effects by dissolving in the lipid bilayer that forms the cell membrane, and by disrupting the structural properties of the cell membrane in a nonspecific manner (Meyer, 1901). To explain alteration in physicochemical properties by general anesthetics, a number of mechanisms have been proposed, including fluidisation and a thickening of the membrane bilayer by general anesthetics (Albrecht and Miletich 1988; Seeman 1972). However, there is no experimental evidence that these effects *per se* reduce neuronal excitability. Therefore, an indirect action is considered more likely. For example, structural changes of the lipid bilayer may alter the function of membrane integral protein like ion channels, thereby inducing anesthesia.

Current thinking, however, has moved away from this hypothesis for a number of reasons. Firstly, several compounds show membrane-destabilizing effects, similar to those of anesthetics, but are not anesthetic in nature (Mihic et, 1994). Secondly, many anesthetics exist as enantiomers and show marked enantioselectivity in their anesthetic potency; however, this selectivity is not reflected in their membrane partition coefficient (Tomlin et

al., 1998). Therefore, the current hypothesis is that anesthetics interact with specific proteins and specific pathways to produce anesthesia, which are named as specific theories.

1.2.2.2. Specific theories

Specific theories propose that anesthetics interact with specific proteins, particularly neurotransmitter receptors, which facilitate or inhibit their activity to produce unconsciousness. These theories also propose that anesthetics modulate specific neurons and synaptic pathways in the CNS, which are crucial for maintaining consciousness. This hypothesis is validated by the fact that enantioselectivity matches exactly with anesthetic potency, and non-anesthetic membrane disruptions have no effect on the putative target proteins. In addition, the interaction with specific neurons or synapses in the central nervous system (Ries and Puil, 1999a, 1999b; Nelson, 2002) allows us to make rational and testable conclusions regarding their mechanisms of actions.

Among specific theories, a unitary hypothesis is the GABA hypothesis. This states that enhancement of activity at $GABA_A$ receptors is an important component, perhaps the only component, of relevant mechanisms in anaesthesia. However, some clinical anesthetics, such as xenon, nitrous oxide and cyclopropane, have little effect on $GABA_A$ receptors (Dilger, 2002). Genetic studies (Nash, 2002) and evidence from brain imaging (Heinke and Schwarzbauer, 2002) do not support an exclusive role for $GABA_A$ receptors in anesthesia, although they support the hypothesis that the *in vivo* effects of anaesthetics are mediated at least in part through GABAergic mechanisms. Other receptors and ion channels are also involved, such as glutamate receptor channels and cholinergic neurotransmitter systems (el-Beheiry and Puil, 1989; Puil and el-Beheiry, 1990).

In contrast, multisite hypotheses, which allow that many molecular mechanisms may cause one or many neuronal alterations, do not hold that all anesthetics should show the same correlation between the anaesthetic endpoint and the mechanism-related endpoint. Studies of proteins (Ubran, 1993), brain slices (Ries and Puil, 1999a, 199b; Wan et al., 2003) and functional imaging (Heinke and Schwarzbauer, 2002) all come up with data consistent with multisite theories of anesthetic action.

1.2.3. Anesthesia and the cortico-thalamocortical system

The cortico-thalamocortical system is crucial for maintaining consciousness. Anesthetics modulate synaptic transmission and neuronal excitability in clinically relevant concentrations in this system, which may induce unconsciousness.

1.2.3.1. Anesthesia and neocortical function

What happens in the cerebral cortex when general anesthetics induce unconsciousness? Several investigators have tackled this question in recent years. Brain image studies show that the metabolism of most cortical areas is decreased by roughly 50% in lightly anesthetized subjects (Alkire et al., 1995; Alkire, 1997; Alkire, 1999). The alteration of electrophysiological properties in the neocortex during anesthesia is studied by electroencephalogram (EEG), which represents electrical activities in the cortex. The ensembles of cortical and thalamic neurons discharge synchronously at stereotyped frequencies associated with different consciousness states (McCormick and Bal, 1997; Steriade, 2000). For example, during alert wakefulness, high-frequency oscillations in the gamma range (20-50 Hz; '40Hz' oscillations) occur spontaneously or as part of sensory-elicited events in the relay nuclei of the thalamus and the cortical areas to which they

project (Castelo-Branco et al., 1998; Llinas and Pare, 1991; Murthy and Fetz, 1996). The transition from wakefulness to unconsciousness by anesthetics is accompanied by a depression of these high-frequency oscillations (Uchida et al., 2000). When anesthesia goes deeper, low frequency high-voltage activity becomes more pronounced (Clark and Rosner, 1973). Hence, alteration in cortical function occurs during transition from consciousness to unconsciousness induced by anesthetics.

Most anesthetic agents alter EEG activity patterns in a similar, although not identical, way. MacIver and collaborators (MacIver et al., 1996b) correlated the behavioral state in the rat with the corresponding EEG patterns. They observed increased power in different frequency bands of the EEG: (1) during sedation, a pattern termed activation; (2) during hypnosis, delta oscillations; (3) during anesthesia, a pattern termed burst suppression. Burst suppression is characterized by episodes of low-frequency high-voltage activity, which are separated by periods of neuronal silence. The finding that general anesthetics induce delta activity in the EEG has prompted the suggestion that the brain states of anesthesia and natural sleep are comparable with regards to several aspects (Lukatch and MacIver, 1996; MacIver et al., 1996b). This hypothesis is based mainly on the fact that synchronized cortical delta activity is present during non-rapid eye movement (REM) sleep.

Although thalamocortical neurons play an important role in delta activity, the data obtained from neocortical brain slices provide evidence that anesthetic-induced delta activity may also be related to a cortical site of action (Lukatch and MacIver, 1996; MacIver et al., 1996b). In rat neocortical slices a burst suppression-like pattern can be observed during

thiopental-induced anesthesia. This finding indicates that burst suppression involves a cortical site of action. In fact, recordings in the neocortex in experimental animals, before and after removing the ascending inputs by cutting along the white matter, demonstrated that burst suppression survives this procedure (Henry and Scoville, 1952).

In summary, general anesthetics alter firing of cortical neurons to induce unconsciousness. During anesthesia, two events probably come together: the induction of a sleep-like state by drug actions taking place on a subcortical, e.g. thalamic, level and simultaneously, a massive depression of cortical excitability. Therefore, to understand how anesthetics modulate subcortical function may help to further our knowledge on potential targets of anesthetics in the CNS.

1.2.3.2. Anesthesia and thalamic function

General anesthetics induce unconsciousness by depressing neuronal excitability in the CNS. The thalamus is one of major targets for anesthetics effects, based on the report that anesthetic-induced unconsciousness is associated with selective depression of thalamic function (Fiset et al., 1999; Alkire, 2000). A correlation between a person's level of consciousness and their level of thalamic functioning at various doses of propofol anesthesia has been demonstrated in humans (Fiset et al., 1999). As well, regional thalamic functional activity suppression has been found during halothane anesthesia (Alkire, 1999). Animal studies examining anesthetic-induced changes in evoked potential recordings suggest that one of the primary basis of anesthesia may be the blocking or disruption of sensory information processing through the thalamus (Angel, 1991, 1993). The mechanism of anesthetic-induced disruption of thalamic function appears, based on animal work, to be

dependent on how anesthetics interact with a few specific brain sites including thalamocortical nuclei and nRT (Angel, 1991). An anesthetic-induced decrease in corticothalamic and cortico-reticulothalamic signaling increases inhibition and decreases excitation on thalamic neurons, thereby decreasing their output to cortex (Angel, 1991). Therefore, anesthetics may interact with various targets in the CTC system to produce unconsciousness.

Delta oscillation occurs at anesthetic-induced hypnosis and anesthesia. A number of studies on sleep mechanisms provide evidence that synchronized cortical delta activity originates in the thalamus (Amzica and Steriade, 1998; Contreras and Steriade, 1997; McCormick and Bal, 1997). Considering the mechanism thought to underlie natural sleep, cortical delta rhythms during anesthesia could be explained by a depression of neuronal activity at the thalamic level. Assuming that general anesthetics reduce the excitability of thalamic relay cells either by direct actions on these neurons or by reducing their synaptic input, it seems possible that the cells are forced to enter the burst mode, thereby producing synchronized delta activity in the thalamo-cortical loop. Additional pharmacological properties of anesthetics presumably facilitate the oscillation. For example, intracellular recording from thalamic brain slices shows that low concentrations of pentobarbital increase the low threshold Ca^{2+} spike (LTS) amplitude whereas higher concentrations decrease the LTS amplitude (Puil et al., 1996). This implies that barbiturate anesthetics exert excitatory effects at low doses, which may be attributable to modulation of LTS amplitude (Puil, et al., 1996) or enhancement of synaptic transmission through mechanisms involving $GABA_A$ and NMDA receptors and the HCO_3^- ion. (Archer et al., 2001).

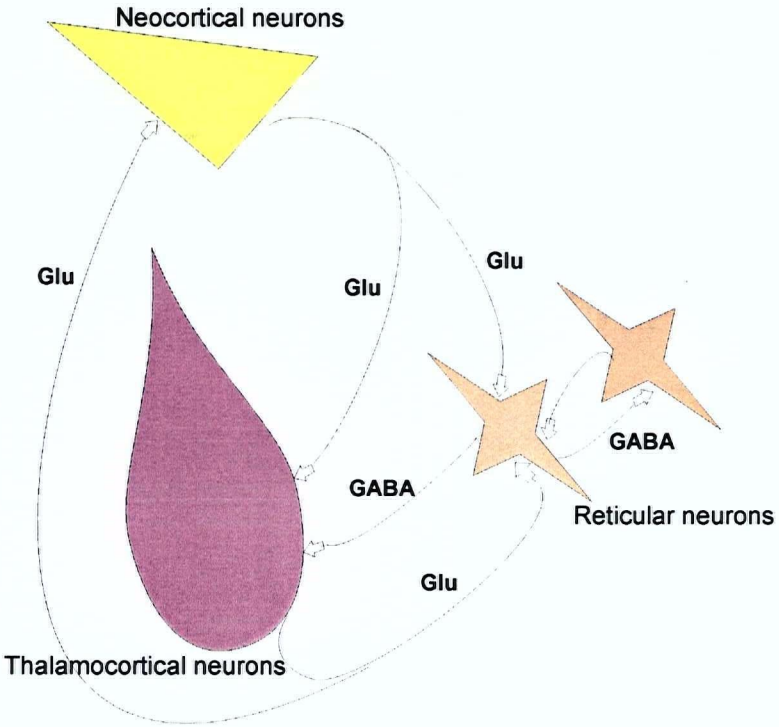

Figure 1.1. Relations between neurons of γ-aminobutyric (GABA)ergic nucleus reticularis thalami, neocortical neurons and their effects on thalamocortical neurons. Thalamocortical and reticular neurons receive prevalent excitatory input from neocortical neurons. Neocortical neurons receive excitatory input from thalamocortical and reticular neurons. Thalamocortical neurons also receive inhibitory input from reticular neurons. Simultaneously, the activity in adjacent nucleus reticularis thalami (nRT) areas is suppressed by axonal collateralization and dendro-dendritic synapses within nRT.

Sleep EEG spindles indicate the loss of consciousness during the transition from wakefulness to sleep. Sleep-like spindles are generated in the thalamus during barbiturate anesthesia (Contreras and Steriade, 1996). One spindle represents a sequence of neuronal oscillatory activity at 7- to 14-Hz that characteristically waxes and wanes and recurs at a frequency<1-Hz. EEG spindle activity depends on intrinsic properties of thalamocortical cells (i.e. the low threshold Ca^{2+} spikes) and network pacing by the nRT neurons. Multiple simultaneous *in vivo* intracellular recordings with barbiturate anesthesia show that spindle activity occurs in phase among nRT, thalamocortical and corticothalamic neurons. During

depolarizing plateaus in nRT neurons, rhythmic spike activity leads to synchronous GABAergic inhibitory postsynaptic potentials (IPSPs) in thalamocoritcal neurons, which in turn lead to synchronous excitatory postsynaptic potentials (EPSPs) in cortical neurons. Rebound spike bursts occur following the IPSPs and action potentials occur with the EPSPs. The waxing pattern consists of a progressive increase in synaptic potential during the first part of spindle sequence. Waxing depends on a progressive recruitment and sychronization of thalamic and cortical neurons. The waning pattern at the end of the spindle occurs due to a progressive desynchronization of the thalamocortical afferent input to corticothalamic neurons such that the EEG oscillation fades.

Spindle-like activity is reported with other anesthetics such as ketamine, urethane (Contreras and Steriade 1996) and halothane (Avramov 1991; Keifer et al., 1994). Prolonged membrane hyperpolarization precedes each spindle sequence in cortical, nRT and thalamocortical neurons (Contreras and Steriade 1996). A decrease in stimulation during anesthesia, as in sleep, would lead to a decrease in the release of arousal neurotransmitters, hyperpolarization and thalamic oscillation.

The thalamic mechanisms that underlie spindle generation can also account for generalized absence epilepsy. In absence or petit-mal, individuals exhibit a few seconds of staring while a synchronous slow oscillatory rhythm occurs in thalamocortical circuits (Snead, 1995). Positron emission tomography studies of regional blood flow show that thalamic perfusion selectively increases during an absence seizure (Prevett, 1995). Therefore, although a thalamic origin has not been confirmed in humans during absence epilepsy, animal models strongly suggest that nRT is involved.

In summary, general anesthetics modulate function of the CTC system, including decreases of excitation and increases of inhibition. A numerous nodes in this system may be altered by anesthetics through a variety of mechanisms (Figure. 1.2), which may contribute to the anesthetics-induced unconsciousness.

1.2.4. Anesthesia and spinal cord

Anesthesia mainly involves changes in the CTC system. However, there is evidence that the suppression of pain-evoked activity by inhalational anesthetics partly involves the spinal cord. The evidence for this comes in three parts. Firstly, the immobility response to noxious stimulation during anesthesia may mainly be due to interaction with spinal cord (Dutton et al., 1996; Rampil and Laster, 1992). Secondly, neither parietal cortical lesions, nor decerebration change minimal alveolar concentration (MAC) of inhalational anesthetics to block motor responses in rats (Rampil et al., 1993; Rampal, 1994). And thirdly, low MAC of inhalational anesthetics is required in spinal cord, compared to neocortex, thalamus, midbrain and cerebellum, for blocking movement in the goat (Antognini and Schwartz, 1993; Borges and Antognini, 1994). Taken together, these investigations suggest that the principal site of anesthetic action for movement blockade during noxious stimulation is the spinal cord.

1.2.5. Pharmacological properties of barbiturates

The barbiturates can produce all degrees of depression of the CNS, ranging from mild sedation to general anesthesia (Table 1.2). Anesthetic barbiturates are derivatives of barbituric acid (2,4,6-trioxohexahydropyrimidine), with either an oxygen or sulfur at the 2-

position. Barbiturates containing 5-phenyl substituent have selective anticonvulsant activity, e.g. phenobarbital. Pain perception and reaction are relatively unimpaired until the moment of unconsciousness, and in small doses the barbiturates, e.g. pentobarbital increases the reaction to painful stimuli. However, recently, amobarbital, a pentobarbital isomer, has recently been used in the treatment of central and neuropathic pain (Koyama et al., 1998) and chronic regional pain syndrome (CRPS; Mailis et al., 1997). The mechanism underlying this effect is still unclear.

Table 1.2. Clinical effects of three barbiturates

	Clinical effects			
	Sedative/hypnotic	Analgesic	Anti-epileptic	Anesthetic
Pentobarbital	(++)	(+/-)	(-)	(++)
Amobarbital	(++)	(+)	(-)	(++)
Phenobarbital	(+)	(-)	(++)	(-)

(++) indicates strong effects; (+) indicates significant effects; (+/-) indicates unclear or controversial effects; (-) indicates no effects.

Potentiation of GABAergic transmission is considered one of the major mechanisms of barbiturate actions in the CNS; however, barbiturates may exert distinct effects on inhibitory synaptic transmission. Barbiturates prolong $GABA_A$ergic synaptic currents in neurons and enhance burst duration of single $GABA_A$ receptor channels (Eghbali et al., 2000; Macdonald et al., 1989; Mathers, 1985; Steinbach and Akk, 2001). At higher concentrations, they directly activate $GABA_A$ receptors (Eghbali et al., 2003; Krasowski

and Harrison, 1999; Mathers and Barker, 1980; Thompson et al., 1996). Pentobarbital potentiates GABA-induced increases in Cl^- conductance below 10 μM in isolated hippocampal neurons; above 100 μM, pentobarbital can directly activate Cl^- conductance in the absence of GABA (Mathers and Barker, 1980). Phenobarbital, is less efficacious and much less potent in producing GABAmimic effects compared with pentobarbital (MacDonald and Barker, 1978). Amobarbital enhances GABA-dependent Cl^- flux in synaptic vesicles (Allan and Harris, 1986), but it is not known whether this barbiturate potentiates $GABA_A$ergic inhibition in CNS neurons.

Besides GABA potentiation and GABA-mimic effects, barbiturates may exert GABA-independent actions in the CNS (ffrench-Mullen et al., 1993; Nicoll and Madison, 1982; O'Beirne et al., 1987; Werz and Macdonald 1985). Pentobarbital, for instance, has effects on the intrinsic membrane properties that depress the excitability of neurons. This depression occurs in the similar or lower concentrations, at which pentobarbital potentiates GABA action. A prominent effect of pentobarbital is to increase K^+-conductance, which shunts the current required for excitation (Nicoll and Madison 1982; O'Beirne et al., 1987). Pentobarbital also inhibits Ca^{2+}-currents (ffrench-Mullen et al., 1993; Werz and Macdonald 1985) and suppresses Ca^{2+}-dependent transmitter release (Weakly 1969). High concentrations of barbiturates depress Na^+-dependent action potentials and currents in axons (Blaustein 1968). Hence, barbiturates have multiple actions, unrelated to GABAergic inhibition, which may contribute to, or account for, anesthetic-induced decreases in neuronal excitability.

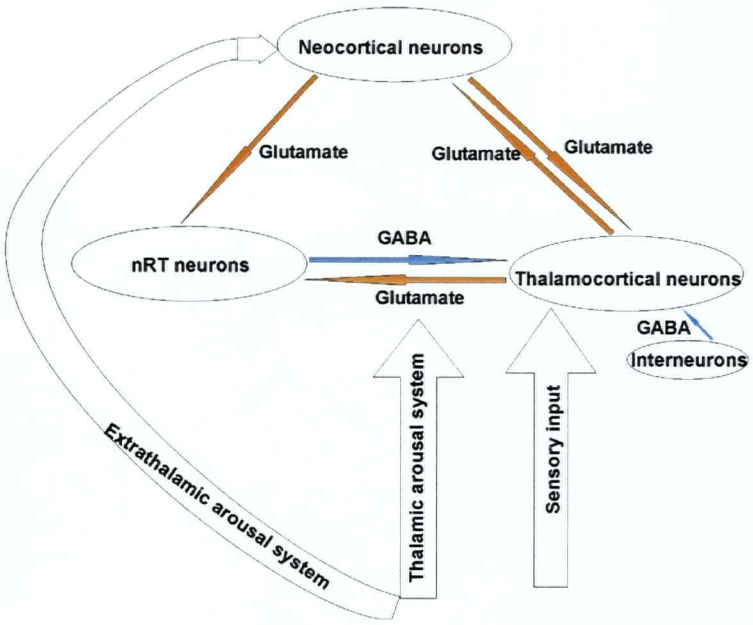

Figure 1.2. The basic cortico-thalamocortical network involved in anesthesia. The depicted neurons and impulse pathway (marked by arrows) are assumed to be the main targets for general anesthesia (Angel 1993; Ries and Puil 1999a and Alkire et al., 2000).

1.2.6. Concentration criteria for anesthetic- induced unconsciousness

The goal of *in vitro* studies is to explain how anesthetics produce unconsciousness. The question that arises is how does one correlate the results of such studies to unconsciousness? Historically, several criteria have been applied, but these criteria are inadequate. For example, the correlation of MAC to anesthetic potency in *in vitro* experiments is considered one of the most important criteria for applicability to explain how inhalational anesthetics produce unconsciousness. However, MAC is not very helpful for the following reasons: (1) there are different ways of measuring MAC, thus causing the variation of MAC obtained from different investigators; (2) the measurement of MAC doesn't distinguish unconsciousness from analgesia; (3) the measurement to determine human MAC cannot be used on animals; and (4) at MAC 50% of animals are NOT

anaesthetized. The concentration of anesthetics in the neuronal membrane is relevant for correlations to their mechanisms of action because the excitable membrane represents the most likely target for blocking signal transmission. Extracellular concentration of general anesthetics during anesthesia at nerve cells, e.g. CSF concentrations, may represent the relevant concentrations of drugs for inducing unconsciousness, as this concentration correlates to equilibrium membrane concentration of anesthetics in the brain. Based on this criterion, various synaptic and non-synaptic targets have been identified, which may contribute to anesthetic-induced unconsciousness.

1.2.7. Multiple sites of general anesthetics to induce unconsciousness

A number of mechanisms found *in vitro* have been proposed for *in vivo* general anesthetic effects (Franks and Lieb, 1994; Ries and Puil, 1999a; Wan et al., 2003). Low concentrations (sedative doses) of general anesthetics induce sedation-hypnosis. When applied in higher concentrations (anesthetic doses), general anesthetics cause loss of consciousness. This suggests that general anesthetics may interact with different sites in various concentrations, which exert varying levels of depression in the CNS *in vivo*.

1.2.7.1. Excitatory neurotransmission and anesthetics

Suppressing excitatory neurotransmission in the CTC system may be a potential *in vitro* mechanism for anesthetics. Glutamate is a major excitatory neurotransmitter in the CNS and activates two distinct classes of receptors. It binds to ligand-gated ion channels, called ionotropic glutamate receptors, and to G-protein coupled receptors, termed metabotropic glutamate receptors (mGluR; Gasic and Hollmann, 1992). Ionotropic glutamate receptors are commonly divided into two classes (Table 1.1). The alpha-amino-3-hydroxy-5-methyl-

4-isoxazoleproprionate (AMPA)/Kainate may be activated rapidly upon glutamate release and inactivated within a few milliseconds, showing little voltage-dependence. The N-methyl- d-aspartate (NMDA) subtype may be activated and inactivated more slowly, exhibiting steep voltage dependence.

General anesthetics depress excitatory postsynaptic potentials (EPSPs) by presynaptic and postsynaptic mechanisms. Halothane, isoflurane, and enflurane decrease glutamatergic excitatory postsynaptic potentials or currents at clinically relevant concentrations (el-Beheiry and Puil, 1989; Cheng and Kendig, 2003; Kitamura et al., 2003). This action may be attributable to anesthetic-induced decreases of postsynaptic responsiveness by inhibiting postsynaptic NMDA or non-NMDA receptors (Stucke et al., 2003), to glutamate by anesthetics (Puil and El-Beheiry 1990). As well, it could be due to depressing the release of glutamate from nerve terminals via presynaptic actions (Nishikawa and MacIver, 2000). The intravenous anesthetic, pentobarbital, suppresses EPSPs in hippocampal and neocortical neurons (Richards, 1971; Sawada and Yamamoto, 1985). This suppression is attributable to the fact that pentobarbital reduces the probability of channel opening, which results from a shortening of the lifetime of the channel's open state, and by a decrease in burst length (Charlesworth et al., 1995). Pentobarbital also causes use and concentration-dependent depression on AMPA receptor mediated currents by facilitating AMPA receptor desensitization (Jackson et al., 2003). Although the molecular mechanisms underlying the interactions between excitatory neurotransmission and anesthetics are not clear, inhibition of Nitric Oxide (NO) synthesis potentiates anesthesia in animals (Johns et al., 1992; Ichinose et al., 1998; Motzko et al., 1998), which implicated that NO pathway may be involved in general anesthetics-induced unconsciousness.

In summary, disruption of glutamate dependent processes is an operative mechanism of anesthetic action. Many anesthetics inhibit glutamatergic neurotransmission in clinical relevant concentrations, which may contribute to unconsciousness. However, up to now, there has been no study on the anesthetic action on the cortico-thalamocortical system based on concentration-dependence, which is one objective that this thesis will achieve.

Table 1.1. Pharmacology of GABA and glutamate receptors

	GABA receptors			Glutamate receptors		
	$GABA_A$	$GABA_B$	$GABA_C$	NMDA	AMPA/Kainate	mGluR
Associated ion(s)	Cl^-	G protein coupled K^+	Cl^-	Ca^{2+}, Na^+, K^+	Na^+, K^+ (Ca^{2+})	G-protein-coupled Ca^{2+}, K^+
Specific Agonists	GABA, Muscimol	GABA, Baclofen	GABA, CACA	NMDA,	AMPA, Kainate,	1S, 3R, ACPD
Specific Antagonists	Bicuculline	CGP 35348, Saclofen	TPMPA	APV, CPP	CNQX, NBQX	S-4C3HPG, MCCG, MAP4

1.2.7.2. Enhancement of inhibitory neurotransmission

Many general anesthetics enhance inhibitory neurotransmission mediated by GABA, a major inhibitory neurotransmitter in the CNS. Three subtypes of GABA receptors have been identified: $GABA_A$, $GABA_B$ and $GABA_C$ receptors (Table 1.1). $GABA_A$ receptor belongs to a superfamily of ligand-gated ion channels (Macdonald and Olsen, 1994), and is considered a major target of general anesthetics. Anesthetics enhance $GABA_A$ receptor mediated currents in neurons, GABA-activated Cl^- flux in brain slices, cells and

homogenates, and allosteric modulation of GABA receptor radioligand binding assays in homogenates (reviewed by Olsen et al., 1991). The $GABA_A$ receptor is considered an important anesthetic target since anesthetic effects occur at concentrations close to the EC_{50} for general anesthesia and a considerable number of agents affect $GABA_A$ receptor gated Cl^- channels (Olsen et al., 1991).

General anesthetics may directly activate, and potentiate the $GABA_A$ receptor, which causes alteration in amplitude and decay of IPSPs. Enflurane, for example, prolongs the GABAergic inhibitory postsynaptic currents (IPSC) decay but simultaneously decreases the amplitude of IPSCs, in cerebellar Purkinje cells and hippocamal pyramidal cells, by a postsynaptic mechanism (Antkowiak and Heck, 1997; Banks and Pearce, 1999). This differs from the actions of etomidate, which prolongs the IPSC decay and increases the amplitude of synaptic events (Yang and Uchida, 1996). Pentobarbital, halothane and propofol prolong IPSC decay, leaving amplitude affected (Banks and Pearce, 1999; Orser et al., 1994; Wan et al., 2003). However, potentation of IPSPs may not necessarily cause inhibition. *In vivo*, the potentation of IPSPs induces hyperpolarization, which activates low threshold Ca^{2+} currents (Williams et al., 1997). This action may contribute to excitation period during emergence from anesthesia.

It seems that different subunits of $GABA_A$ receptor could differ in their ability to interact with barbiturates, despite a rather uniform sensitivity of GABA receptors to anesthetics in CNS neurons. $GABA_A$ receptors are composed of five subunits. In mammals, α (1-6), β (1-3), γ (1-3), δ (1), ε (1), θ (1) subunit isoforms exist (Mehta and Ticku, 1999). α subunits of $GABA_A$ receptors are crucial for direct activation of $GABA_A$ receptors by pentobarbital.

Among α subunits, $GABA_A$ receptors containing α_6 subunits showed the highest affinity and efficacy for direct activation (Thompson et al., 1996). Among β subunits, pentobarbital was significantly more potent in enhancing [^{3}H] flunitrazepam binding to WSS-1 cells transfected with the β_2 subunit, compared with the β_3 subunit (Harris et al., 1995). The presence of γ subunit is required for the action of benzodiazepines, but not for barbiturates, propofol or steroid anesthetics.

Although the evidence showing that the $GABA_A$ receptor is one of the major molecular targets of general anesthetics in the CNS, pentobarbital and other anesthetics depress membrane excitability by actions that are not sensitive to blockade with $GABA_A$ receptor antagonists (Sugiyama et al., 1992; Belelli et al., 1999). Indeed, observations of greater GABAergic inhibition during anesthesia are not universal in different preparations. The questions that arise are how general anesthetics modulate GABAergic IPSPs (IPSCs) in the CTC system in the range of clinically relevant concentrations, and are there concentration-dependent effects? These questions will be discussed in this thesis.

The inhibitory neurotransmission by another inhibitory neurotransmitter in the CNS, glycine, is also reported to be potentiated by general anesthetics (reviewd by Belelli et al., 1999). Glycine contributes to fast inhibitory synaptic transmission within the brainstem and the spinal cord via activation of strychnine-sensitive glycine receptors. Inhalational anesthetics, including cloroform, enflurane, methoxyflurane, and sevoflurane, greatly potentiate Cl^- currents mediated by a homo-oligomeric glycine receptor (Krasowski and Harrison, 1999). By contrast, pentobarbital, propofol and alphaxalone only moderately potentiate glycine receptors at clinically relevant concentrations (Belelli, et al., 1999).

Thus, current available evidence suggests that any putative role for glycine receptors in clinical anesthesia is likely to be restricted to the mediation of an aspect of volatile anesthetics.

1.2.7.3. Non-synaptic intrinsic ion channels

Although alteration of synaptic transmission is a common mechanism for anesthetic actions *in vitro*, general anesthetics may inhibit neuronal excitability by other mechanisms. Puil and Gimbarzevsky (1987) reported an increase of input conductance in trigeminal root ganglion neurons induced by halothane and isoflurane. Since these neurons are believe to be devoid of synaptic inputs, the modulation of intrinsic ion channels likely account for this action. These intrinsic ion channels may include K^+, Ca^{2+} and Na^+ channels (Haydon and Urban, 1983; Nicoll and Madison, 1982; Weakly, 1969).

K^+ channels and general anesthetics

Anesthetics may activate K^+ channels to inhibit neuronal excitability. Nicoll and Madison (1982) found that small hyperpolarization of vertebrate neurons, accompanied by increases in K^+ conductance, correlated with anesthetic potency. Inhalational anesthetics, isoflurane, halothane and sevoflurane, activate K^+ currents, which shunt the firing activity of thalamocortical neurons, motoneurons and cerebellar granule neurons (Ries and Puil, 1999a; Shin and Winegar, 2003; Sirois et al., 1998). Pentobarbital, at low doses, hyperpolarizes hippocampal and cerebellar Purkinje neurons with occasional decreases in input resistance, which may be due to activation of calcium-activated K^+ channels (Carlen, et al., 1985; O'Beirne, et al., 1987). Thus, K^+ channel activation, including voltage-

dependent and voltage-independent K^+ channels, may be a common mechanism for different anesthetics.

General anesthetics may interact with voltage-independent leak K^+ channels. Leak K^+ selective channels are characterized by a lack of voltage and time dependence and by a linear current voltage relationship in a symmetrical K^+ gradient. Leak K^+ channels play an essential role in setting the resting membrane potential, tuning the action potential duration and modulating the responsiveness to synaptic input. General anesthetics induce small hyperpolarization (Nicoll and Madison, 1982) of vertebrate central neurons, accompanied by increases in K^+ conductance (Ries and Puil, 1999a, 1999b). Single channel experiments establish that this hyperpolarization is due to volatile anesthetic activation of leak K^+ channels (Siegelbaum et al., 1982; Patel et al., 1999).

Inhalational anesthetics interact with different subtypes of leak K^+ channels, especially with TWIK-related K^+ channel (TREK) and TWIK-related acid-sensing K^+ channel (TASK) channels. In rat somatic motoneurons, locus coeruleus neurons and cerebellar granule neurons, volatile anesthetics similarly activate a leak TASK-1 like conductance, causing membrane hyperpolarization and suppressing action potential discharge (Maingret et al., 2001; Sirois et al., 2000). In motoneurons and cerebellar granule neurons, opening of TASK-1 probably contributes to anesthetic-induced immobilization, whereas in locus coeruleus, it might support analgesic and hypnotic action (Maingret et al., 2001; Sirois et al., 2000). In recombinant leak K^+ channels, isoflurane, halothane, diethyl ether and chloroform activate TREK-1 and TREK-2 channels on recombinant channels expressed in COS cells (Patel et al., 1999; Lesage et al., 2000). Recombinant TASK channels are

activated by isoflurane and halothane (Patel et al., 1999). This activation effect of TASK-1 induced by halothane is greater than by isoflurane, whereas TASK-1 channels are insensitive to chloroform and inhibited by diethylether (Patel et al., 1999). These studies suggest that leak K^+ channels are activated by various volatile anesthetics in different preparations.

The interaction between intravenous anesthetic and leak K^+ channels is not unknown. However, some intravenous anesthetic agents, e.g. pentobarbital, inhibit neuronal voltage-dependent K^+ currents in different preparations (Benoit, 1995; Brau et al., 1997; Carlen et al., 1985; O'Beirne et al., 1987; Kulkarni et al., 1996; Friederich and Urban, 1999). Further investigation on how intravenous anesthetics modulate different types of K^+ channels in the CTC system may clarify the mechanisms of anesthetics.

Na^+ channels and Ca^{2+} channels and general anesthetics

Anesthetics may inhibit Na^+ channels to inhibit neuronal excitability at concentrations that are higher than clinically relevant doses. Studies on rat and human neurons reveal that anesthetics decrease the rate of rise of action potentials, which is consistent with a change in sodium channel properties (MacIver and Roth, 1988; Berg-Johnson and Langmoen, 1990). The threshold potentials become more depolarized with application of anesthetics, consistent with anesthetic modification of sodium channels (Berg-Johnsen and Langmoen, 1990; Fujiwara et al., 1988; Yoshimura et al., 1985). Additionally, anesthetic blockade of sodium channels may directly inhibit glutamate release *in vitro* (Ratnakumari and Hemmings, 1996; Schlame and Hemmings, 1995), which may contribute to the anesthetic-

induced depression of glutamatergic neurotransmission in the hippocampus (MacIver et al., 1996a).

The molecular interactions between Na^+ channels and general anesthetics that may lead to alteration in neuronal function have been first studied in non-mammalian tissue. In the 1980s, experiments on squid giant axon (Haydon and Urban, 1983) revealed that at least five functional properties of sodium channels are altered by anesthetics: average channel conductance, steady-state channel activation (m_∞) and inactivation (h_∞), and the time constants of channel activation and inactivation. Most importantly, volatile anesthetics decrease peak sodium current (I_{Na}) and shift steady-state inactivation to more hyperpolarization potentials while shifting steady-state activation to more positive potentials (Haydon and Urban, 1983; Urban, 1993). The net result of all these anesthetic effects is a significant decrease in sodium conductance.

The study to examine anesthetic interaction with mammalian CNS sodium channels shows that the anesthetics have two effects: (1) a reduction in single channel current, and (2) a shift in channel steady-state activation to more hyperpolarization potentials (Frenkel et al., 1989, 1990; Frankel and Urban, 1991, 1992). These effects occur at high concentrations. Pentobarbital blocks human sodium channels in a frequency-dependent manner, at 3-5 fold of clinical concentration in transfected CHO cell lines (Rehberg et al., 1995). Volatile anesthetics also block sodium channels with IC_{50} of 6-10 fold larger than concentrations that yield anesthesia (Rehberg et al., 1996). Since neither intravenous nor volatile anesthetics inhibit Na^+ channels in clinically relevant concentrations, it is unlikely that Na^+ channel suppression contributes to general anesthetics-induced depression in the CNS.

Ca^{2+} channels are another potential targets for anesthetic actions in the CNS. Both volatile and intravenous anesthetics have been found to block low-threshold Ca^{2+} channels (Todorovic and Lingle, 1998). Halothane and isoflurane at 1 MAC produce 20% and >50% reduction of T-type Ca^{2+} currents in dorsal root ganglia cells (Todorovic and Lingle, 1998). Pentobarbital inhibits Ca^{2+}-currents (ffrench-Mullen et al., 1993; Werz and Macdonald 1985) and Ca^{2+}-dependent transmitter release (Weakly 1969). However, pentobarbital produces a complete blockade of low threshold T-type Ca^{2+} currents with an EC_{50} of 334 μM (Todorovic and Lingle, 1998). Because this concentration is significantly higher than concentrations that produce anesthesia *in vivo*, it is unlikely that the blockade of low threshold T-type Ca^{2+} currents significantly contribute to barbiturate-induced anesthesia.

There has been tremendous progress in our understanding of the mechanisms of anesthetic actions over the past few years. A lot of evidence points to the activity of the majority of anesthetics at ligand-gated ion channels, providing an excellent rationale for their pharmacological effects. Enhancement of inhibitory GABAergic and/or glycinergic neurotransmission, interaction with potassium, sodium, calcium channels or inhibition of excitatory pathways, clearly provide potential targets and testable hypotheses for the mechanisms of anesthetics. Thus, another object of this thesis is to assess the interaction of these potential targets with barbiturates in the CTC system.

1.3. Rationale

Knowledge of the interaction between general anesthetics and intrinsic membrane properties, network connectivity, synaptic and neuromodulatory inputs in the CTC system is a prerequisite to understand the mechanisms of these agents in the CNS. This thesis will

study three major types of neurons in the CTC system: neocortical neurons, reticular thalamic neurons and thalamocortical neurons. Comparing barbiturate actions in these neurons will therefore further our understanding on the potential targets for these agents' effects *in vivo*. The actions of barbiturates on interneurons, other types of neocortical neurons in the CTC system will not be investigated in this thesis.

Although a number of mechanisms, especially GABA mechanism, may contribute to anesthetic-induced unconsciousness, assessment of possible *in vitro* targets will depend on further electrophysiological investigations of these agents in a nervous tissue relevant to neurological mechanisms of consciousness discussed above. In this thesis, the actions of an anesthetic barbiturate, pentobarbital, in the CTC system will be studied, because it is a benchmark drug that potentiates GABA receptors. Another barbiturate anesthetic, amobarbital, and anti-epileptic barbiturate, phenobarbital, are studied in the same system for comparison. Other possible mechanisms, including interaction with excitatory neurotransmission and intrinsic ion channels are studied based on concentration-dependence in the same system. In this thesis, we apply extracellular concentrations of barbiturates close to CSF concentrations according to the previous reports (Sato et al., 1995), which correlate with relevant concentrations to induce unconsciousness.

Taken together, the hypothesis of the thesis is that barbiturates depress neuron excitability by interacting with synaptic neurotransmission and non-synaptic intrinsic ion channels by GABA-dependent and GABA-independent mechanisms in the CTC system, which may contribute to the alteration of consciousness.

1.4. Major objective and questions

In view of the role of the corticothalamocortical system in anesthetic-induced unconsciousness and the potential mechanisms of anesthesia, the objective of this thesis was to study the effects of barbiturates in neurons of the CTC system and to ascertain the most likely mechanisms underlying the observed effects. This study contributes to an understanding of the mechanisms of barbiturate actions, and hence, to the mechanisms of general anesthesia, anticonvulsant activity and analgesia. The investigation addressed the following questions:

1. Does pentobarbital, at clinically relevant concentrations, modulate intrinsic membrane properties of neurons in the CTC system?
2. How does pentobarbital modulate intrinsic ion channels and synaptic properties in the CTC neurons?
3. How do amobarbital and phenobarbital alter neuronal excitation and synaptic transmission?
4. What are the concentration-response relationships for the effects of the barbiturates on neurons of the CTC system?

Chapter 2
METHOD

2.1. Whole-cell patch clamp recording

2.1.1. Preparation of slices

The experiments received approval from the Committee on Animal Care of The University of British Columbia. At the beginning of each experiment, a Sprague-Dawley rat (range from 13 to 15 days) was put at room temperature under an inverted glass funnel (volume, 300cc) to provide a gas-tight induction chamber. The rat was anesthetized by ~4% halothane or ~4% isoflurane. After 30 seconds to 1 min, the immobile but still breathing rat were quickly removed from anesthetic chamber and decapitated. After decapitation of the breathing animal, the skull cap was opened, the cerebral hemispheres were gently retracted rostrally and a spatula was inserted to sever the brainstem. The brain was removed from the cranial vault and immersed in ice-cold (1-4°C), modified artificial cerebrospinal fluid (ACSF). The ACSF, used to enhance slice viability, contained sucrose as a replacement for NaCl. This solution was used for the first 1 to 2 minutes of the immersion. The entire surgical procedure was performed in less than 2 min. Coronal slices (300 μm thick), containing the medial geniculate body (MGB) or ventroposterolateral (VPL) nuclei or lateral geniculate nucleus (LGN) and neocortex, were cut by a Vibroslice (Campden Instruments Ltd., London, England). Horizontal slices containing ventrobasal complex of thalamus, nucleus reticularis thalami (nRT), internal capsule were used in some experiments to investigate synaptic transmission.

Slices were maintained on a polypropylene mesh in a holding chamber containing normal ACSF (23- 25° C) for at least 1 hr before recording.

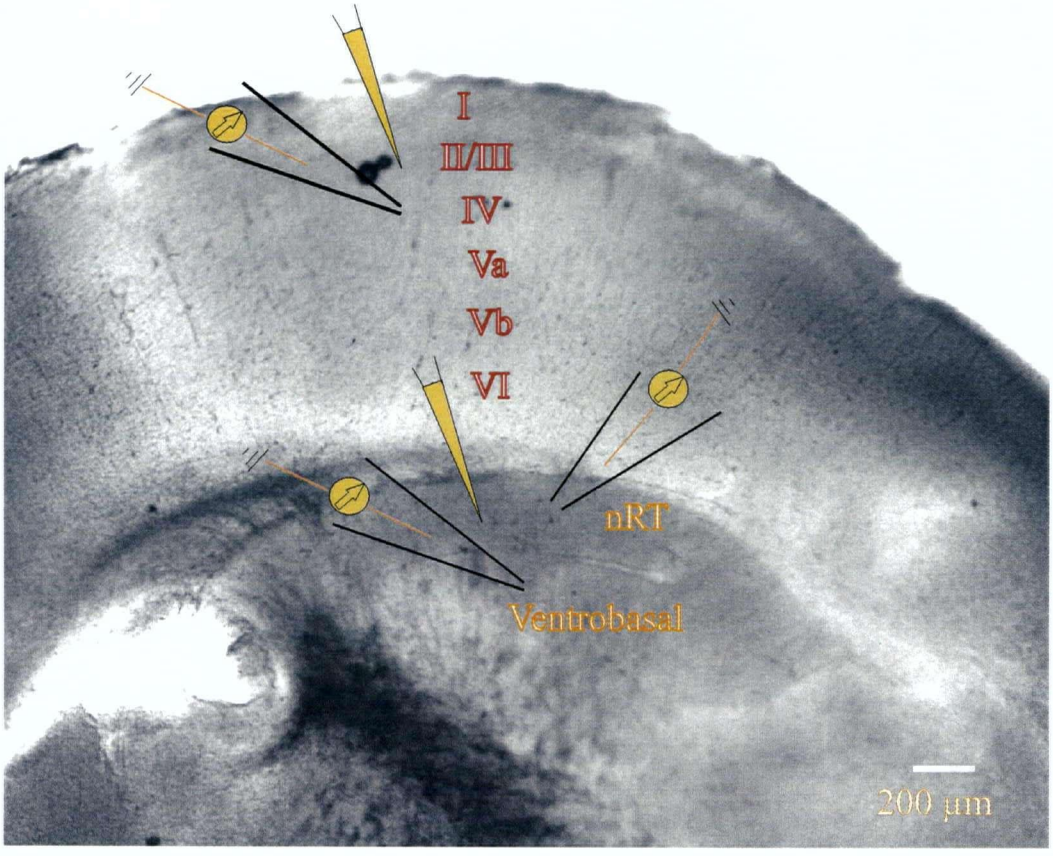

Figure 2.1. Photograph of a coronal slice of rat somatosensory cortex and thalamus. The whole-cell patch clamp recording was performed in layer IV neocortical neurons, nRT neurons or ventrobasal neurons as showed in the picture. Scale bar, 200 μm.

2.1.2. Physiological solutions

Except for the initial preparation, the ACSF used for the experiments contained (in mM): NaCl, 124; $NaHCO_3$, 26; glucose, 10; KCl, 4; $CaCl_2$, 2; $MgCl_2$, 2; and KH_2PO_4, 1.25. The ACSF modified for the slice preparation contained a low $[Na^+]$ because of substitution with sucrose (125 mM). The ACSF solutions were saturated with 95% O_2 : 5% CO_2 and had a pH = 7.4.

2.1.3. Electrical recording

Whole-cell patch-clamp recording was performed using an Axoclamp 2A amplifer (Axon Instruments, Inc., Foster City, CA, U.S.A) in the current-clamp and voltage-clamp mode. The recording pipettes were drawn from borosolicate glass tubing with internal filament (WPI Instruments, Inc., Sarasota, FL, U.S.A.), using a vertical puller (Narishige Instruments, Tokyo, Japan). The pipette solution contained (in mM): K-gluconate, 140; KCl, 5; ethylene-glycol-bis-(β-aminoethyl ether)-N, N, N′, N′-tetraacetic-acid (EGTA), 10; NaCl, 4; $MgCl_2$, 3; N-[2-hydroxyethyl] piperazine-N′-[2-ethanesulfonic acid] (HEPES; free acid), 10; disodium ATP, 2.8 or 3; monosodium GTP, 0.3 and $CaCl_2$, 1 (~10 nM Ca^{2+}, calculated using Max Chelator software). Just prior to electrical recording, ATP and GTP were added to the pipette solution. E_{Cl} was -55 mV, E_K, -84 mV, and E_{Na}, 92 mV, calculated from the Nernst equation. The pH was adjusted to 7.4 with 10% gluconic acid. The electrode resistances ranged between 5 and 9 MΩ.

For recording, a slice was placed in a Perspex chamber that had a volume of 1.2 cc. A polypropylene mesh in the chamber immobilized the slice which was perfused with

oxygenated (95% O_2: 5% CO_2) ACSF at a flow rate of 1 ml/min^{-1}. The nuclei were identified, visually aided by differential interference contrast (DIC) microscopy (400x magnification). The measurements of drug effects were conducted on visually selected neurons at 23-25 °C. The neurons were accepted for further study if they had stable resting membrane potentials and responded to depolarizing current pulse injections with overshooting action potentials. The input resistance (R_i) was determined from the hyperpolarizing voltage responses of usually ~5 mV, evoked by intracellular injections of current. The neurons were held at –66 mV for construction of current-voltage (I-V) relationships. Tonic firing was elicited by injection of depolarizing current pulses into neurons held near the resting potential, as typical for neurons of dorsal thalamic nuclei. Bursts of action potentials were elicited on injection of depolarizing pulses while holding the membrane potential at a hyperpolarized value (usually at –86 mV). Leak conductance was obtained from current response to -10 mV hyperpolarizing steps from -50 mV. Slope conductance was obtained from linear regression fits of current responses to -10 mV hyperpolarizing steps from V_H = -50 mV. Whole cell voltage clamp were made using a single-electrode voltage-clamp amplifier (Axoclamp 2A) in discontinuous mode (switching frequencies, 3-8 kHz, clamp gains 3-5 mV/nA). Electrode settling was monitored on a separate oscilloscope. In recording synaptic responses, a bipolar tungsten electrode (tip diameter ~100 μm) was placed at 0.2–0.3 mm above the slices for electrical stimulation. Signals were lowpass filtered at 5 kHz, digitized at 10 kHz with a 16-bit data acquisition system (Axon Instruments, USA), using pClamp 8 software running on a Pentium computer.

2.2. Single channel recording

2.2.1.Acute dissociation of neurons

Horizontal slices containing ventrobasal thalamus and nRT were cut to prepare acute dissociated neurons. The ventrobasal nuclei and nRT of the slices were further blocked using a razor blade and incubated for 10 min at 21 °C in oxygenated, calcium-free media of composition (in mM): 120 NaCl; 5 KCl; 1 $MgCl_2$; 5 D-glucose; 20 piperazine-N,N'-bis (2-ethanesulfonic acid) PIPES; 3 EGTA, and 2 mg/ml bovine serum albumin (BSA). The pH was 7.3. Tissue was then transferred to a stirring chamber and incubated for 45 min at 32°C in an enzyme solution containing (in mM): 120 NaCl; 5 KCl; 1 $MgCl_2$; 1 $CaCl_2$; 20 PIPES; 2 mg/ml BSA, and 14 Units/ml papain (Sigma , St. Louis, MO). The pH was 7.0. The tissue was carefully rinsed with enzyme-free PIPES buffered solution and kept in the stirring chamber for 15 min at room temperature. Mechanical dispersal was performed by trituration in 2 ml Ca^{2+}-free and BSA-free PIPES solution using fire-polished, silicon-coated Pasteur pipettes. Ventrobasal cells were plated onto uncoated 35 mm diameter tissue culture dishes (Corning, Midland MA) and kept at 21 °C in PIPES buffered solution until needed for recording.

2.2.2.Electrical recording

Single channel currents were recorded at room temperature (21-23°C). The dispersed ventrobasal or nRT cells, were bathed in a saline containing (in mM): 4 KCl; 135 NaCl; 10 $CaCl_2$; 1 Mg Cl_2; 10 HEPES; and 5 D-glucose (pH = 7.3). Patch pipettes (10-15 MΩ) were made by using a vertical puller (PP-83, Narishige, Japan). The pipettes were silicone-coated near the tip and contained a solution of composition (mM): 135 CsCl; 1

$MgCl_2$; 0.267 $CaCl_2$; 10 HEPES; 3 EGTA; and 5 D-glucose, and pH = 7.3. The $[Ca^{2+}]$ was 50 nM. Outside-out membrane patches were voltage-clamped usually at a holding potential (V_h) = -60 mV (List EPC-7 amplifier, Darmstadt, Germany). The currents were filtered at DC to 1 kHz, digitized (8 kHz) and analyzed off-line (Instrutech Corp., New York, U.S.A.).

2.3. Drugs

Stock solutions were prepared in distilled water or ACSF and diluted for immediate administration or frozen until just before experiment. (+/-)-Pentobarbital was purchased from Dumex Medical Surgical Products Ltd. (Pickering, ON, Canada). Amobarbital (Eli Lilly, Indianapolis, Indiana, USA) was a generous gift of Dr. Juhn Wada. Phenobarbital was purchased from The British Drug House (Toronto, ON, Canada). GABA, (±)-2-amino-5-phosphononopentanoic acid (APV), bicuculline methiodide, 6-cyano-7-nitroquinoxaline-2,3-dione (CNQX), picrotoxinin, tetrodotoxin (TTX), CGP 35348, CsCl and $BaCl_2$ were purchased from Sigma-Aldrich Canada Ltd. (Mississauga, ON, Canada). 2-hydroxysaclofen was purchased from Precision Biochemicals Inc. (Vancouver, B.C., Canada). (1,2,5,6-tetrahydropyridine-4-yl)methylphosphinic acid (TPMPA) from RBI/Sigma. ZD-7288 was purchased from Tocris Cookson Inc. (Ballwin, MO, USA). Drugs were applied by perfusion of the slices or to the external face of outside-out membrane patches excised from dispersed neurons.

2.4. Data Analysis

The data have been compensated for the junction potential between ACSF and the electrode solution. The junction potential of −11 mV was subtracted from all membrane potentials, e.g., a recorded resting potential of −55 mV corresponds to an actual potential of −66 mV. PClamp 8 (Clampfit, Axon Instruments), Prism GraphPad (San Diego, CA, U.S.A.), and CorelDraw (Ottawa, ON, Canada) software were used in data analysis. IPSCs were recorded at clamp potentials of -40 to -80 mV. Single exponential functions were fitted to the averaged decay phase of fast IPSCs, yielding their decay time constant. Data were expressed as mean ± S.E.M. and n denoted the number of cells tested. Student's t-test was used for comparing two groups. Analysis of variance (ANOVA) for multiple comparisons, and Student-Newman-Keuls tests for comparing groups were used. Significance was defined as $P < 0.05$. The probability, P_o, of a single amobarbital or GABA-activated channel opening during a period, T_{tot}, was calculated as $P_o = (T_1 + 2\ T_2 + \ldots N\ T_N)/N\ T_{tot}$, where N was the number of agonist activated channels and T_1, T_2, T_N, were times when at least 1, 2....N channels were open. The open time distributions were transformed by plotting the exponential fit function $y = A.e^{-t/\tau}$ on a logarithmic time scale, yielding a curve with peak amplitude at a time constant, τ. The mean open time of amobarbital or GABA-activated channels were calculated as the weighed sum of biexponential fits. Bursts of openings are defined as groups of openings that are separated by gaps that are all shorter than some specified length, t_c. t_c was chosen so as to make the proportion of long intervals that were misclassified (as short) equal to the proportions of short intervals that were misclassifed (as long). This was achieved by solving for t_c the equation $1-e^{-t_c/\tau_s} = e^{-t_c/\tau_m}$, where τ_s and τ_m are the slow and intermediate time constants in

the distribution of all shut times. (Colquhoun and Sakmann 1985). Gaussian terms were fitted to the amplitude distributions of single channel currents.

Chapter 3
RESULTS

Parts of the results in this chapter have been published in the Journal of Neurophysiology (Wan and Puil, 2002), Neuroscience (Wan et al., 2003). Parts of results now are in revision in British Journal of Pharmacology (2004)

Part I. Mechanisms of pentobarbital action on neurons of medial geniculate body (MGB) and ventrobasal (VB) nuclei

This part studied the actions of pentobarbital on two types of thalamocortical neurons and studies whether pentobarbital exerted specific action in these neurons.

3.1.1. Action potential firing and membrane conductance

The data were obtained from 66 neurons, located in the ventral division of the MGB, and 47 neurons located in the VB nuclei. There were no significant differences in resting membrane potentials of these neurons (n = 40; $P>0.05$). In 40-pooled neurons, mean resting potential was -66 ± 2.1 mV and mean input resistance (R_i) was 236 ± 24 MΩ.

3.1.1.1. Tonic and burst firing

When neurons were held at a potential near resting membrane potential, e.g., –66 mV, intracellular injection of depolarizing pulses elicited the tonic firing pattern of action potentials. (Figure 3.1A). When the membrane potential was held at a hyperpolarized potential, e.g., –86 mV, injection of similar depolarizing pulses elicited a low threshold Ca^{2+} spike (LTS). Pentobarbital application reversibly decreased or eliminated tonic firing as well as burst firing and the associated low threshold Ca^{2+}-spike (LTS), evoked by current pulses. The effects of pentobarbital on the tonic firing of 4 or 5 action potentials or LTS bursts of 2 or 3 action

potentials were determined in MGB neurons. Figure 3.1A shows the reduction in tonic firing due to pentobarbital application (20 μM) in a neuron held at –66 mV.

Pentobarbital application decreased or eliminated bursts of action potentials. Pentobarbital over a 0.01 to 50μM range produced a marked elevation in the amount of current required for evoking multiple action potentials in MGB neurons (Figure. 3.1) but only small changes (<10%) in action potential amplitude (Figure. 3.1D). The blockade of firing in tonic and burst modes was surmountable by increasing the amplitude of current pulses. The tonic firing rate decreased with an increase in the pentobarbital concentration (Figure. 3.2A). The data were fitted with a sigmoidal function and showed an IC_{50} at 7.2 ± 0.7 μM (n = 5).

Pentobarbital induced changes in the LTS, despite co-application of TTX to block voltage-dependent Na^+-conductances. On blockade of the transient Na^+ conductance of action potentials and persistent Na^+ conductance (Stafstrom et al., 1982), pentobarbital (10 μM) reversibly decreased the maximal rate of rise (dV/dt_{max}) of the LTS by 29% (from 2.2 ± 0.7 to 1.5 ± 0.5 mV/ms). The LTS evoked by current pulse injection decreased gradually in amplitude during the application. At 4 min the voltage response likely reflected the passive membrane properties (Figure. 3.1C, *middle*). The LTS appeared shunted because an increased amplitude of injected current produced a return of the LTS despite continuing pentobarbital application (Figure. 3.1C, *middle*).

Pentobarbital had similar actions on VB neurons. Pentobarbital inhibited tonic and burst firing in ventrobasal neurons in a concentration-dependent manner. The IC_{50} for inhibition of tonic firing is 8.2 ± 0.8 μM (n = 6).

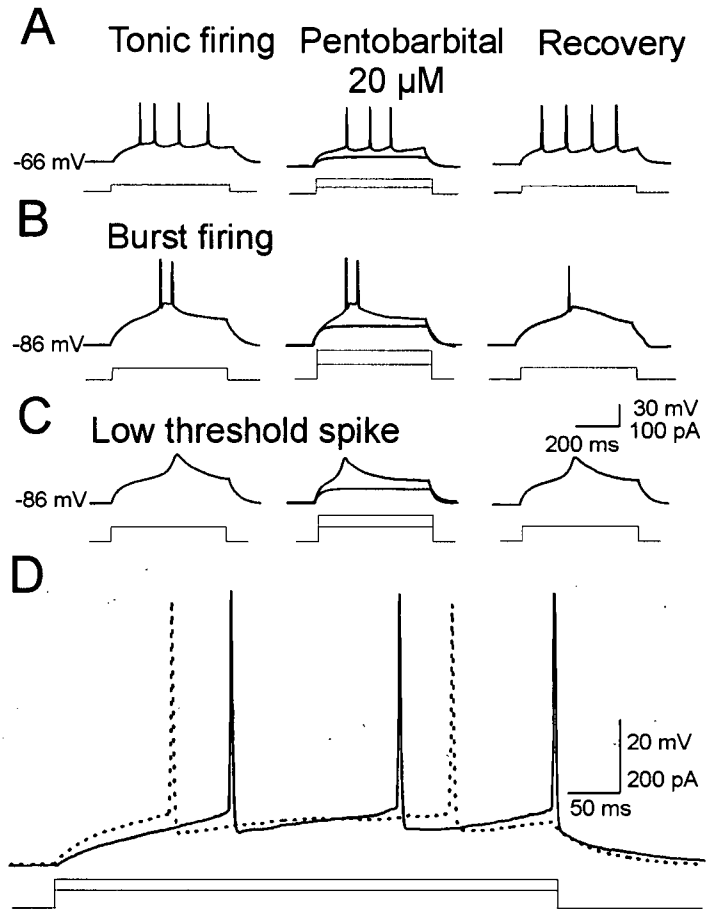

Figure. 3.1 Depressant effects of pentobarbital application on the firing modes of MGB neurons. (A) Pentobarbital (20 μM) eliminated the tonic firing of action potentials evoked by current pulse injection (middle, *lower trace*) in a neuron held with DC at -66 mV. (B) In the same neuron held at –86 mV, pentobarbital (20 μM) eliminated the burst of action potentials elicited by current pulse injection (middle, lower trace). (C) During blockade of action potentials with TTX application, pentobarbital (20 μM) abolished the low threshold Ca^{2+} spike evoked by current pulse injection. In the middle (*upper*) records of A-C, a larger current pulse returned the firing of action potentials or the low threshold Ca^{2+} spike, characteristic of a shunt-type of blockade. In A-C, recovery was observed at ~20 min after discontinuing pentobarbital application. (D) Pentobarbital (10 μM; dotted line) did not greatly affect the configuration of action potentials during control (solid line) evoked by 500 ms current pulses of 60 and 100 pA amplitudes. These effects were reversible on terminating the application in all neurons. Complete recovery required 20 to 30 min in ~75% of all neurons.

These indicated that different types of thalamocortical neurons had similar sensitivity to pentobarbital-induced depressant effects on neuronal firing.

3.1.1.2. Low resistance shunt mechanism

The reversible blockade of tonic and burst firing in VB and MGB neurons induced by pentobarbital was overcome by larger depolarizing current pulse injections (Figure. 3.1). This implied that a low resistance shunt mechanism may be involved in the pentobarbital-induced blockade of action potentials in these two types of neurons.

3.1.1.3. Alteration of input resistance (R_i) and membrane potential

Pentobarbital produced changes in electrical membrane properties that corresponded to the observed decrease in firing. Neurons that exhibited a decrease in evoked firing by 10 μM pentobarbital showed a 28 ± 9% reduction in R_i in MGB neurons (n = 5) and 25 ± 5% in ventrobasal neurons (n = 5), both measured with hyperpolarizing pulses (Figure. 3.2C). This concentration of pentobarbital did not reduce R_i in 4 out of total 10 neurons. Overall, pentobarbital application hyperpolarized neurons by a mean of 3 mV (range, 1 to 4 mV), which was not significantly different from the control (n = 50).

3.1.1.4. Concentration-responses for R_i decreases

Figure 3.2B shows the pooled data in a concentration-response relationship for the depressant effects of pentobarbital on R_i. The data, fitted with a sigmoidal function, showed an IC_{50} at 7.8 ± 0.5 μM in 20 MGB neurons and 8.1 ± 0.6 μM in 17 ventrobasal neurons. There was no significant difference in IC_{50}s between these two types of neurons (n = 5, $P>0.05$). The effects of 10 μM pentobarbital are summarized in Figure 3.2C which shows input resistance data,

measured with hyperpolarizing and depolarizing current pulses that displaced the membrane potential by ~8 mV.

3.1.2. Involvement of GABA receptors

To study the interactions between pentobarbital with GABA receptors in thalamocortical neurons, the effects of GABA receptor antagonists on pentobarbital-induced inhibition were studied in another series of experiments.

3.1.2.1. Interactions with bicuculline

The interactions with a $GABA_A$ receptor antagonist, bicuculline (20 to 100 μM), was applied to assess the possibility that pentobarbital produced its inhibiting effects by activating $GABA_A$ receptors. In these experiments on 5 neurons, bicuculline (100 μM) were applied for 4 min before co-applying pentobarbital (10 μM) and bicuculline (100 μM) for an additional 4 min. Bicuculline, alone, had an excitatory effect (cf. Debarbieux et al., 1998), depolarizing neurons by 4-5 mV and producing a small leftward shift in the latency of evoked action potentials (Figure. 3.3A). Under these conditions, pentobarbital decreased tonic and burst firing, as well as the LTS during TTX-blockade of Na^+-conductance.

We also reversed the procedure, applying pentobarbital (10 μM) for 4 min, observing the depressant effects and a small hyperpolarization, and then co-applying bicuculline (100 μM) for an additional 4 min. In such cases, bicuculline did not antagonize the depressant effects of pentobarbital (n = 4). Despite bicuculline co-application which itself caused little or no change in membrane properties of thalamocortical neurons, pentobarbital significantly reduced R_i (Figure. 3.3C).

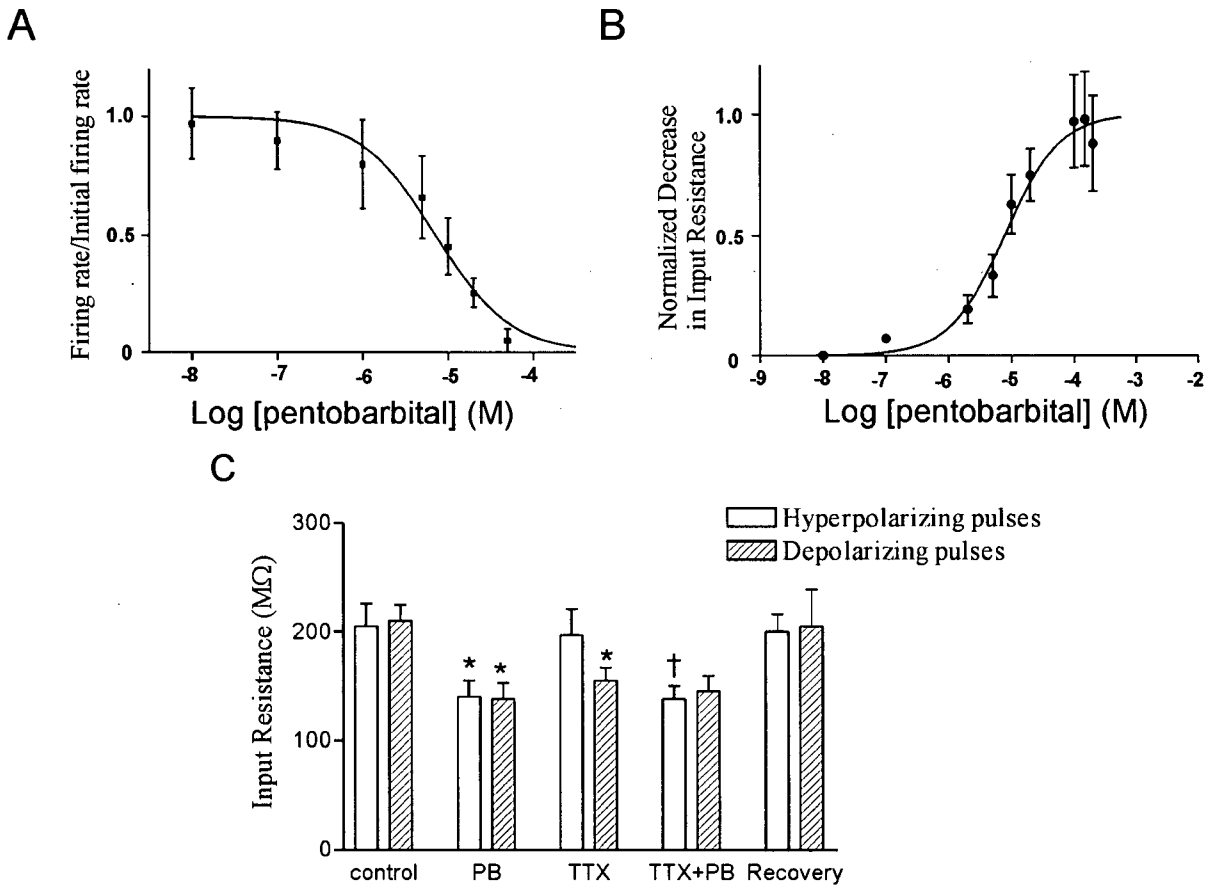

Figure. 3.2 Concentration-response relationships for depressant effects and summary of effects on input resistance induced by pentobarbital application in MGB neurons. (A) Pentobarbital decreased firing frequency in a concentration-dependent manner in a range from 10 nM to 50 μM. The relationship was fitted with a sigmoidal function (equation: $Y = 1/[1+10^{\log(IC_{50} - X)}]$) and each point represents a mean ± SE of 3 to 4 neurons. The IC_{50} for pentobarbital was 7.2 ± 0.7 μM. Vertical axis is the ratio of tonic firing rate to initial firing rate. (B) Pentobarbital induced a concentration-dependent decrease in R_i, measured with hyperpolarizing current pulse injection. The inhibition was calculated as a percentage of averaged control values. The IC_{50} for pentobarbital was 7.8 ± 0.5 μM. The relationship was fitted with the same sigmoidal function as above. The error bars for the data points at 10^{-8} and 10^{-7} M are within the symbols. Each point represents a mean ± SE of 3 to 8 neurons with or without TTX application. (C) Summary of depressant effects of pentobarbital (PB, 10 μM; n = 5) on input resistance obtained from depolarizing or hyperpolarizing responses (8 mV), with or without TTX. * $P< 0.05$, significantly different from Control. † $P< 0.05$, significantly different from TTX.

3.1.2.2. Muscimol Activation of $GABA_A$ receptors

The $GABA_A$ agonist, muscimol, were used to verify that the $GABA_A$ receptors in the slices remained intact and were susceptible to antagonism by bicuculline. Application of muscimol (20 μM) to 3 neurons held at –66 mV decreased R_i from the control value of 252 ± 30 MΩ, to 90 ± 17 MΩ (n = 3). Muscimol depolarized 2 neurons by ~1 mV and the third neuron by 4 mV. As expected for a Cl^- conductance increase, the depolarizing direction of these values is consistent with a relatively positive E_{Cl}. The E_{Cl} in these experiments was –55 mV (cf. Methods). Co-application of muscimol (20 μM) and bicuculline (50 μM) for 6 min and did not result in significant changes in R_i (n = 3). Approximately 10 min after termination of the co-application, an application of muscimol, alone, again produced fully reversible decreases in R_i in all 3 neurons. Muscimol-induced depressant actions, which were susceptible to blockade by $GABA_A$ receptor antagonist, implying that $GABA_A$ receptors were functional in the preparation.

3.1.2.3. Interactions with picrotoxinin

In view of the above results, we attempted to block pentobarbital actions by applying picrotoxinin (50 or 100 μM), which blocks a $GABA_A$-linked Cl^--channel site. That is distinct from the site antagonized by bicuculline. The effects of pentobarbital (10 μM) application were observed during the first 4 min and then again during an additional 4 min co-application with picrotoxinin (50 μM; n = 3). The reversed procedure was applied in 3 additional neurons, by applying picrotoxinin before pentobarbital. Picrotoxinin applied to the 6 neurons, did not significantly alter the membrane potential and R_i (Figure. 3.3C). Pentobarbital, applied according to both procedures, decreased tonic and burst firing, as well as the LTS on TTX-blockade of voltage-dependent Na^+-conductances (Figure. 3.3B). Pentobarbital also increased

the threshold current requirement for a LTS. After a 20 min recovery period from the co-application, a second application of pentobarbital, alone, produced depressant effects of approximately the same magnitude as in the initial control. Therefore, picrotoxinin-blockade of the Cl^- channels did not prevent the depressant effects of pentobarbital on thalamocortical neurons.

3.1.2.4. Interactions with saclofen, a $GABA_B$ receptor antagonist

Saclofen, a $GABA_B$ receptor antagonist, was applied to assess a possible involvement of $GABA_B$ receptors in pentobarbital actions. An initial application of pentobarbital (10 μM) during TTX-blockade of voltage-dependent Na^+-conductances eliminated the LTS and decreased R_i from 260 ± 40 MΩ to 180 ± 28 MΩ (n = 5). After recovery of the LTS, a subsequent application of saclofen (200 μM) for 4 min, followed by the co-application at 10 μM of pentobarbital (4 min), still resulted in elimination of the LTS (Figure. 3.4A) and a decreased R_i from 256 ± 35 MΩ to 175 ± 30 MΩ (Figure. 3.4C; n = 5). Despite the co-application with a saclofen concentration that antagonizes $GABA_B$ responses in MGB neurons (Peruzzi et al., 1997), pentobarbital produced depressant responses.

3.1.2.5. Interactions with a $GABA_C$ receptor antagonist

The interactions of pentobarbital and (1,2,5,6-tetrahydropyridine-4-yl) methylphosphinic acid (TPMPA), a $GABA_C$ receptor antagonist (Ragozzino et al., 1996) were observed, in order to assess a possible contribution of $GABA_C$ receptor activation to the depressant effects of pentobarbital. TPMPA (20-50 μM), itself, did not alter membrane properties. The same procedure was used as above for saclofen, for TPMPA. Before TPMPA, pentobarbital application (10 μM) abolished the LTS and decreased R_i by 30%, from 244 ± 30 MΩ to 170 ±

24 MΩ (n = 4). An 8 min application of TPMPA, in concentrations that ranged between 10 and 50 μM, did not block the inhibition of the tonic and burst firing (Figure. 3.4B) or the LTS and R_i decrease induced by co-applied pentobarbital. During co-application of TPMPA and pentobarbital (10 μM), R_i was decreased by 31%, from 238 ± 40 MΩ to 168 ± 33 MΩ (Figure. 3.4C; n = 4). In summary, pharmacological blockade of $GABA_C$ receptors produced no antagonism of the depressant effects of pentobarbital on MGB thalamocortical neurons.

3.1.2.6. Combined application of $GABA_A$, $GABA_B$, and $GABA_C$ antagonists

The effects of co-applied pentobarbital with picrotoxinin (50 μM), saclofen (200 μM) and TPMPA (20 μM) were determined, in order to verify that known GABA receptors did not mediate the pentobarbital-induced depression. Before applying the 3 antagonists in 3 neurons, application of pentobarbital (20 μM) induced a 33 ± 7% decrease in R_i. During co-application with the antagonists, pentobarbital decreased R_i by 31 ± 6 %. In summary, combined blockade of $GABA_A$, $GABA_B$, and $GABA_C$ receptors did not significantly alter the ability of pentobarbital to decrease R_i.

To identify whether pentobarbital-induced GABA independent action is nucleus specifiC, the effects of GABA receptor antagonists on pentobarbital-induced inhibition were examined in ventrobasal neurons. The procedures of these experiments were performed by the same way as previously in MGB neurons (see above). Bicuculline (n = 5), saclofen (n = 5), or TPMPA (n = 5), did not block pentobarbital-induced inhibition on neuronal firing and a decrease in R_i ($P>0.05$).

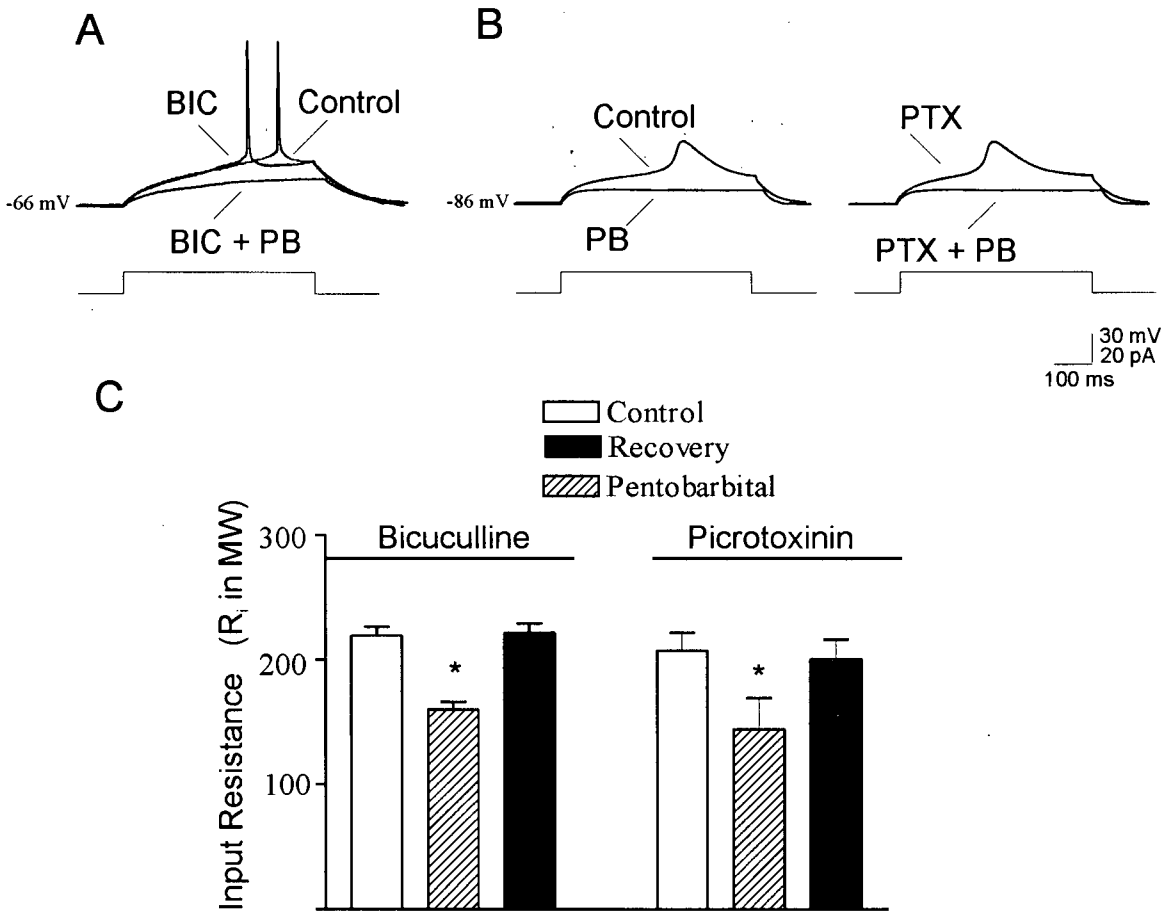

Figure. 3.3 $GABA_A$ antagonists, bicuculline and picrotoxinin, did not greatly affect the depressant effects of pentobarbital on MGB neurons. (A) Co-application with bicuculline (BIC; 100 μM) did not block the depressant effects induced by pentobarbital (PB; 10 μM) on evoked tonic firing. Bicuculline application, alone, caused a small leftward shift in the latency of evoked action potentials. Holding potential, -66 mV. (B) With TTX blockade of action potentials, pentobarbital (10 μM) depressed the low threshold spike (*left*). After recovery from pentobarbital, picrotoxinin (PTX; 50 μM) was applied for 4 min, followed by a co-application of picrotoxinin (50 μM; right). Under these conditions, pentobarbital still depressed low threshold spikes. Holding potential, -86 mV. (C) Summary of the depressant effects of pentobarbital (10 μM) on R_i during application of bicuculline (100 μM, n = 4) or picrotoxinin (50 μM, n = 3). * $P< 0.05$, significantly different from Control.

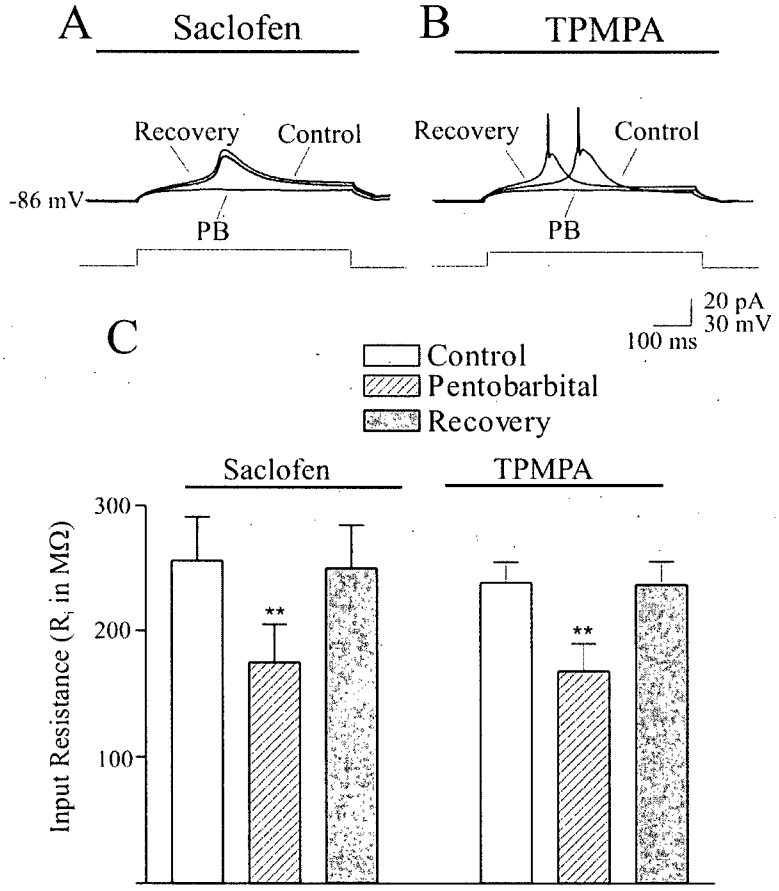

Figure. 3.4 Depressant effects of pentobarbital on MGB neurons are independent of $GABA_B$ and $GABA_C$ receptor activation. (A) Co-application of saclofen (200 μM) and pentobarbital (PB; 10 μM) depressed low threshold spike (TTX present). (B) With TPMPA (20 μM) present, pentobarbital (10 μM) depressed the low threshold spike and action potential. The recovery was obtained at 15 to 20 min after terminating the application of pentobarbital in A and B. Holding potential, -86 mV. (C) Summary of pentobarbital (10 μM)-evoked depression of input resistance during saclofen (200 μM, n = 5) or TPMPA (20 μM, n = 4) application. ** $P< 0.01$, significantly different from Control.

Co-application of $GABA_A$, $GABA_B$, and $GABA_C$ receptor antagonists as well did not block depressant effects of pentobarbital (n = 5). This indicated that pentobarbital-induced inhibition on neuronal firing and a decrease in membrane resistance, which is independent of GABA receptor, may not be nucleus specific in the thalamus.

Table 1. Membrane properties of neurons showing depressant or excitatory effects of pentobarbital.

	Neurons exhibiting depressant effects (n = 50, 76%)		Neurons exhibiting excitatory effects (n = 11, 17%)	
	Control	TTX	Control	TTX
R_i (MΩ)	204 ± 20	190 ± 22	276 ± 56	270 ± 54
R_{depol} (MΩ)	207 ± 25	152 ± 30*	283 ± 60	196 ± 59*
dV/dt of LTS (mV/ms)	2.0 ± 0.3	2.1 ± 0.4	1.4 ± 0.1	1.4 ± 0.1

R_i was obtained from hyperpolarizing voltage responses (5-8 mV) to current pulses. Input resistance in depolarizing direction (R_{depol}) was obtained from depolarizing voltage responses (5-8 mV) to current pulses. dV/dt was obtained from just-threshold LTS. The values are expressed as mean ± SE. Number of pooled MGB neurons and percentages of total are given in parentheses. * significantly different from Control, $P < 0.05$.

3.1.3. Actions of selective ion channel blockers

Pentobarbital inhibited neuronal firing, accompanied by a decrease in R_i with EC_{50}s = ~8 μM in thalamocortical neurons. These actions were independent of interactions with GABA receptors. To investigate the mechanisms underlying these actions, various ion channel

blockers were applied in another series of experiment to study interactions between pentobarbital and intrinsic ionic channels.

3.1.3.1. Neuronal firing and R_i

3.1.3.1.1. External Cs^+ blockade

The effects of co-applied 3 mM Cs^+ and pentobarbital (20 μM) were observed, in order to investigate the effects of blockade of hyperpolarization-activated inward rectifiers (Pape 1996) on neuronal firing and a decrease of R_i in 5 neurons. These experiments were performed during concomitant TTX application, to block voltage-dependent Na^+ conductance. TTX itself did not significantly alter R_i and membrane potential (c.f. Table 3.1).

Prior to co-application with Cs^+, pentobarbital induced a 29% decrease in R_i (control, 214 ± 20 MΩ and pentobarbital, 151 ± 16 MΩ, n = 6). Application of Cs^+ alone increased R_i by 71 % (control, 214 ± 20 MΩ and Cs^+, 368 ± 31 MΩ; n = 6; Figure. 3.5A). The neurons depolarized by 8 ± 4 mV (n = 5) during the application, presumably due to a decreased leak conductance. During co-application with Cs^+, the depressant effects of pentobarbital were not apparent (Cs^+, 368 ± 31 MΩ and Cs^+ + pentobarbital, 365 ± 34 MΩ; n = 6; Figure. 3.5A). Application of Cs^+ also greatly increased the slope of I-V relationship in the same 5 neurons in a membrane potential range of –65 to –100 mV (Figure. 3.5B). Co-application of Cs^+ and pentobarbital (20 μM) did not result in a further change in the slope (Figure. 3.5B). In summary, the depressant effects of pentobarbital on the input and slope resistances in the hyperpolarizing quadrant may be involved in an increase in conductances that were sensitive to Cs^+ blockade.

3.1.3.1.2. TTX blockade of action potentials

Before pentobarbital application, the relationships between current and voltage (I-V) for neurons exhibiting depressant responses were either approximately linear or S-shaped curves. In neurons with either I-V relationship, pentobarbital application resulted in an approximately linear relationship with a reduced slope. As in Figure 3.6A, a reduction in the slope of the relationship over a membrane voltage range from -90 mV to threshold (~-50 mV) were observed in 29 out of 31 neurons that were administered pentobarbital in concentrations ≥10 μM. The reversal potential for pentobarbital action, provided by the intersection of the control and pentobarbital curves (cf. Fig. 3.6A), was -74 ± 3.8 mV (n = 5). This value is close to the theoretical E_K, implying a K^+ involvement.

The I-V relationship did not greatly change during application of TTX to 46 neurons at membrane potentials hyperpolarized from rest. During TTX application, pentobarbital retained an ability to decrease the slope of the I-V relationship over a –90 to –65 mV range (Figure. 3.6B). Application of TTX reduced the apparent input resistance at depolarized potentials (Figure. 3.6B), presumably by eliminating a voltage-, Na^+-dependent type of rectification in this quadrant (Jahnsen and Llinas 1984; Tennigkeit et al., 1996). In the neuron of Figure. 3.6B, a co-application of TTX with pentobarbital did not result in a further decrease in the slope of the I-V relationship from –65 mV to –40 mV compared to TTX application alone. In this voltage range, there was a close superposition of the curves for TTX, alone, and co-application of TTX with pentobarbital in 15 out of 24 neurons. In this group of 15 neurons, the reversal potential for pentobarbital action was –79.1 ± 2.9 mV (n = 9). In the remaining 9 neurons, however, there was a significant decrease of 18 ± 7 % in the slope of the I-V relationship.

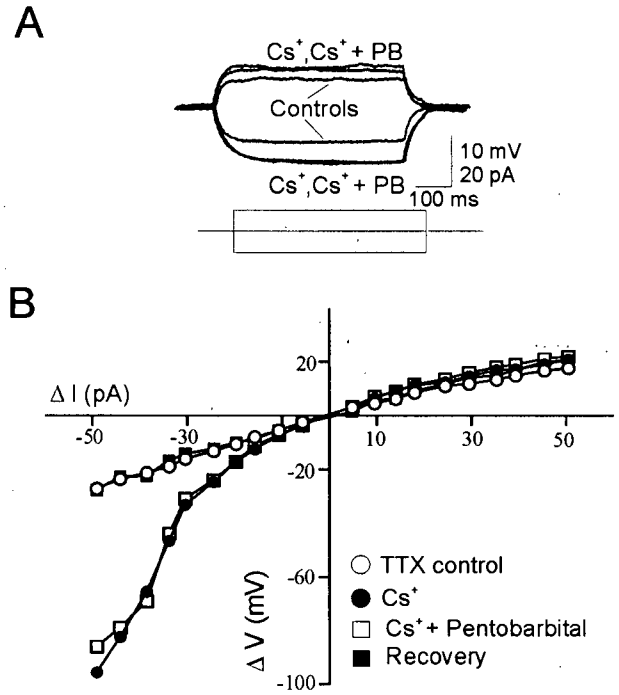

Figure 3.5. External Cs^+ blockade of pentobarbital effects on voltage responses and current-voltage relationships of a MGB neuron. (A) Superimposed hyperpolarizing and depolarizing responses to current pulses taken during control period, application of 3 mM Cs^+, and co-application of Cs^+ and pentobarbital. (B) Cs^+ significantly increased the slope of current-voltage relationship in the lower left quadrant while inducing a small increase in the slope in the upper right quadrant. Co-application of Cs^+ with pentobarbital did not induce changes additional to the effects of Cs^+ alone.

Consequently, an action of pentobarbital on TTX-insensitive forms of rectification (e.g., a K^+-rectifier) was apparent in the top right quadrant in the 9 neurons. In these neurons, the reversal potential for pentobarbital action was –74.3 ± 4.1 mV (n = 9). There was no significant difference in the reversal potentials between these two groups of neurons. These results indicated that TTX eliminated or partially blocked pentobarbital action in the depolarization quadrant.

3.1.3.2. Pentobarbital-induced current and intrinsic ion channel blockers

To further study intrinsic ionic mechanisms of pentobarbital action in thalamocortical neurons, whole-cell voltage clamp and selective ion channel blockers were applied in ventrobasal neurons. The aim of this series of experiments was to study ionic mechanisms underlying the low concentration of pentobarbital actions in thalamocortical neurons.

3.1.3.2.1. Pentobarbital induced an outward current

The effects of pentobarbital on membrane currents during TTX blockade of action potential activated neurotransmission were determined first. When measured at V_H = -60 mV, pentobarbital (8 μM, 6 min) reversibly induced a sustained outward current (Figure. 3.7A). The mean outward current induced by pentobarbital was 9 ± 2 pA (n = 10).

The effects of pentobarbital on I-V relationships, obtained with 10 mV hyperpolarizing step commands in 15 neurons, were determined. Inspection of the raw currents revealed both fast and slow activating forms of rectification, with little inactivation during the voltage commands (Figure. 3.7B). Pentobarbital affected both forms of rectification. Pentobarbital appeared to

prolong the slowly developing inward currents and increase the steady state currents, especially with the larger hyperpolarizing commands. The control steady-state currents exhibited an inwardly rectifying I-V relationship, evident at potentials more negative than -70 mV (Figure. 3.7C). Pentobarbital increased the slope conductance between -50 and -140 mV and net inward rectification at voltages between -76 and -140 mV. In this voltage range, pentobarbital-induced inward current (I_{PB}) that was evident from subtraction of the currents obtained during control and pentobarbital application (Figure. 3.7C). In the neuron of Figure 3.7C, I_{PB} reversed to an outward current at -76 mV. The average reversal potential for I_{PB} was -75 ± 4 mV (n = 15). This implied more than one ion species in pentobarbital action, with a major contribution by K^+ (E_K = -84 mV). It was evident that pentobarbital, despite increasing slope conductance, differentially affected rectifying currents activated at hyperpolarized potentials (Figure. 3.7B).

3.1.3.2.2. Cs^+ blockade of rectifying and leak conductances eliminated I_{PB}

The interaction of pentobarbital with extracellular Cs^+ which reversibly blocks hyperpolarization-activated rectifiers, I_h and I_{Kir}, as well as leak current, I_{leak}, in thalamocortical neurons, was examined (Larkman and Kelly, 2001; Williams et al., 1997). Application of Cs^+ (3 mM) induced an inward current (Figure. 3.8A) that averaged 2 ± 0.4 pA in 5 neurons held at -60 mV. When co-applied with Cs^+, pentobarbital (8 μM) did not induce a further change in this current (Figure 3.8A; n = 5). During co-application with Cs^+, pentobarbital produced no change in the I-V relationship (Figure. 3.8B). Alone, Cs^+ greatly reduced the slope conductance between -90 and -140 mV, consistent with substantial blockade of K^+ channel-related rectification.

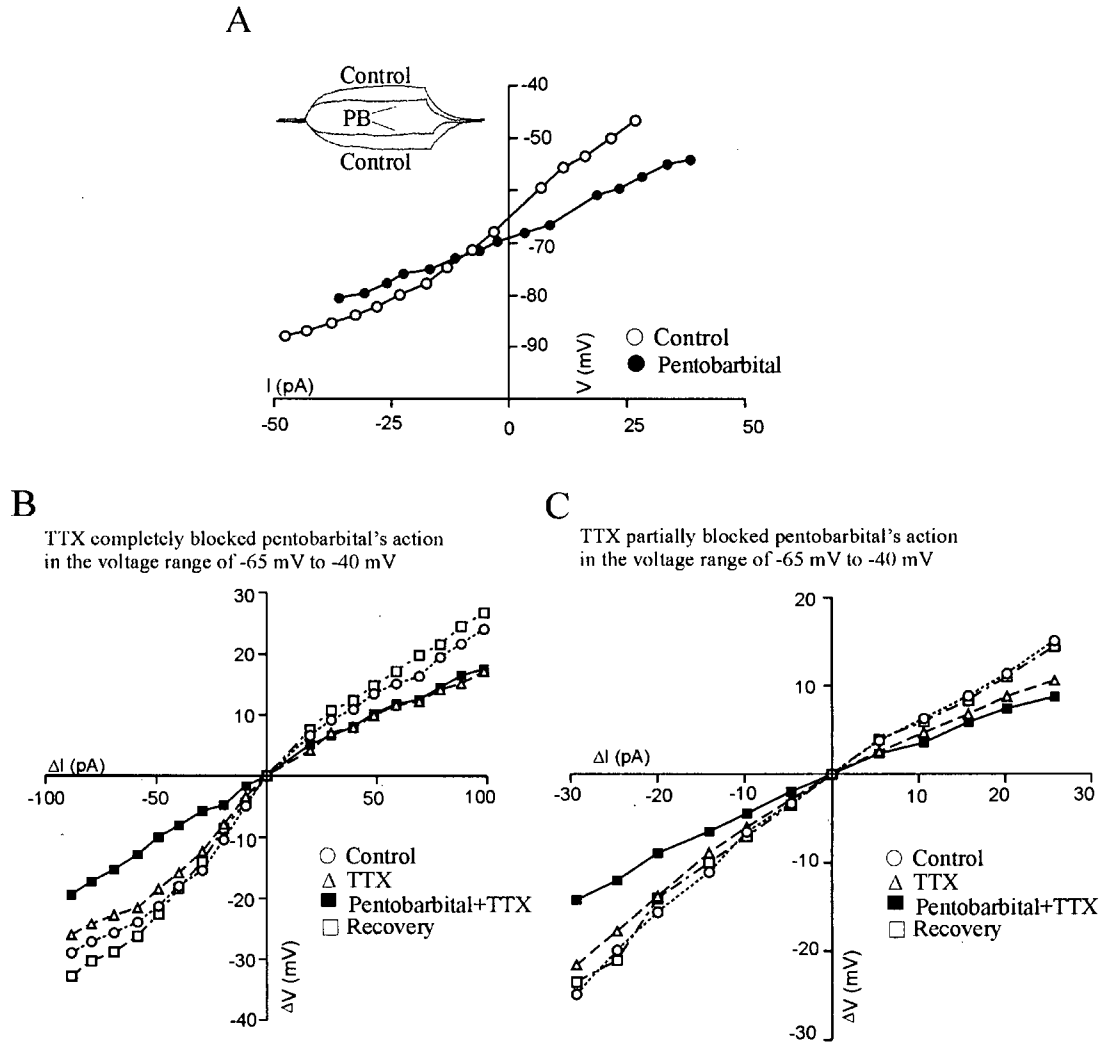

Figure 3.6. Changes in current-voltage relationship produced by pentobarbital and TTX-blockade of Na^+-dependent rectification in MGB neurons. (A) Pentobarbital (20 μM) decreased the resistance, resulting in an approximately linear relationship between current input and voltage response. The reversal potential for pentobarbital action, provided by the intersection of the control and pentobarbital curves, was -72 mV. Membrane potential, -66 mV. Inset shows superimposed depolarizing and hyperpolarizing responses (5-10 mV) to current pulses taken during a control period and application of pentobarbital (PB). (B) During TTX-blockade, pentobarbital (20 μM) decreased slope resistance only in the lower left quadrant in 15 out of 24 neurons. Membrane potential, -67 mV. (C) During TTX-blockade in the remaining 9 out of 24 neurons, pentobarbital (20 μM) decreased slope resistance in lower left and upper right quadrants. Membrane potential, -66 mV.

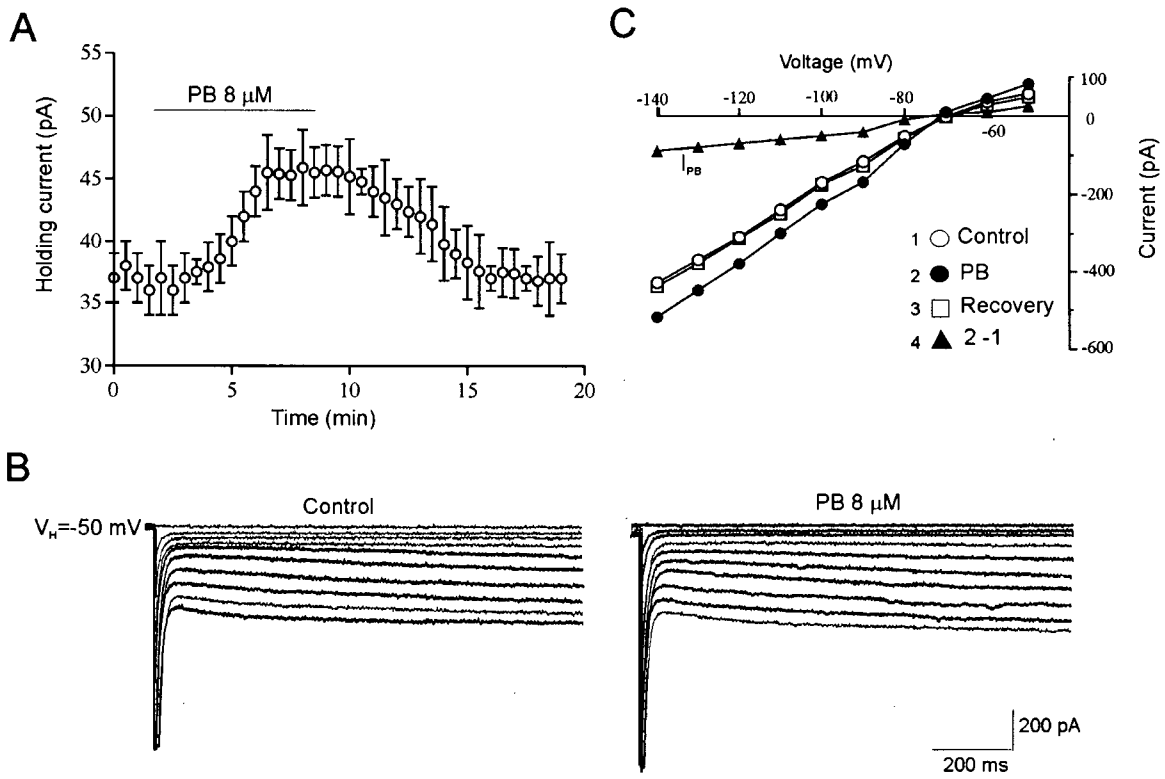

Figure 3.7. Pentobarbital (PB) increases outward current and slope conductance. (A) Time course of the changes in holding current (V_H = -60 mV) caused by PB (8 μM) in the presence of TTX. Data were averaged from 10 neurons. (B) Currents obtained using hyperpolarizing commands (1 s duration, 10 mV) from -50 mV to -140 mV, before and during PB application. (C) Steady-state I-V curves were constructed before (Control), during PB (8 μM) and recovery (15 min). PB increased the slope of the I-V relationship, which intersected with the control curve at -76 mV. The PB induced current (I_{PB}) was obtained by subtracting control currents from those during PB application and is shown in curve labelled 2-1, which reversed polarity at -76 mV.

Subtraction of the currents evoked under control and Cs^+ conditions revealed an inward current that was >250 pA at V_H = -140 mV and reversed in polarity at -80 mV (Figure. 3.8C). This represented the Cs^+-sensitive current. Subtraction of the currents evoked during application of Cs^+ from Cs^+ with pentobarbital showed that pentobarbital did not elicit significant changes in current over the voltage range of -50 to -140 mV (Figure. 3.8C). These data implicate an involvement of hyperpolarization-activated rectifying Na^+-K^+ dependent I_h currents in I_{PB} at potentials negative to -80 mV, and a small net outward current at potentials positive to -80 mV. Given the observed elimination of I_{PB} by Cs^+, we proceeded to investigate the role of specific rectifiers in the pentobarbital response.

3.1.3.2.3. ZD-7288 blockade of hyperpolarization activated inward I_h current reduced I_{PB}

The effects of ZD-7288 on I_{PB} were determined, in order to assess an involvement of the inward Na^+/K^+ rectifier, I_h. ZD-7288 at 10-25 μM selectively and irreversibly blocks I_h (Larkman and Kelly, 2001; Williams et al., 1997).

ZD-7288 application (25 μM) to four neurons clamped at V_H = -60 mV induced an outward current (7 ± 2 pA) and completely blocked I_h. In the neuron of Figure 3.9A, co-application of pentobarbital (8 μM) and ZD-7288 produced ~40% less net outward current than the control I_{PB}. Inspection of the current evoked by stepping from V_H = -50 to -140 mV revealed that pentobarbital inhibited an I_h like current, characterized by slow activation and little or no inactivation (Figure. 3.9B). Figure 3.9C shows the effects of pentobarbital and ZD-7288 interaction on the steady-state I-V relationship. ZD-7288 decreased the net inward current between -80 and -140 mV (Figure. 3.9C). Before ZD-7288 application, the reversal potential for I_{PB} was -77 mV in this neuron. Co-application of ZD-7288 with pentobarbital yielded an I-

V relationship which intersected with the ZD-7288 curve at -86 mV (Figure. 3.9C, arrow). The mean hyperpolarizing shift in reversal potential for I_{PB} during ZD-7288 application was 9 ± 1 mV (n = 4). The mean reversal potential of ZD-7288-sensitive current estimated by extrapolation was -40 ± 2 mV (n = 4). The characteristics of the ZD-7288-sensitive current were consistent with known properties of I_h (McCormick and Pape, 1990; Williams et al., 1997; Pape, 1996). Subtraction of the currents during ZD-7288 application and co-application with pentobarbital yielded a ZD-7288-insensitive current which represented voltage-dependent and -independent components of pentobarbital action with a reversal potential near -86 mV (Figure. 3.9D). During the blockade of I_h by ZD-7288, pentobarbital increased the fast activating, leak subtracted currents between V_H = -50 and -100 mV (Figure. 3.9E), presumably attributable to the inward K^+ rectifier, I_{Kir}. These results indicated that the outward current induced by pentobarbital was partially due to blocking I_h.

3.1.3.2.4. Ba^{2+} blockade of I_{Kir} and I_{leak} reduced I_{PB}

The effects of 2 mM extracellular Ba^{2+} on I_{PB} were examined to further assess involvement of I_{Kir} and I_{leak}, which Ba^{2+} blocks in ventrobasal thalamic neurons (McCormick and Pape, 1990; Pape, 1996; Willams et al., 1997). Ba^{2+} application to neurons clamped at V_H = -60 mV induced an inward current (14 ± 4 pA, n = 6). As shown in Figure. 3.10A, co-application with Ba^{2+} reduced I_{PB} by ~45 %. In 6 neurons, a mean reduction of 48 ± 4 % were observed. In the neuron of Figure 3.10B, the magnitude of current evoked by stepping from V_H = -50 mV to -140 mV was significantly increased on application of pentobarbital. Alone, Ba^{2+} decreased the slope conductance in the I-V relationship between -50 and -140 mV. When co-applied with pentobarbital, Ba^{2+} reduced the magnitude of the evoked net inward currents, as well as the net inward currents induced by pentobarbital (Figure. 3.10B).

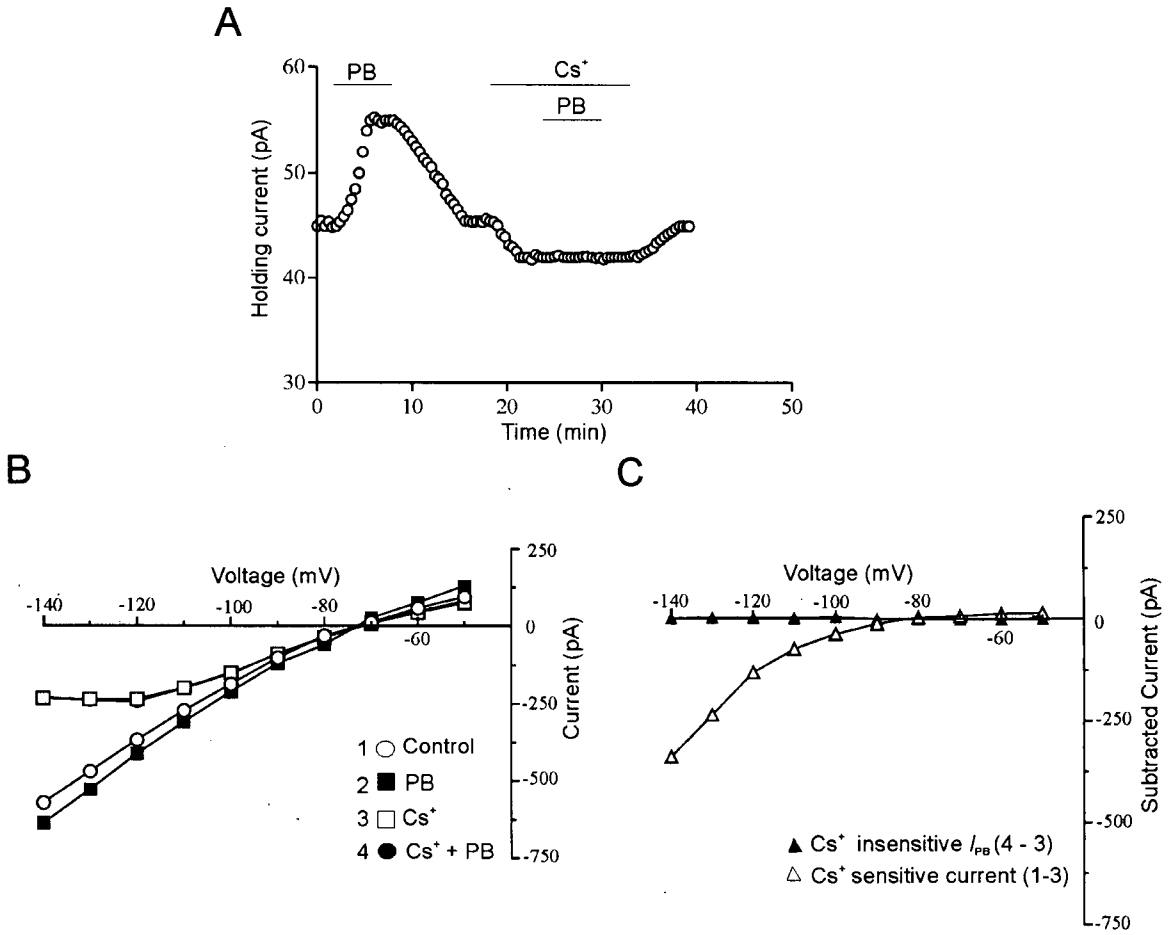

Figure 3. 8. Cs^+ blocked PB induced effects on membrane current. (A) PB (8 μM) induced outward current which was completely and reversibly blocked by co-application of Cs^+ (3 mM). V_H = –60 mV. (B) Steady-state I-V curves obtained using -10 mV command steps in a neuron from V_H = -50 mV. The curves were obtained during control, PB (8 μM), Cs^+ (3 mM) and co-application of PB and Cs^+. (C) The Cs^+ sensitive current was obtained by subtracting the current during Cs^+ application from control current. The Cs^+ insensitive I_{PB} was obtained by subtracting the current during Cs^+ from that during co-application of Cs^+ and PB.

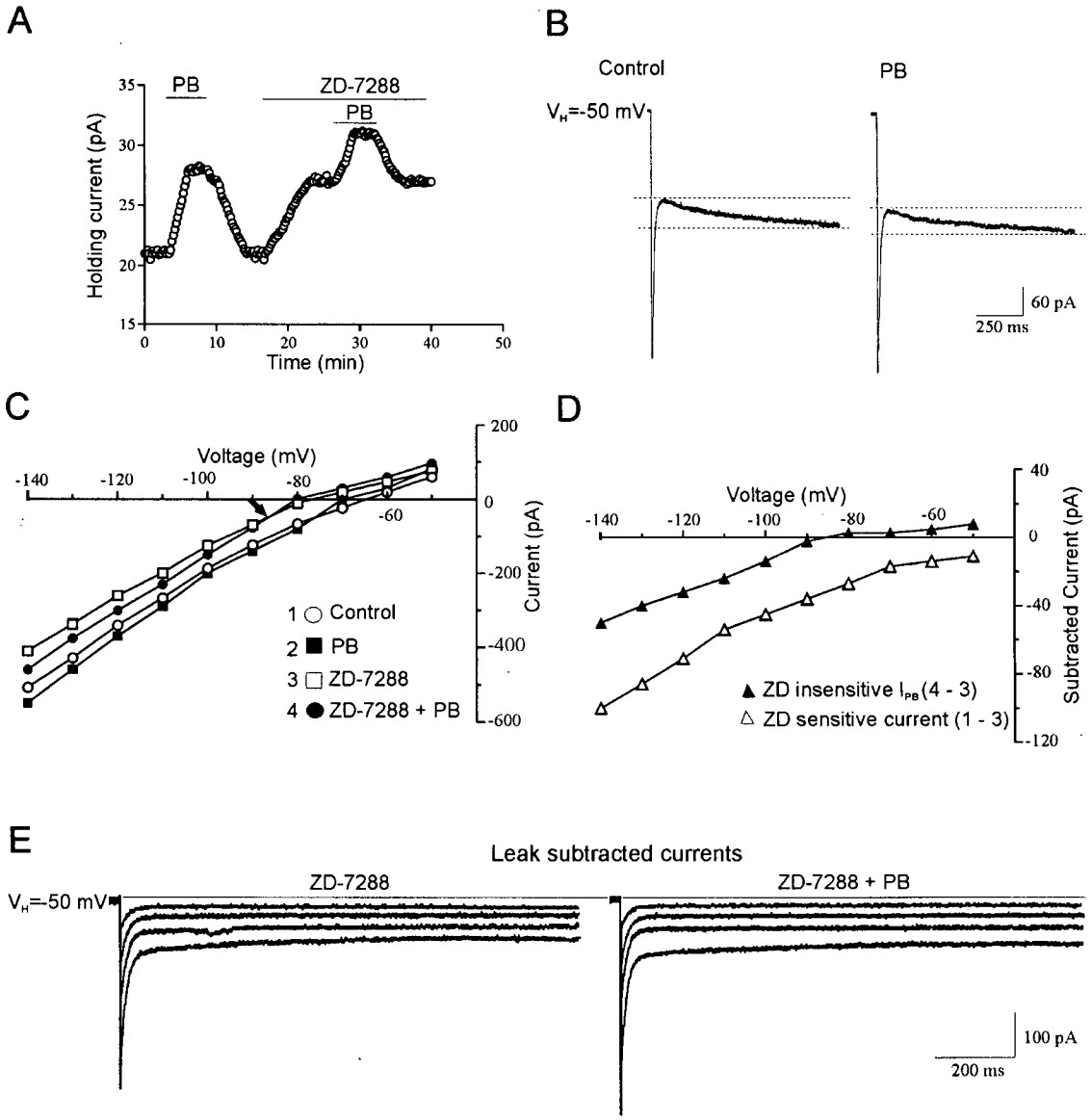

Figure 3.9. ZD-7288 reduced effects of PB on membrane currents. (A) Changes in holding current induced by PB (8 μM) were partially blocked by co-application with ZD-7288 (25 μM). V_H = -60 mV. (B) Currents evoked by hyperpolarizing steps from V_H = -50 mV to -140 mV, before and during PB (8 μM). Note that the I_h like current was inhibited by PB application. (C) Steady-state I-V curves were obtained by hyperpolarizing steps (1 s duration) from V_H = -50 mV during PB (8 μM), ZD-7288 (25 μM) and co-application of PB and ZD-7288. Note that the intersection between control and PB curves shifted from -77 to -86 mV (solid arrow) during ZD-7288. (D) The ZD sensitive current was obtained by subtracting the ZD-7288 current from control. The ZD insensitive I_{PB} was obtained by subtracting the ZD-7288 current from that during co-application of ZD-7288 and PB. (E) Leak subtracted currents were obtained during application of ZD-7288 and co-application with PB. Currents were evoked by voltage steps (1 s duration) from V_H= -50 mV to -70, -80, -90 and -100 mV. Note PB increased leak subtracted inward current during ZD-7288, presumably due to activation of I_{Kir}.

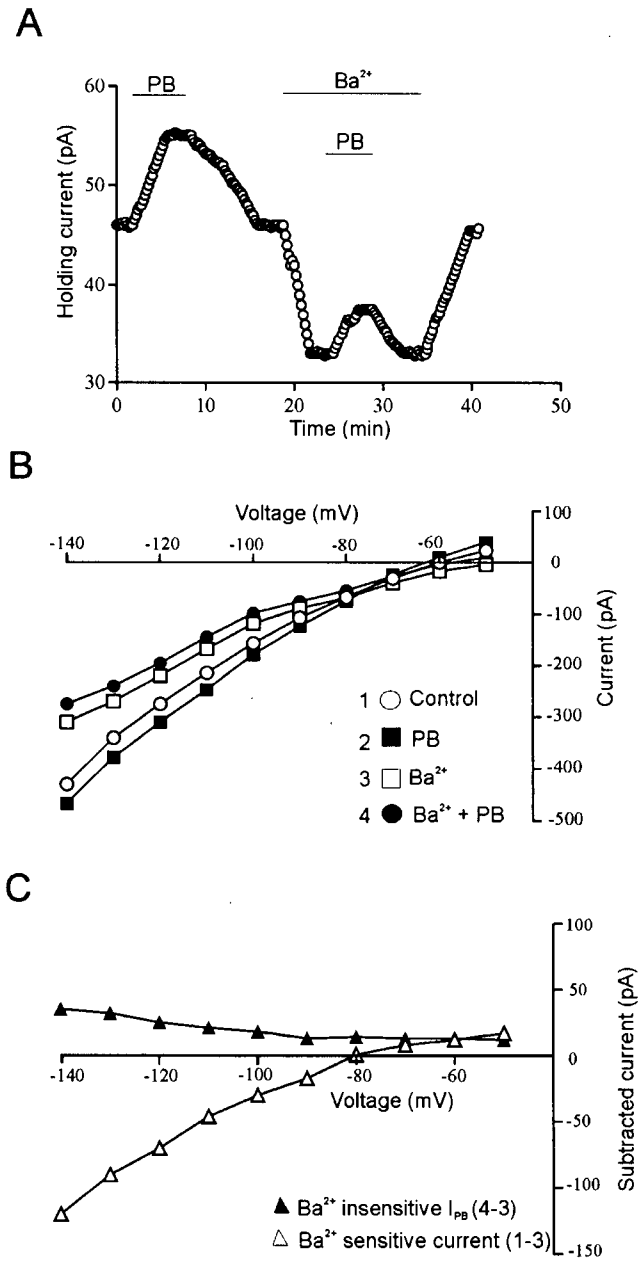

Figure 3.10. Ba^{2+} reduced effects of PB on membrane currents. (A) PB (8 μM) induced an outward current which reversibly decreased during co-application with Ba^{2+} (2 mM). V_H = -60 mV. (B) Steady-state I-V curves obtained by hyperpolarizing voltage steps (1 s duration) from V_H = -50 mV during control, PB (8 μM), Ba^{2+} (2 mM), and co-application of PB and Ba^{2+}. (C) The Ba^{2+} sensitive current was obtained by subtracting the Ba^{2+} and control currents. The Ba^{2+} insensitive I_{PB} was obtained by subtracting the currents during Ba^{2+} and co-application of Ba^{2+} and PB.

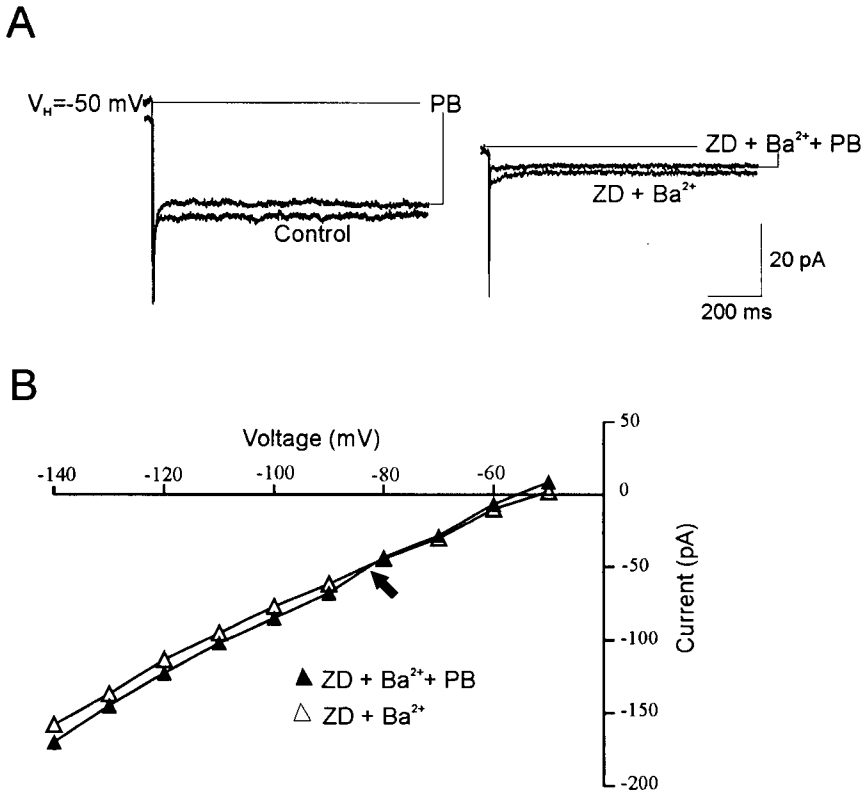

Figure 3.11. PB increased I_{leak} (A) Currents were measured in a neuron during the command step from -50 mV to -60 mV. PB (8 μM) caused an increase in the outward holding current, evident as a shift at V_H = -50 mV. The voltage command evoked more outward current during PB application. Co-application of Ba^{2+} (2 mM) and ZD-7288 (25 μM) decreased the outward holding current, as well as the current responses to hyperpolarizing commands (right), compared to control (left). PB produced a smaller shift in outward current during co-application with Ba^{2+} and ZD-7288 (right, upper trace), compared to PB alone (left). (B) Steady-state I-V curves obtained by hyperpolarizing steps (1 s duration) from V_H = -50 mV during co-application of ZD-7288 and Ba^{2+}, and combined application of PB, Ba^{2+} and PB. The arrow indicates the reversal potential for I_{PB} which was -82 mV.

Subtraction of Ba^{2+} and control currents showed the Ba^{2+}-sensitive current (Figure. 3.10C). These experiments demonstrated a probable contribution of I_{Kir} and I_{leak} to I_{PB}. The Ba^{2+}-insensitive current reflected a summation of pentobarbital actions on I_h and I_{leak} (Figure. 3.10C). Hence, it was of interest to isolate the effect of pentobarbital on I_{leak} that was insensitive to Ba^{2+}. To do this, ventrobasal neurons were held at -50 mV where there may be small contribution of I_h (cf. Figure. 3.9). In the neuron of Figure 3.11A (left), pentobarbital application decreased the magnitude of the inward current evoked by stepping from V_H = -50 to -60 mV. During Ba^{2+} and ZD-7288 blockade of both I_{Kir} and I_h, pentobarbital produced a smaller decrease in the magnitude of the inward current, representing residual I_{leak} in the same neuron (Figure. 3.11A, right). This smaller increase, compared to that evoked by pentobarbital alone, is attributable to partial blockade of I_{leak} by Ba^{2+}. Figure 3.11B shows that the I-V relationship is approximately linear over a wide range during application of ZD-7288 and Ba^{2+}. In the neuron of Figure 3.11B, pentobarbital increased the magnitude of this leak current which reversed at -82 mV, close to E_K (mean, -83 ± 1.5 mV; n = 4). These results implied that pentobarbital activated Ba^{2+} sensitive and Ba^{2+}-insensitive I_{leak}.

3.1.3.2.5. Co-application of ZD-7288 and Ba^{2+} and outward currents

Figure 3.12A summarizes the interactions of ion channel blockers with I_{PB}, showing the total blockade of I_{PB} by Cs^+ and partial reductions of I_{PB} by ZD-7288 and Ba^{2+} at V_H = -60 mV. ZD-7288 and Ba^{2+} each resulted in <50% reduction in I_{PB} (ZD-7288, 39 ± 4%, n = 7; Ba^{2+}, 48 ± 5%, n = 6) whereas when applied in combination, they decreased I_{PB} by 87% of control (87 ± 4 %, n = 4). The residual, outward current observed during ZD-7288 and Ba^{2+} application (cf. Fig. 3.11B) likely represented Ba^{2+} insensitive I_{leak}, eliminated by Cs^+. Figure 3.12B shows the concentration-response relationship for the actions of pentobarbital on the normalized input

conductance, which includes conductances for I_h, I_{Kir} and I_{leak}. Pentobarbital effects on input conductance spanned more than two log concentration units. Note that appreciable increases in conductance occurred at pentobarbital concentrations that were below 10 μM, whereas response saturation was evident at 100-200 μM. The shallow concentration-response relationship is consistent with pentobarbital actions on multiple membrane currents.

3.1.4. *Excitatory actions in minority of MGB and ventrobasal neurons*

In 11 of the 66 MGB neurons and 4 of 47 ventrobasal neurons, application of pentobarbital (0.1-50 μM) produced excitatory effects. The number of excited neurons was too small for a systematic comparison with the 50 neurons that exhibited depressant responses to pentobarbital application

3.1.4.1. Neuronal firing

The excitation induced by pentobarbital in MGB and VB neurons consisted of an increased action potential discharge in the tonic and burst patterns evoked by current pulses (Figure. 3.13A). In 5 of 15 neurons, there were a greater number of action potentials following an evoked burst. Pentobarbital (20 μM) decreased the current requirement for evoking a LTS and increased its rate of rise and amplitude. TTX-blockade of Na^+-conductances did not greatly alter pentobarbital-induced effects on the LTS (Figure. 3.13A).

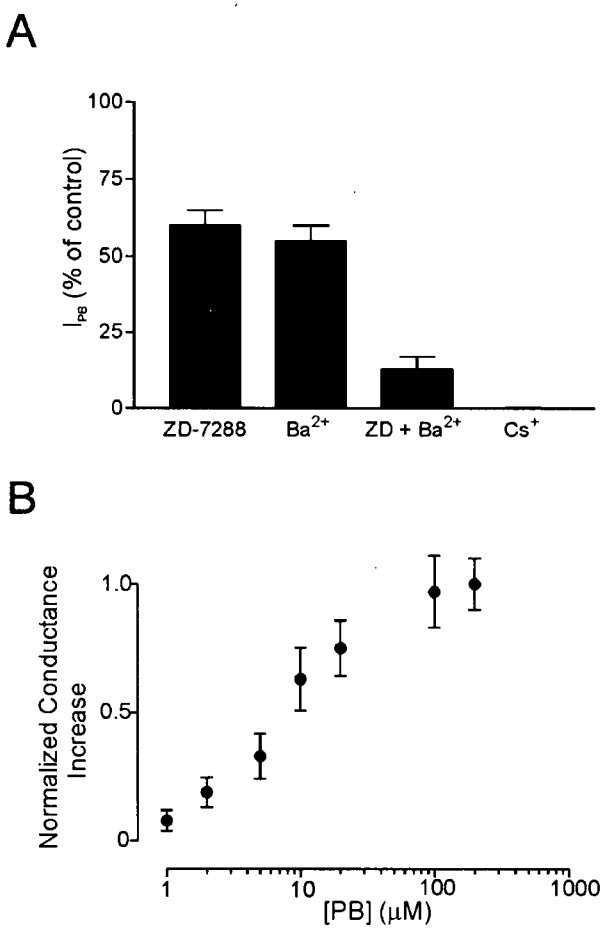

Figure 3.12. Summary of PB-induced changes in holding currents during ion channel blockade and concentration-dependent increase of input conductance. (A) The outward current (I_{PB}) evoked by PB (8 μM) during ZD-7288 (25 μM), Ba^{2+} (2 mM), and Cs^{+} (3 mM) is expressed as a percentage of current evoked by PB alone (% of control) in neurons at V_H = -60 mV. In each case, there was a significant reduction in the outward current ($P < 0.05$). The effect of co-application of ZD-7288 and Ba^{2+} was significantly greater than the effect of either blocker ($P < 0.01$). The effect of Cs^{+} was significantly greater than application of ZD-7288 or Ba^{2+} alone ($P < 0.01$). The data were obtained from 5 to 7 cells in each condition. (B) PB increased input conductance in a concentration range from 1 to 200 μM and had an apparent EC_{50} = ~8 ± 0.5 μM. Input conductance was determined from small hyperpolarizing responses to current pulse injection from neurons at V_H = -50 mV and normalized to maximal effect induced by PB.

3.1.4.2. Alteration on membrane conductance concomitant with excitation

The alteration of membrane conductance were examined during pentobarbital excitation. Pentobarbital induced reversible excitatory effects that included a small depolarization and increased R_i, measured with hyperpolarizing pulses (see Methods). At 20 μM, pentobarbital produced 3 ± 1 mV depolarization and a 22 ± 4% increase in R_i (n = 3). Pentobarbital also increased the slope resistance in 4 neurons at subthreshold potential values (Figure. 3.13C). The higher resistance reduced the threshold and increased the tonic firing.

The pentobarbital-induced increase in input and slope resistances, measured with depolarizing current pulses, was not evident after TTX-blockade of Na^+-dependent action potentials and rectification. Application of TTX, alone, produced a 32 ± 5 % decrease in input resistance, measured with 5-8 mV depolarizing current pulses (n = 7). This decrease was attributable to a TTX-blockade of a voltage-dependent Na^+-conductance (Crill 1996). Prior to TTX-blockade, pentobarbital evoked a 30 ± 3 % increase in R_i, measured with depolarizing current pulses (n = 4). During TTX application, pentobarbital had no significant effects on resistance measured with depolarizing pulses. In contrast, co-application with TTX did not significantly affect the pentobarbital-induced increase in R_i (26 ± 6 %; n = 7) or slope resistance, measured with hyperpolarizing pulses (Figure. 3.13D). Hence, TTX-blockade of Na^+-dependent rectification appeared to nullify the ability of pentobarbital to increase membrane resistance at potentials depolarized from rest.

3.1.4.3. Concentration-response relationship

Figure 3.13B shows the concentration-response relationship of pentobarbital for the 15 neurons that showed increases in R_i, due to pentobarbital application. Recovery was complete in 11 out

of 15 neurons at 20 to 25 min after discontinuing the application. In cumulative concentration-response studies on 9 neurons, pentobarbital application produced a reversible, biphasic response in 3 neurons. These were concentration-dependent (1-50 μM), consisting of 10-15 min of enhanced tonic or burst firing, a decreased R_i, and subsequent ~5 min reductions in the evoked firing and R_i. In summary, pentobarbital induced excitation in a small number of thalamic neurons in a concentration-dependent manner.

3.1.5. Synaptic neurotransmission in VB neurons

To study pentobarbital actions on cortico-thalamocortical synaptic transmission, nRT neurons were electrically stimulated and IPSPs or IPSCs were recorded in VB neurons. EPSPs recorded in VB neurons were evoked by electrical stimulation of the internal capsule.

3.1.5.1. Thalamocortical IPSC amplitude and decay

Before quantifying the effects of PB on IPSCs, the components of IPSCs were examined, which were evoked by stimulation of nRT axons, using antagonists of $GABA_A$ and $GABA_B$ receptor subtypes (Kao and Coulter, 1997). The contributions of glutamatergic excitatory postsynaptic currents (EPSCs) were eliminated by co-applying APV (50 μM) and CNQX (20 μM), antagonists of NMDA and non-NMDA receptors, respectively.

The isolated IPSCs had fast and slow inward components at V_H near -70 mV. At V_H = -40 mV, application of 2-hydroxysaclofen (200 μM), a $GABA_B$ receptor antagonist, blocked a slow component, revealing a fast outward IPSC (Figure. 3.14A). The fast IPSC reversed to an inward current at E_{Cl} = -55 mV (n = 7).

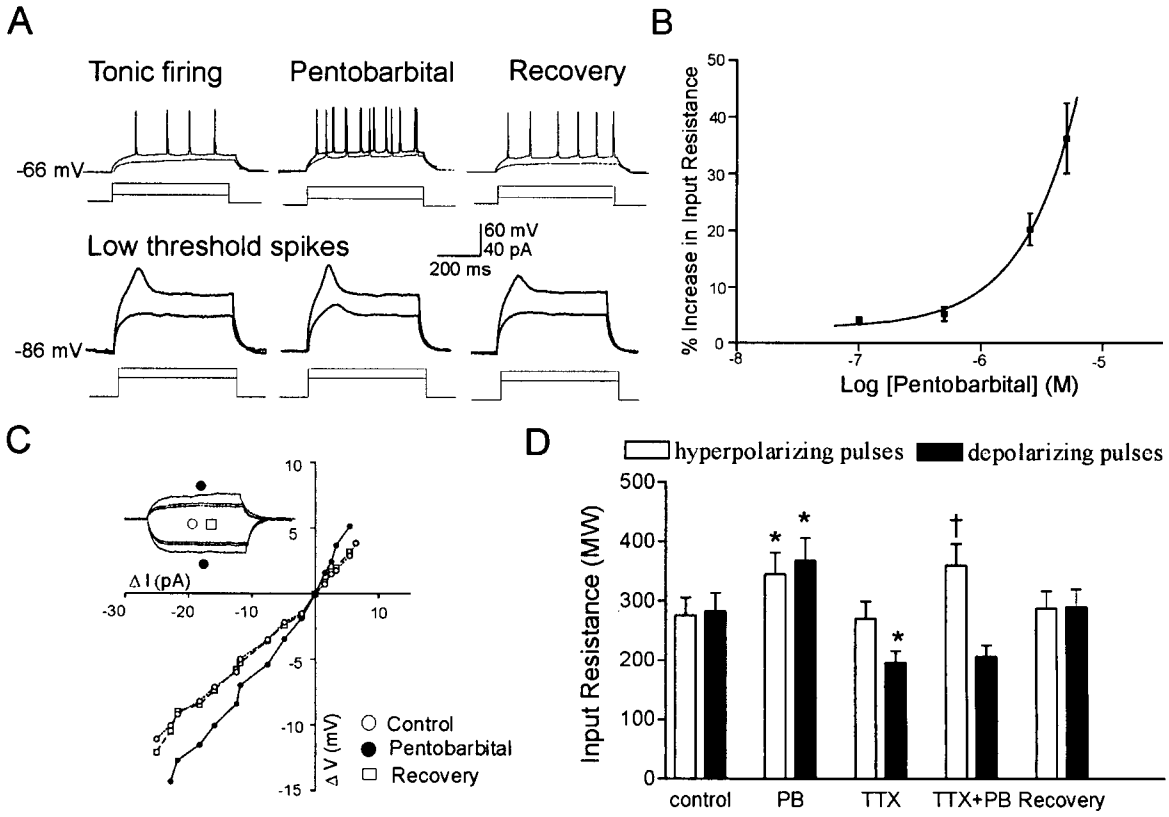

Figure 3.13. Excitatory effects of pentobarbital application in MGB neurons. (A) Rate of tonic firing and the rate of rise and amplitude of the LTS are increased during pentobarbital application (20 μM). Lower traces show that the current pulse amplitude which was "just-threshold" evoked a LTS during pentobarbital application. Holding potential in tonic firing record, –66 mV. Holding potential in LTS record, –86 mV. Recovery was observed at 15-20 min after discontinuing pentobarbital application. (B) Pentobarbital, induced a concentration-dependent increase in R_i in the concentration range of 0.1 to 50 μM. The increase was calculated as a percentage of the averaged control values. The relationship was fitted with a sigmoidal function. (C) Pentobarbital (20 μM) increased slope resistance in the relationship of injected current to voltage response. Recovery was observed at 15-20 min after discontinuing pentobarbital application. Inset of C shows superimposed hyperpolarizing and depolarizing responses (5-10 mV) to current pulses taken during a control period and application of pentobarbital, as well as during recovery. Membrane potential, -65 mV. (D) Summary of excitatory effects of pentobarbital (PB; 20 μM, n = 6) on the input resistance obtained from depolarizing or hyperpolarizing responses (8 mV), with or without TTX. * $P< 0.05$, significantly different from Control. † $P< 0.05$, significantly different from TTX.

Application of picrotoxinin (50 μM, n = 4) or bicuculline (50 μM; n = 3) greatly reduced the fast component, leaving a slow outward IPSC component measured at a V_H = -40 mV (Figure. 3.14B). The slow IPSC reversed to an inward current at V_H = -80 mV, close to E_K (n = 4). Co-application of bicuculline (50 μM) and 2-hydroxysaclofen (200 μM) eliminated the IPSC (not shown, n = 10). The data provided confirmation that $GABA_A$ and $GABA_B$ receptors respectively mediated all fast and slow IPSC components and we deduced that no $GABA_C$ response was present.

Pentobarbital (50 μM) had little effect on the IPSC amplitude, but prolonged the decay of the fast component, isolated with 2-hydroxysaclofen (Figure. 3.15A). During $GABA_A$ receptor blockade with bicuculline or picrotoxinin (Figure. 3.15B), pentobarbital did not affect the IPSC amplitude (control amplitude, 10 ± 2 pA; 50 μM PB, 9.7 ± 2 pA; n = 7) or duration of the slow component (control duration, 204 ± 30 ms; 50 μM PB, 210 ± 36 ms; n = 7). These data indicated that pentobarbital potentiated $GABA_A$ergic inhibitory neurotransmission.

3.1.5.2. Concentration-responses for IPSC decay prolongation

The effects of pentobarbital on the decay of fast IPSCs were quantified with and without blockade by 2-hydroxysaclofen. These neurons were voltage-clamped at V_H = -80 mV, in order to reduce a K^+ channel-related contribution. The averaged IPSC decay phases were fitted with a single exponential function (Figure. 3.15C). Pentobarbital prolonged the decay time constant (τ_{decay}) while producing no significant changes in amplitude of IPSCs (Figure. 3.15C). In contrast to the PB effects on input conductance, the concentrations of pentobarbital below

10 μM had negligible effects on τ_{decay}. Pentobarbital acted in a concentration-dependent manner with an EC_{50} of 53 ± 4 μM (n = 16; Figure.3.15D).

3.1.5.3. $GABA_A$ receptor mediation

The effects of pentobarbital on τ_{decay} were likely attributable to interactions at $GABA_A$ receptors. Co-application of pentobarbital and $GABA_A$ receptor antagonist, bicuculline or picrotoxinin, did not result in prolongation of IPSC decay. In summary, pentobarbital potentiated $GABA_A$ergic IPSCs by prolonging τ_{decay} in a concentration-dependent manner.

3.1.5.4. Action on EPSP amplitude and duration

Due to problems in clamping EPSCs, the effects of pentobarbital on corticothalamic EPSPs were examined, which were evoked by electrical stimulation of the internal capsule and recorded them in ventrobasal neurons (Figure. 3.16). The evoked potentials occasionally had a biphasic configuration. In such cases, application of picrotoxinin (50 μM) and 2-hydroxysaclofen (200 μM) eliminated the second, negative-going phase which resulted in a monophasic depolarizing potential. In all neurons, application of these GABA receptor antagonists increased the amplitude of the monophasic depolarizing potential, evidently an EPSP (Figure. 3.16A). After GABA receptor blockade, pentobarbital decreased the amplitude of EPSPs (Figure. 3.16A).

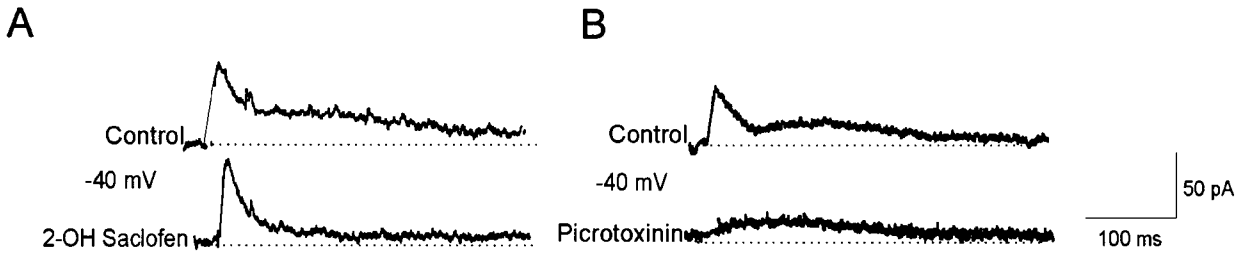

Figure 3.14. Thalamocortical IPSCs were identified by selective receptor antagonists. (A) 2-hydroxysaclofen (2-OH Saclofen, 200 μM) eliminated a slow IPSC component visible in control, isolating fast component in the neuron at V_H = -40 mV. (B) $GABA_A$ receptor antagonist, picrotoxinin (100 μM) in the neuron at V_H = -40 mV completely blocked a fast IPSC component, isolating slow IPSC component.

As expected (Goldshani et al. 1998), the corticothalamic EPSPs were glutamatergic and had NMDA and non-NMDA receptor mediated components, as demonstrated by their complete blockade on co-application of the glutamate receptor antagonists, APV and CNQX. The non-NMDA component during GABA receptor blockade was isolated by application of APV (50 μM), which slightly reduced EPSP amplitude. Pentobarbital (50 μM) significantly decreased the amplitude of EPSPs but did not alter EPSP duration (Figure 3.16A). This depression was reversible after the 15 min termination of pentobarbital application (Figure. 3.16A).

3.1.5.5. Concentration-responses of EPSP amplitude suppression

Pentobarbital decreased corticothalamic EPSP amplitude in a concentration-dependent manner with an IC_{50} of 36 ± 5 μM (Figure. 3.16B; n = 15). This IC_{50} was significantly higher than the IC_{50} of pentobarbital action to decrease input resistance (n = 5; $P<0.05$). This implied that the decrease on membrane resistance by pentobarbital may not account for the suppression of EPSP amplitude.

3.1.5.6. Non-NMDA receptor mediation

Selective glutamate receptor subtype antagonists were applied to determine the mechanism of pentobarbital-induced depression on EPSP amplitude. In the presence of APV (50 μM; Figure 3.16B), pentobarbital application (50 μM) decreased the amplitude of the remaining non-NMDA component (control: 8.5 ± 1.8 mV; pentobarbital: 5.5 ± 1.5 mV; $P<0.01$; n = 5) but did not significantly alter its duration (control: 95 ± 5 ms; pentobarbital: 93 ± 7 ms; $P>0.05$, n = 5).

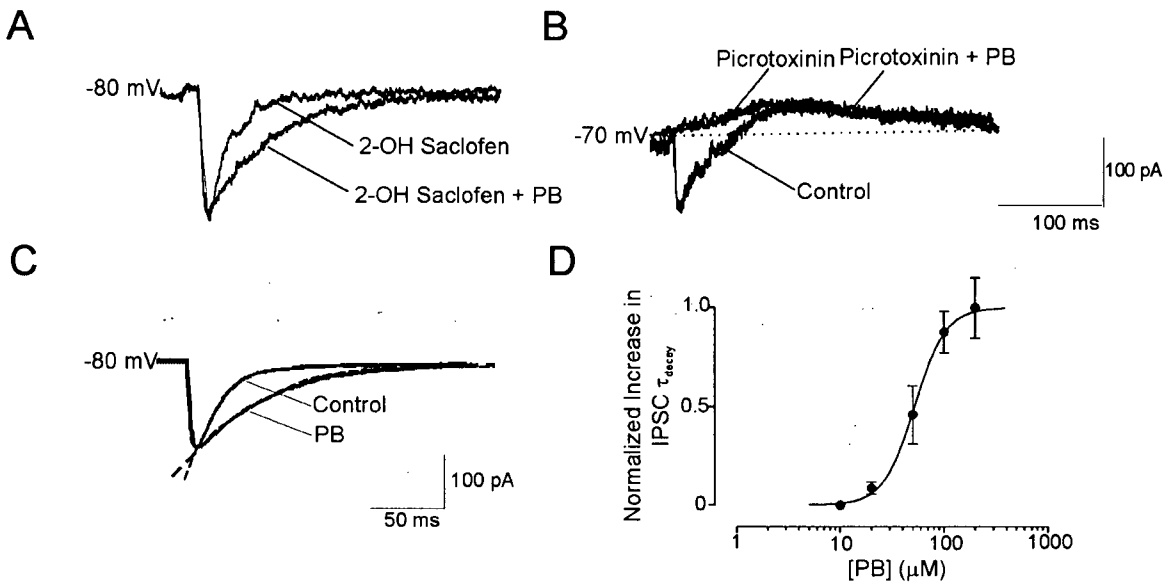

Figure 3.15. Pentobarbital potentiated $GABA_A$ergic IPSCs in ventrobasal neurons. (A) During $GABA_B$ receptor blockade by 2-OH Saclofen (200 μM), PB (50 μM) greatly prolonged fast IPSC component. (B) During $GABA_A$ receptor blockade by picrotoxinin (50 μM), PB (50 μM) did not alter the slow IPSC component. (C) IPSC decay time was fitted with single exponential in control and PB application to obtain τ_{decay}. (D) PB increased IPSC decay time constant (τ_{decay}) in a concentration-dependent manner with an EC_{50} = 53 ± 7 μM obtained from sigmoidal fit. Prolonged IPSCs after PB application were normalized to maximal response. Each data point represents a mean value from 3 to 6 neurons. The IPSCs were isolated from glutamatergic EPSCs by co-applying CNQX (20 μM) and APV (50 μM).

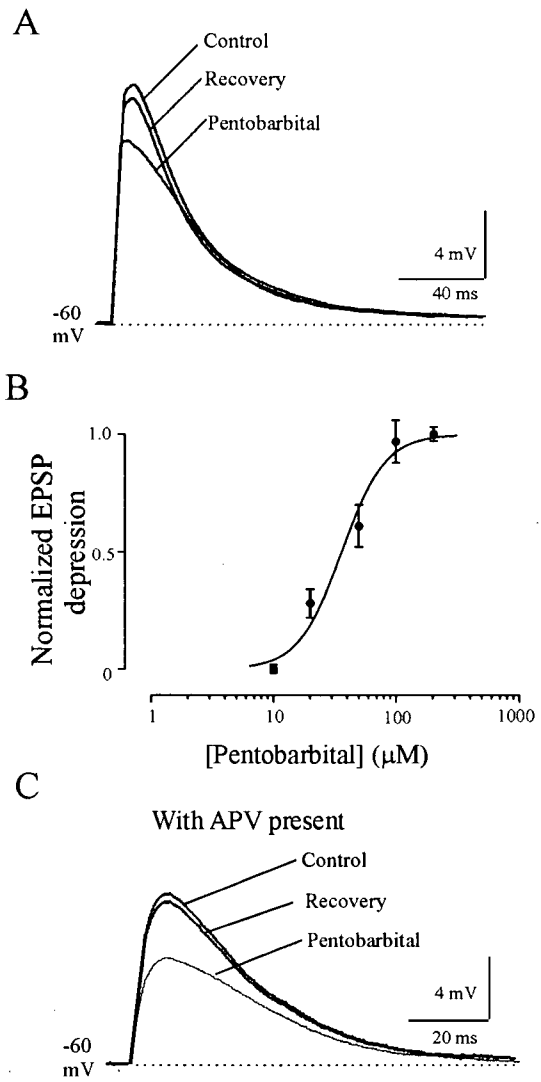

Figure 3.16. Pentobarbital depressed non-NMDA receptor mediated EPSPs in a concentration-dependent manner. (A) Pentobarbital (50 μM) decreased the amplitude of EPSPs recorded in ventrobasal neurons, isolated from GABAergic potentials by co-application of picrotoxinin and 2-hydroxysaclofen. (B) Pentobarbital decreased EPSP amplitude in a concentration-dependent manner, acting with an IC_{50} of 36 ± 5 μM. Each data point represented a mean value obtained from 3-4 neurons. (C) With APV present, pentobarbital (50 μM) decreased the amplitude of the non-NMDA component of EPSPs and recovery was obtained 15 min after termination of the drug application.

The NMDA component was isolated by co-application of picrotoxinin, 2-hydroxysaclofen, and CNQX. Pentobarbital application (50 μM) did not significantly alter the amplitude of the NMDA component (control: 1.9 ± 0.2 mV; pentobarbital: 1.9 ± 0.2 mV; $P>0.05$, n = 4). In summary, pentobarbital selectively reduced the non-NMDA component, decreasing the amplitude of glutamatergic EPSPs by a mechanism that did not likely depend on a concomitant increase in membrane conductance, whereas possibly by the depression of postsynaptic non-NMDA receptors.

3.1.6. Single channel currents in VB neurons

The previous experiments showed that pentobarbital at higher concentration, e.g,. 50-100 μM potentiated GABAergic IPSCs. To further understand the observation that pentobarbital prolonged IPSC decay without changing IPSC amplitude, the effects of pentobarbital on GABA mediated currents were examined by single channel recordings.

3.1.6.1. Lack of activation of single channel currents

The effects of pentobarbital on single $GABA_A$ receptor channels were investigated, because changes in their kinetic behavior could account for the prolonged decay of the IPSCs. This was tested, by employing single channel recordings and applied GABA or muscimol to neurons that were acutely dispersed from the slice preparation. These VB neurons showed a mean resting potential of -60 ± 3 mV when measured on formation of the whole-cell recording condition (n = 14). Single channel currents occurred spontaneously at low frequency in the majority of outside-out patches examined at membrane potentials between -80 mV to +80 mV. Application of 5-10 μM GABA, but not of control bathing solution, evoked inwardly-directed single channel currents in 5 out of 8 outside-out patches, clamped at V_H = -60 mV (Figure.

3.17A). These currents reversed polarity at the equilibrium potential for Cl^- (E_{Cl} = 0 mV). Application of pentobarbital (10-100 μM) did not evoke single channel activity in outside-out membrane patches (Figure. 3.17A).

3.1.6.2. Alterations in open time of GABA activated single channel currents

On the other hand, the co-application of pentobarbital (100 μM) with GABA (10 μM) resulted in the appearance of channel openings with enhanced open state durations (Figure. 3.17A). This change in kinetic behaviour was associated with a pentobarbital-induced increase in the open probability, P_o of GABA-activated channels. At a concentration of 100 μM, pentobarbital increased P_o from 0.04 ± 0.01 to 0.10 ± 0.02 (P<0.05, n = 5). Kinetic analysis showed that open time distributions for GABA-activated single channel currents were well fitted by the sum of 2 exponential terms, $y = A_f.e^{-t/\tau_f} + A_s.e^{-t/\tau_s}$. Here, A_f and A_s represent the amplitudes of fast and slow components with the respective time constants τ_f and τ_s (Figure. 3.17B). Closed time distributions for GABA-activated currents were well described by the sum of three exponential terms and were barely altered by pentobarbital (100 μM). The mean open time of $GABA_A$ receptor channels was calculated from the relationship, $\tau_{mean\ open} = A_f/(A_f + A_s).\tau_f + A_s/(A_f + A_s).\tau_s$., A value of 2.5 ± 0.3 ms was obtained at V_h = -60 mV (n = 5). These results showed that pentobarbital increased open probability but did not alter close time of GABA single channels.

3.1.6.3. Actions on amplitude of GABA-activated single channel currents

GABA-activated single channel currents displayed amplitude distributions that were well described by single Gaussian terms (Figure. 3.17C). The mean value of the currents corresponded to a single channel conductance of 21 ± 1.0 pS at V_H = -60 mV (n = 5). Similar

means for both open time and conductance have been reported for $GABA_A$ receptors in thalamic ventrobasal neurons of the P13-P15 rat (Browne et al., 2001). As also shown in Figure. 3.17C, pentobarbital had no effect on the amplitude of the currents flowing through ion channels activated by GABA (10 μM). When measured during pentobarbital application (100 μM), the mean conductance of GABA-activated channels was 20 ± 0.8 pS. This conductance did not differ significantly from control values given above (P>0.05, n = 5).

3.1.6.4. $GABA_A$ receptor mediation

As further confirmation of the identity of ion channels activated by GABA in our preparation, the effects of the $GABA_A$ receptor-selective agonist, muscimol were examined. As shown in Figure 3.18A, muscimol (10 μM) activated single channel currents with amplitudes (mean conductance 23 ± 1.1 pS, P>0.05, n = 5) that were similar to GABA. Open time distributions for muscimol-activated channels were well described by the sum of two exponential terms (Figure. 3.18B). However, muscimol-activated channels showed a two-fold longer mean open time ($\tau_{mean\ open}$ = 6.5 ± 0.4 ms at V_h = -60 mV; p<0.05, n = 5) than GABA-activated channels. This effect has also been reported for $GABA_A$ receptor channels in mouse spinal cord neurons (Mathers and Barker, 1981). Hence, $GABA_A$ receptors were functional in our preparation. Pentobarbital interacted with $GABA_A$ receptors to increase GABA activated single channel open time in the dissociated neurons.

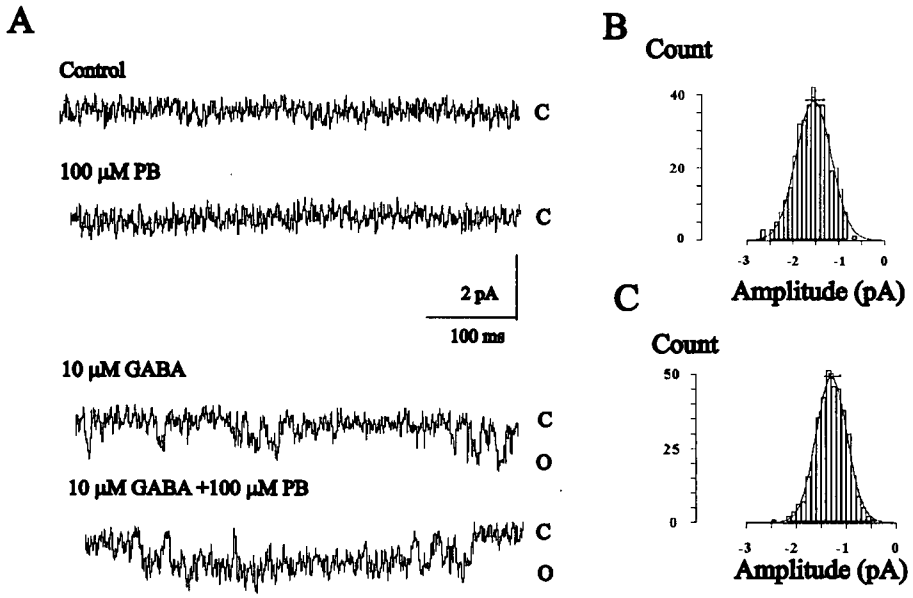

Figure 3.17. Pentobarbital modulates kinetics but not amplitude of GABA activated single channel currents. A, currents were recorded (21°C) in outside-out membrane patch (V_h = -60 mV), excised from acutely dispersed ventrobasal neuron with symmetrical 140 mM Cl^- solutions (E_{Cl} = 0 mV). Baseline current is denoted by C whereas O indicates current flow in GABA-activated channels. Neither control solution nor pentobarbital (PB, 100 μM) did not activate currents. GABA (10 μM) resulted in brief, inward currents (downward deflections). Co-applied GABA (10 μM) and PB (100 μM) resulted in channel openings with enhanced open state durations. Bandwidth, DC-1 kHz. B, open time distribution (n = 734), shown for currents activated by 10 μM GABA in same patch (V_h = -60 mV), was well fitted by sum of 2 exponential terms (smooth curves, $y = A_f.e^{-t/\tau_f} + A_s.e^{-t/\tau_s}$). τ_f and τ_s were 1.0 ms and 8.4 ms, respectively, with $A_f/(A_f + A_s)$ = 0.84 and $A_s/(A_f + A_s)$ = 0.16. Mean channel open time for GABA-activated channels was calculated from $\tau_{mean\ open} = A_f/(A_f + A_s).e^{-t/\tau_f} + A_s/(A_f + A_s).e^{-t/\tau_s}$ = 2.2 ms. C, amplitude distribution (n = 367) for currents activated by GABA (10 μM) in patch (A, V_h = -60 mV) was well fitted by Gaussian function (smooth curve) with mean ± S.D. of -1.55 ± 0.30 pA. Amplitude distribution for currents (n = 380) recorded from same patch during co-application of GABA (10 μM) and PB (100 μM) was well fitted by Gaussian term of mean –1.30 ± 0.31 pA.

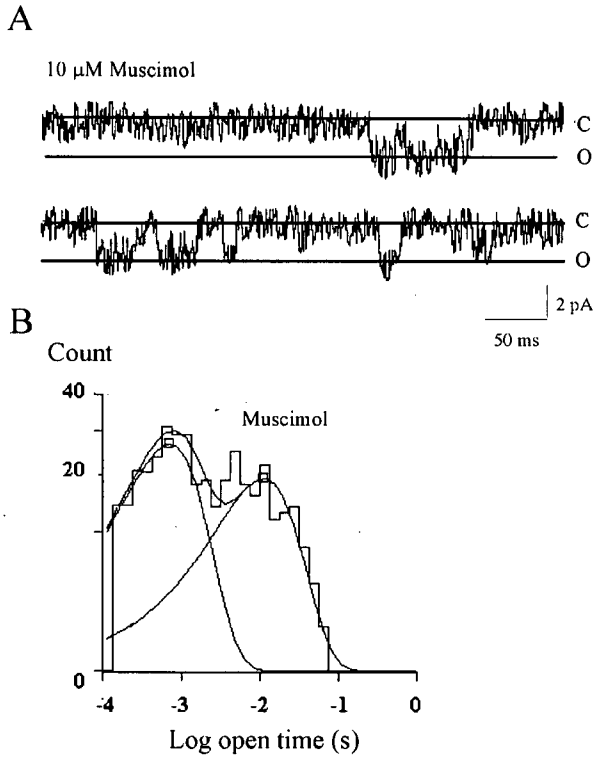

Figure 3. 18. Muscimol, $GABA_A$ receptor agonist, activated single channel currents that had similar amplitude but longer mean open time than channels activated by GABA. Recordings were obtained from an outside-out membrane patch at V_h = -60 mV. A, currents activated by muscimol (10 μM). C and O denote baseline and open channel current level. B, open time distribution (n = 724) for currents activated by muscimol (10 μM) in same patch was well fitted by sum of 2 exponential terms (smooth curves), utilizing τ_f = 0.71 ms; τ_s = 11.2 ms; $A_f/(A_f + A_s)$ = 0.58; $A_s/(A_f + A_s)$ = 0.42. The calculated $\tau_{mean\ open}$ for muscimol activated channels was 5.1 ms.

Part II. Pentobarbital actions in nucleus reticularis thalami and neocortex

To examine pentobarbital actions on reticular thalamic and neocortical neurons in the cortico-thalamocortical system, the effects of pentobarbital on synaptic and non-synaptic properties were studied in these two types of neuron. nRT is the major inhibitory source and layer IV neocortex is the major excitatory source of thalamocortical neurons; we hypothesized that pentobarbital modulated the synaptic and non-synaptic processes in nRT and neocortical neurons to alter neuronal excitability.

3.2.1. Firing properties and membrane conductance on nRT neurons

The data were obtained from 36 neurons in nRT. The resting membrane potential was -71 ± 4 mV and mean R_i was 245 ± 29 MΩ (n = 20) at ~2 min before drug application. The resting membrane potential and R_i were not significantly different from these values obtained in ventrobasal neurons (n = 20; $P>0.05$).

3.2.1.1.Tonic and burst firing of action potentials

When nRT neurons were held at –66 mV, depolarizing current injection elicited neuronal firing at a "wakefulness mode", similar to ventrobasal neurons at tonic firing mode. When held at –86 mV, depolarizing current injection evoked neuronal firing at "sleep mode". nRT neurons fired at higher firing frequency compared to ventrobasal neurons (n = 10; $P<0.05$). Pentobarbital (30 μM) reversibly suppressed neuronal firing in nRT neurons (Figure. 3.19A, B). The recovery can be obtained after 10-15 min termination of drug application.

3.2.1.2.Membrane potential and membrane resistance

Pentobarbital (10-100 μM) slightly hyperpolarized membrane potential by -3 ± 2 mV (n = 10; $P>0.05$). At concentrations higher than 100 μM, pentobarbital depolarized membrane potential by 3 ± 1 mV (n = 4; $P>0.05$). Pentobarbital (30 μM) significantly decreased R_i in nRT neurons (control: 220 ± 21 MΩ, pentobarbital: 181 ± 15 MΩ; n = 4; $P<0.05$). I-V curve showed that pentobarbital (30 μM) significantly decreased slope resistance ($P<0.05$; n = 6; Figure. 3.19C) in nRT neurons.

3.2.1.3.Concentration-response relationship

Pentobarbital inhibited neuronal firing in a concentration-dependent manner in nRT neurons. The IC_{50} of pentobarbital for inhibition of neuronal firing in nRT neurons was 35 ± 4 μM (n = 16; Figure.3.19D). This value was significantly higher than IC_{50}s, at which pentobarbital inhibited neuronal firing in VB and MGB neurons (n = 5, $P<0.05$). Hence, action potential firing in thalamocortical neurons like VB and MGB neurons was more sensitive to pentobarbital-induced suppression than that in nRT neurons.

3.2.1.4.GABA-independent mechanism

To study the interactions between GABA receptors with pentobarbital-induced inhibition on action potential firing in nRT neurons, $GABA_A$, $GABA_B$, and $GABA_C$ receptor antagonists were co-applied with pentobarbital (30 μM). Bicuculline (20-50 μM) or picrotoxinin (50 μM), CGP 33584 (100 μM) and TPMPA (10-50 μM) did not alter pentobarbital-induced decreases on neuronal firing and R_i. These results implicated that pentobarbital inhibited neuronal firing and decreased R_i by a mechanism that was independent of GABA receptors in nRT neurons, however by a low resistance shunt mechanism. This mechanism was similar to what we found in thalamocortical neurons.

3.2.2. Reticular synaptic transmission

Intra-reticular IPSCs were evoked by locally stimulating nRT neurons and recorded in a neighbouring nRT neuron. The IPSCs were pharmacologically isolated by co-application of APV (50 μM) and CNQX (50 μM). Corticothalamic EPSPs were evoked by stimulating the internal capsule and recorded in an nRT neuron. EPSPs were pharmacologically isolated by co-application of bicuculline (50 μM) and CGP-33584 (100 μM).

3.2.2.1. Intra-reticular IPSC amplitude and decay

Intra-reticular IPSCs have larger amplitude and longer decay time constant compared to IPSCs recorded in thalamocortical neurons (Huntsman and Huguenard, 2000). When neurons were held at –80 mV, the intra-reticular IPSC amplitude and decay time constant were 54 ± 5 pA (n = 5) and 41 ± 5 ms (n = 5) respectively, while the mean IPSC amplitude and decay time constant recorded in VB neurons were 42 ± 4 pA (n = 5) and 20 ± 4 ms (n = 5) respectively (cf. Table 3.2). When nRT neurons were held at –80 mV, only a fast component of IPSCs was observed, which was blocked by bicuculline (50 μM) or picrotoxinin (50 μM; Figure. 3.20A), indicating $GABA_A$ receptor mediation. When neurons were held at –40 mV, a slow component, which was blocked by CGP-33584 (100 μM; Catsicas and Mobbs, 2001), could occasionally (~ 30%) be observed. This indicated that the slow component was mediated by $GABA_B$ receptors.

Pentobarbital (40-200 μM) produced 10-30% increase of the intra-reticular IPSC amplitude (Figure. 3.20B). Different from pentobarbital's effects on IPSC amplitude, IPSC decay was greatly prolonged by pentobarbital application with a range from 10% to 900% of the control IPSC decay (Figure. 3.20B).

3.2.2.2. Concentration-response relationship

Pentobarbital increased intra-reticular IPSC amplitude and prolonged intra-reticular IPSC decay in concentration-dependent manners. The EC_{50} for increasing IPSC amplitude by pentobarbital was 62 ± 7 μM (n = 15; Figure. 3.20C), while EC_{50} for prolonging IPSC decay was 84 ± 9 μM (n = 15; Figure. 3.20D). The EC_{50} for prolongation of intra-reticular IPSC decay time constant by pentobarbital was significantly higher than the EC_{50} recorded in thalamocortical IPSCs (n = 5; $P<0.05$). The hill coefficients (hill slopes) of the concentration-response relationships were 2.9 and 4.2 respectively for pentobarbital-induced prolongation in thalamocortical IPSCs and intra-reticular IPSCs. These indicated that the interaction between pentobarbital and the $GABA_A$ receptor might not be identical in thalamocortical neurons and reticular thalamic neurons.

3.2.2.3. $GABA_A$ receptor mediation

The mechanism underlying the potentiation of IPSCs by pentobarbital were determined in nRT neurons. Bicuculline (50 μM) abolished the pentobarbital-induced increase in IPSC amplitude and prolongation of decay time constant (n = 5; Figure. 3.20B). Picrotoxinin (50 μM) also completely blocked pentobarbital-induced IPSC potentiation, similar to the effects of bicuculline (n = 5). These results indicated that the potentiation of intra-reticular IPSCs by pentobarbital was mediated by $GABA_A$ receptors.

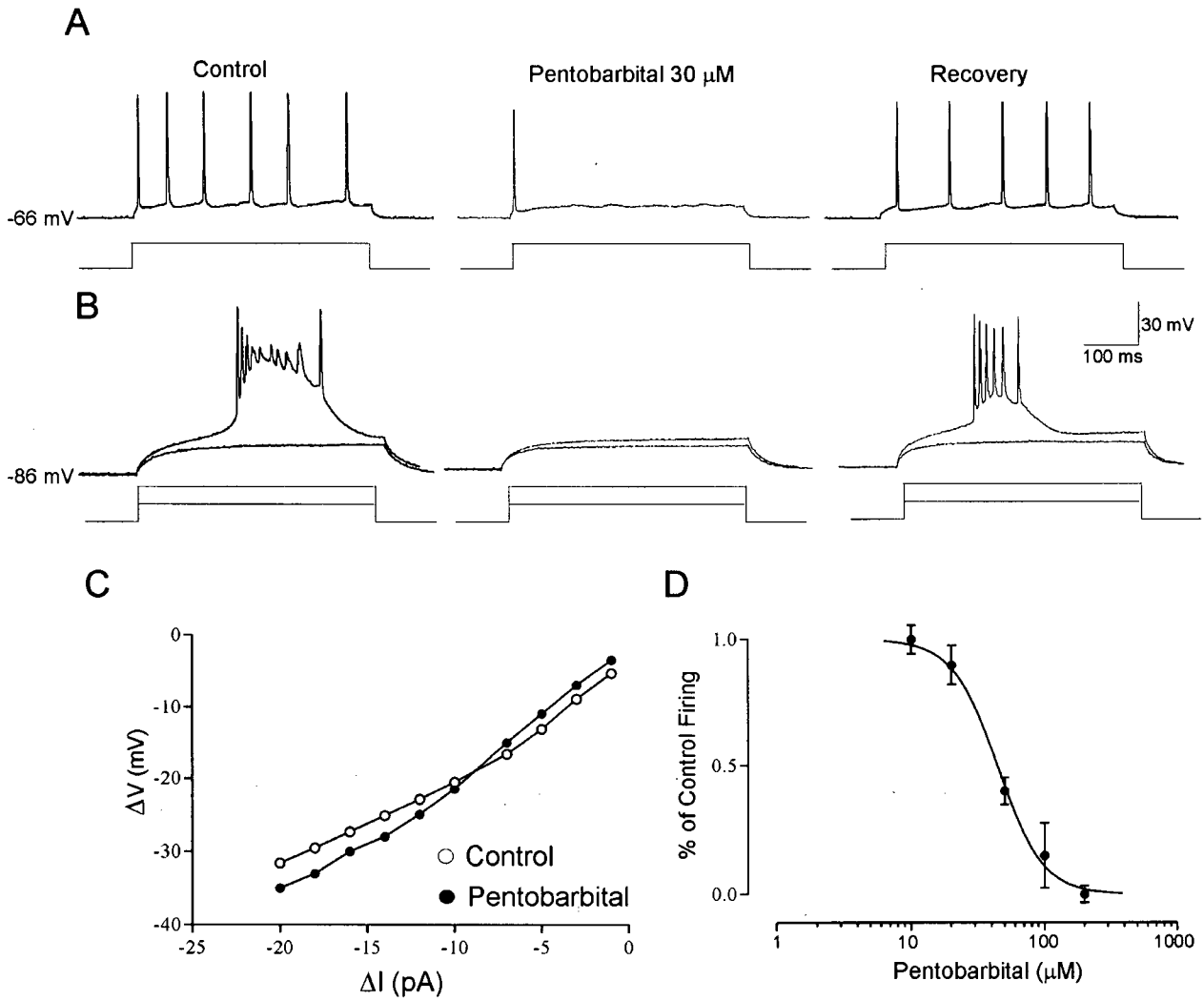

Figure 3.19. Pentobarbital depressed neuronal firing and increased membrane conductance in a concentration-dependent manner in nRT neurons. (A) Pentobarbital (30 μM) reversibly inhibited tonic firing in a neuron held at –66 mV. (B) In the same neuron held at –86 mV, pentobarbital (50 μM) depressed burst firing and recovery could be obtained 15 min later after termination of the drug application. The blockade induced by pentobarbital was surmountable by larger current injection. (C) Pentobarbital (50 μM) increased membrane conductance measured by slope of I-V curve. (D) The inhibition on neuronal firing induced by pentobarbital was concentration dependent. The IC_{50} was 35 ± 4 μM. Each data point was the mean ± S.E.M of 3-5 neurons.

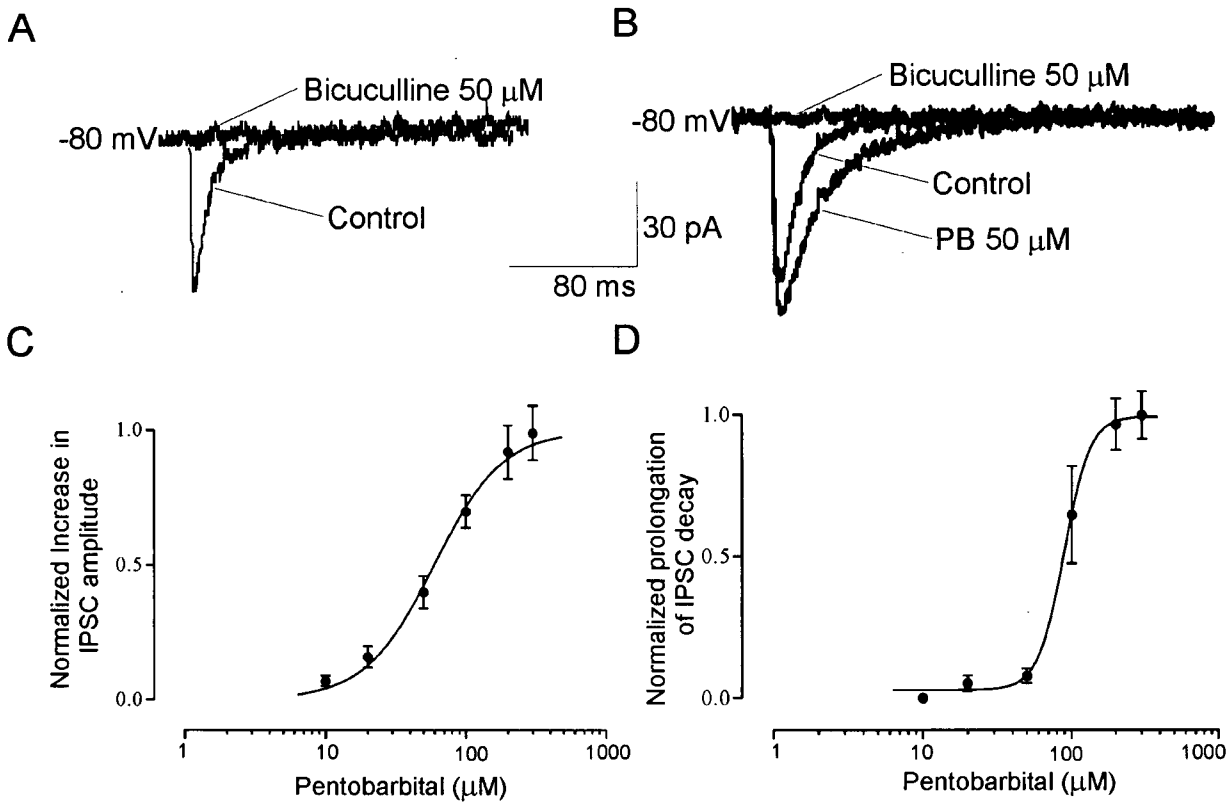

Figure 3.20. Pentobarbital potentiated $GABA_A$ergic IPSCs in nRT neurons. (A) Intra-reticular IPSCs were isolated by co-application of APV (50 μM) and CNQX (25 μM). When a neuron was held at –80 mV, inwardly IPSCs were recorded, which were blocked by co-application with bicuculline (50 μM). (B) Pentobarbital (100 μM) significantly increased IPSC amplitude and decay time constant. This effect was blocked by co-application with bicuculline (50 μM). The effects of pentobarbital to increase in IPSC amplitude and to prolong IPSC decay time constant were concentration-dependent with EC_{50}s = 62 ± 7 μM and 84 ± 9 μM respectively (C, D). Each data point was Mean ± S.E.M of 3-5 neurons.

3.2.2.4. Corticothalamic EPSPs in nRT neurons

Corticothalamic EPSPs recorded in nRT neurons were composed of two components, which were blocked by CNQX (25 μM) and APV (50 μM) respectively. This indicated that NMDA and non-NMDA receptors mediated corticothalamic EPSPs in nRT neurons. Pentobarbital (40-300 μM) decreased corticothalamic EPSP amplitude in nRT neurons, though it did not change EPSP decay (Figure. 3.21 A). The decrease in EPSP amplitude ranged from a 10% to 40% decrease of control value. The pentobarbital-induced decrease in EPSP amplitude was reversible after 15 min termination of drug application. These results indicated that pentobarbital inhibited excitatory neurotransmission in nRT neurons by suppressing EPSP amplitude without altering EPSP decay.

3.2.2.5. Concentration-response relationship

Pentobarbital (10-300 μM) decreased corticothalamic EPSP amplitude in a concentration-dependent manner in nRT neurons with an IC_{50} = 65 ± 7 μM (n = 16; Figure. 3.21C). This IC_{50} was significantly higher than the IC_{50} for decreasing corticothalamic EPSP amplitude in ventrobasal neurons induced by pentobarbital (n = 5; $P<0.05$), which was 36 ± 5 μM.

3.2.2.6. Non-NMDA receptor mediation

During blockade of NMDA receptors by APV (50 μM), pentobarbital (50 μM) decreased EPSP amplitude to the same degree as it would without APV application (Figure. 3.21A, B). Further application of CNQX (25 μM) completely blocked pentobarbital-induced decrease in EPSP amplitude (Figure. 3.21B). This indicated that pentobarbital depressed the amplitude of corticothalamic EPSP mediated by non-NMDA receptors in nRT neurons.

3.2.3.*Membrane properties and synaptic transmission on neocortical neurons*

The data were obtained from 27 neurons from layer IV neocortex. The resting potential and R_i were -69 ± 4 mV and 203 ± 25 MΩ (n = 20) respectively. This thesis only studied the effects of pentobarbital on regular firing neurons in layer IV neocortex.

3.2.3.1. Neuronal firing and input resistance

Unlike actions on thalamic neurons, pentobarbital (10-50 μM) did not significantly alter neuronal firing or R_i in neocortical neurons. Higher concentrations of pentobarbital application (100 μM) inhibited neuronal firing (Figure. 3.22A), which was surmountable by an injection of larger current amplitude, implying a shunt mechanism. Pentobarbital application (100 μM) decreased R_i from 189 ± 20 MΩ to 142 ± 13 MΩ (n = 4; $P<0.05$). The decrease in R_i by pentobarbital was concentration-dependent with an IC_{50}=108 ± 11 μM. This value was significantly higher than IC_{50}s, at which pentobarbital decreased R_i in VB and in nRT neurons (n = 6; $P<0.05$).

3.2.3.2. Modulation of I_h

The interaction between pentobarbital and I_h in neocortical neurons was examined by voltage-clamp studies. Neocortical layer IV neurons had much larger I_h compared to thalamocortical neurons. When neurons hyperpolarized from –50 mV to –140 mV, the amplitude of I_h was 123 ± 14 pA in neocortical neurons and 54 ± 8 pA in ventrobasal neurons (n = 5, $P<0.05$). Though pentobarbital (20-50 μM) significantly increased I_h in neocortical neurons (Figure 3.22B), higher concentrations of pentobarbital (200 μM) decreased I_h (Figure. 3.22B). These effects were distinct from pentobarbital action on I_h in thalamocortical neurons, in which pentobarbital

at all concentrations decreased I_h. These data implied that pentobarbital could exert different actions on intrinsic ion channels in neocortical neurons, compared to thalamic neurons.

3.2.3.3. Neocortical inhibitory synaptic transmission

To examine pentobarbital action on neocortical IPSCs, layer III neocortical neurons were electrically stimulated and IPSCs were recorded in a layer IV neocortical neuron. The components of neocortical IPSCs were identified by applying different receptor antagonists. Strychnine (200 nM), which is a glycine receptor antagonist (Breitinger and Becker, 2002), slightly blocked neocortical IPSCs by 12 ± 4% (Figure. 3.23A). However, bicuculline (20 μM) abolished the remaining IPSCs component (Figure. 3.23A). This indicated that $GABA_A$ receptors-mediated IPSCs were the major component of neocortical IPSCs recorded in layer IV neocortical neurons.

3.2.3.3.1. Neocortical IPSC amplitude and decay

Pentobarbital (40-300 μM) potentiated neocortical IPSCs. In Figure 3.23B, pentobarbital (100 μM) slightly increased IPSC amplitude by ~ 15 % and prolonged IPSC decay time constant in a layer IV neocortical neuron held at –80 mV to eliminate K^+-related contribution. This potentiation was reversible after 20 min termination of pentobarbital application. These results indicated that pentobarbital potentiated neocortical inhibitory neurotransmission by increasing IPSC amplitude and prolonging IPSC decay.

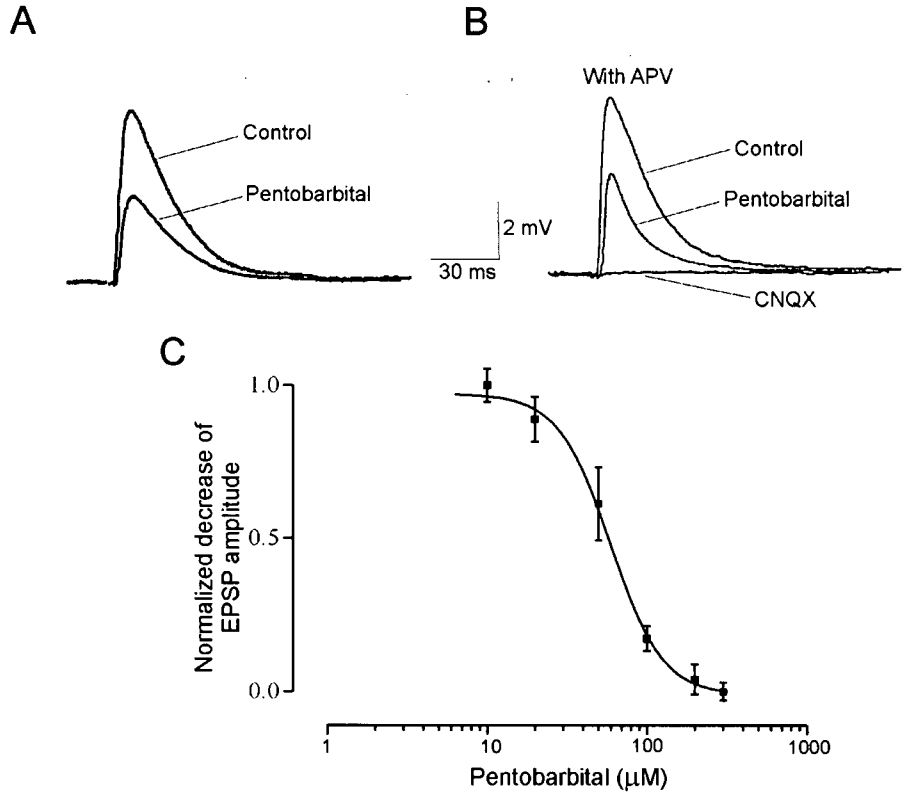

Figure 3.21. Pentobarbital depressed corticothalamic EPSPs. (A) Corticothalamic EPSPs were recorded in an nRT neuron and isolated by co-application of picrotoxinin (50 μM) and 2-hydrosaclofen (200 μM). Pentobarbital (50 μM) decreased EPSP amplitude without altering decay of EPSPs. (B) With NMDA receptor antagonist-APV (50 μM) present, pentobarbital (50 μM) decreased the amplitude of remaining EPSPs. This effect could be abolished by further application of CNQX (25 μM). (C) Pentobarbital decreased corticothalamic EPSP amplitude in nRT neurons in a concentration-dependent manner with an IC_{50}= 65 ± 7 μM. Each data point was Mean ± S.E.M of 3-5 neurons.

3.2.3.3.2. Concentration-response relationship

Pentobarbital potentiated neocortical IPSCs in a concentration-dependent manner. Pentobarbital increased IPSC amplitude with an EC_{50} = 45 ± 5 μM (n = 16; Figure. 3.23C). The EC_{50} for the prolongation of IPSC decay induced by pentobarbital was 101 ± 8 μM (n = 16; Figure. 3.23D). These two EC_{50}s were significantly different (n = 5, $P<0.05$).

3.2.3.3.3. $GABA_A$ mediation

Pentobarbital-induced potentiation on neocortical IPSCs was not blocked by co-application with strychnine (0.1-2 μM), but completely blocked by co-application with bicuculline (50 μM) or picrotoxinin (50 μM). This indicated that pentobarbital-induced potentiation on neocortical IPSCs was mediated by interaction with $GABA_A$ receptors.

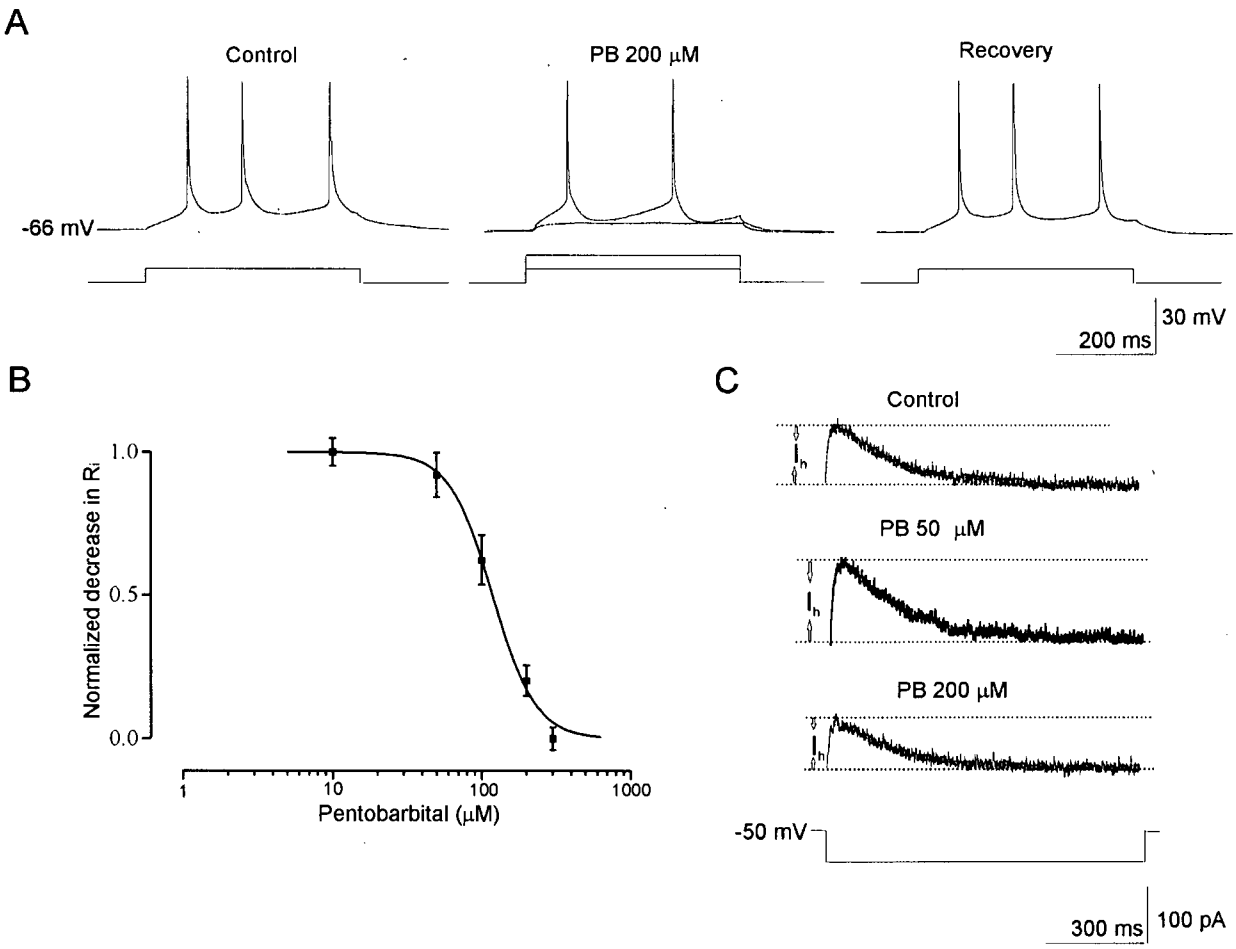

Figure 3.22. Pentobarbital effects on neuronal firing and I_h in neocortical neurons. (A) Pentobarbital (200 μM) inhibited neuronal firing in layer IV neocortical neurons. The full recovery can be obtained after 20 min termination of the drug application. (B) Pentobarbital decreased input resistance in a concentration-dependent manner with an IC_{50}=108 ± 11 μM in neocortical neurons. (C) Pentobarbital (50 μM) increased I_h, whereas 200 μM pentobarbital decreased I_h in neocortical neurons.

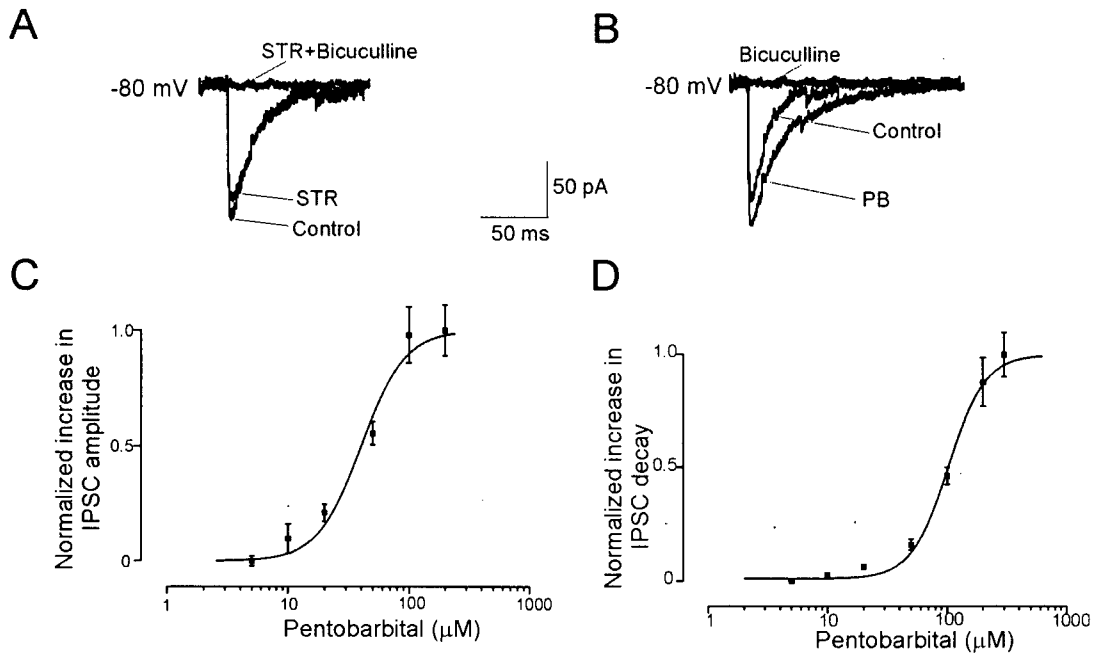

Figure 3.23. Pentobarbital potentiated neocortical IPSCs. (A) Neocortical IPSCs were evoked in a layer IV neuron by electrically stimulating layer III neurons. Neocortical IPSCs were slightly blocked by glycine receptor antagonist- strychnine (200 nM). The remaining IPSCs were completely blocked by bicuculline (25 μM). (B) Pentobarbital (100 μM) increased amplitude and prolonged the decay time constant of neocortical IPSCs. This action can be completely blocked by co-application with bicuculline (25 μM). (C), (D) Pentobarbital increased neocortical IPSC amplitude and decay time constant in concentration-dependent manners with an $EC_{50} = 45 \pm 5$ μM and 101 ± 8 μM respectively.

Part III. Other barbiturate actions on CTC system

To further understand barbiturate mechanisms in the CTC system, the effects and mechanisms of two other barbiturates (amobarbital and phenobarbital), which are much less potent in inducing anesthesia, but have other diagnostic and therapeutic uses in clinical neurology, were studied in neurons of the CTC system.

3.3.1. Amobarbital actions on neuronal firing, synaptic transmission and single channels

The barbiturate, amobarbital, has uses in diagnostic neurology and less commonly in pain therapy (Koyama et al., 1998). The potential mechanisms of anesthetic depression, including rationale for therapeutic uses, are unknown. There are presently few studies on amobarbital actions on central nervous system (CNS) neurons. Amobarbital actions on neurons of the CTC system were examined for a comparison to the effects of pentobarbital and furthering an understanding of possible mechanisms of barbiturates in the CNS.

3.3.1.1.Firing properties and membrane conductance

3.3.1.1.1 Tonic and burst firing

Amobarbital actions were studied on 51 ventrobasal, 25 nRT and 5 intralaminar neurons in the thalamus. Amobarbital (50-500 μM) reversibly inhibited tonic firing of action potentials in 3 types of neurons. As shown for a ventrobasal neuron held at V_h = -66 mV (Figure. 3.24A), amobarbital (100 μM) depressed tonic firing. This depression was concentration-dependent. Amobarbital depressed tonic firing with an IC_{50} = 119 ± 7 μM in ventrobasal neurons, and 99 ± 7 μM in intralaminar neurons (Figure. 3.24D). These values were significantly lower than the IC_{50} = 255 ± 27 μM in nRT neurons (Figure. 3.24D). Tonic firing was approximately twice more susceptible to amobarbital in ventrobasal and intralaminar neurons, than in nRT neurons.

Amobarbital reversibly decreased low threshold spike (LTS) bursts evoked by depolarizing pulses in all neurons held at hyperpolarized potentials (cf. Figure. 3.24B). Action potential discharge associated with the LTS was much less robust in intralaminar neurons. Amobarbital also depressed the LTS and associated firing at the offset of hyperpolarizing pulses in all intralaminar (cf. Figure 3.24C), ventrobasal and nRT neurons.

The suppression of burst firing was at least partly surmountable by injecting larger currents. Tetrodotoxin (TTX; 0.5 μM) was used to isolate the LTS from action potentials in 3 ventrobasal neurons. Subsequent co-application with amobarbital (100 μM) inhibited the LTS to approximately the same extent as in the control, prior to TTX administration. The depression was partly or totally surmountable with larger currents, and antagonised by bicuculline (25 μM, n = 3). Amobarbital suppressed the bursting of ventrobasal and nRT neurons in a concentration-dependent manner (Figure. 3.24D). The IC_{50} was 91 ± 7 μM in ventrobasal neurons, lower than the IC_{50} = 172 ± 19 μM in nRT neurons.

Burst firing was more sensitive than tonic firing to blockade by amobarbital in nRT (n = 7; $P<$ 0.05), and in ventrobasal neurons (n = 7; $P<$ 0.05). Compared with nRT neurons, burst firing in ventrobasal neurons was approximately 80% more susceptible to amobarbital on a concentration basis. Amobarbital suppressed firing also in neurons without manual clamping of the membrane potential to its initial resting value. In summary, a blockade of action potentials and LTS surmountable by larger current inputs, implicated a low resistance shunt.

Amobarbital (100-500 μM) inhibited neuronal firing in neocortical neurons. Figure 3.25A shows that amobarbital (200 μM) reversibly depressed neuronal firing in a neocortical neuron

held at –70 mV. This depression on neuronal firing was blocked by co-application with bicuculline (50 μM) or picrotoxinin (50 μM). The depression of neuronal firing by amobarbital was concentration-dependent with an IC_{50}= 151 ± 17 μM (n = 16; Figure. 3.25B). This IC_{50} was significantly higher than the IC_{50}, at which amobarbital depressed neuronal firing in ventrobasal neurons but not significantly different from IC_{50} of this depression in nRT neurons (n = 5; P<0.05).

3.3.1.1.2. Membrane input resistance

The blockade of tonic and burst firing in both types of neurons was overcome by larger depolarizing current pulse injections (Figure. 3.24A,B), implicating a low resistance shunt. Amobarbital (200 μM) reversibly depolarized ventrobasal neurons and decreased their R_i by 17 ± 6% (Figure. 3.26A; n = 5, P<0.05). In nRT neurons, application of amobarbital at 200 μM did not significantly change R_i. Amobarbital (300 μM) reversibly depolarized nRT neurons by a few millivolts in ventrobasal neurons (Figure. 3.26B; n = 5). The associated decrease in R_i was 16 ± 4% (Figure. 3.26B; n = 5, P<0.05). Amobarbital decreased R_i in concentration-dependent manners with IC_{50}s= 96 ± 7 μM and 194 ± 9 μM in VB and nRT neurons respectively (Figure. 3.26C). These values were not significantly different from IC_{50}s to inhibit burst firing in both nuclei, accorded with the blockade of action potentials by a low resistance shunt mechanism.

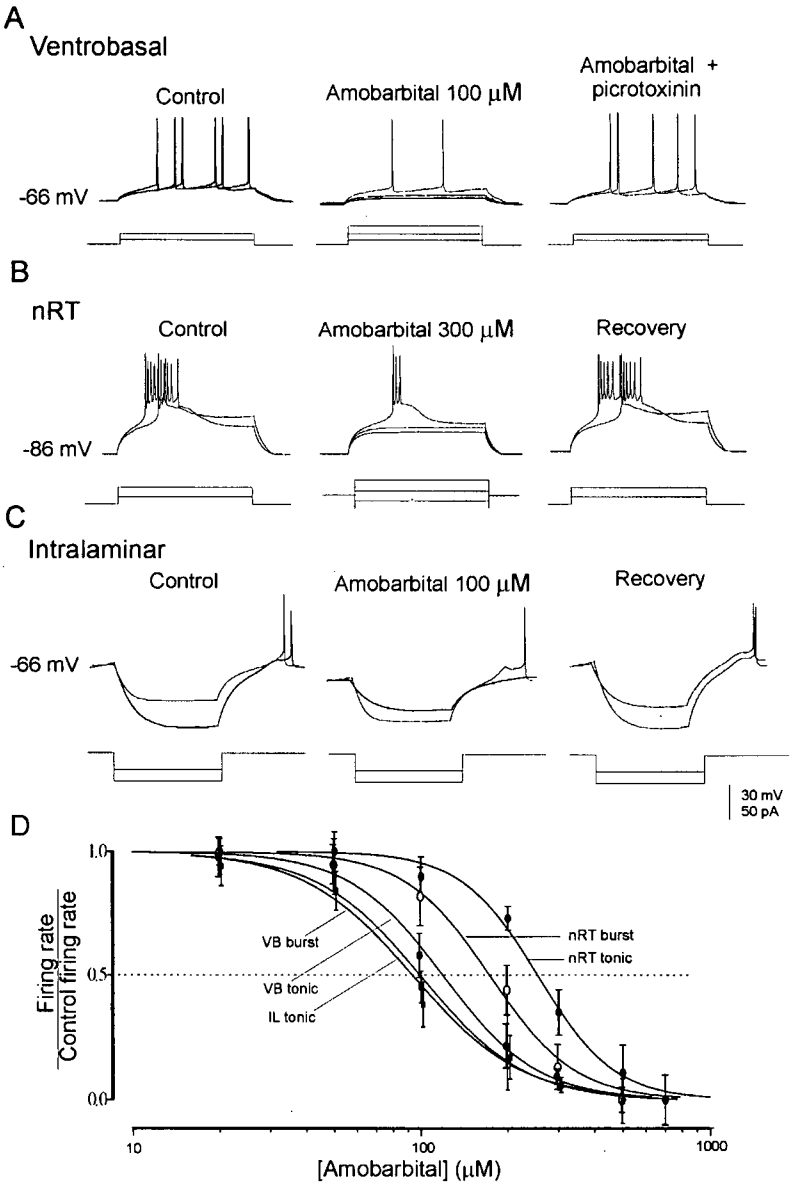

Figure. 3.24. Amobarbital depression of tonic and burst firing in thalamic neurons. (A) Picrotoxinin (50 µM) antagonised depressed tonic firing. Amobarbital depressed burst firing in nRT neuron (B) and at offset of hyperpolarizing pulse in intralaminar neuron (C). Lower records in A-C show 500 ms current stimuli. Note that larger currents partially overcame amobarbital depression. V_h shown at left of voltage records. (D) Relationship of concentration to normalized response shows that IC_{50}s for burst suppression were 91 ± 7 µM in ventrobasal (VB burst), and 172 ± 19 µM in nRT (nRT burst) neurons. IC_{50}s for depression of tonic firing were 99 ± 7 µM in intralaminar (IL tonic), 119 ± 7 µM in ventrobasal (VB tonic), and 255 ± 27 µM in nRT (nRT tonic) neurons. Each point represents mean ± S.E.M of 3-5 neurons. IC_{50} was lower for depression of burst than for tonic firing in ventrobasal and nRT neurons (n = 5, *t*-test, $P<0.05$). IC_{50}s for depression of tonic and burst firing were lower in ventrobasal neurons than in nRT neurons (n = 5, *t*-test, $P<0.05$).

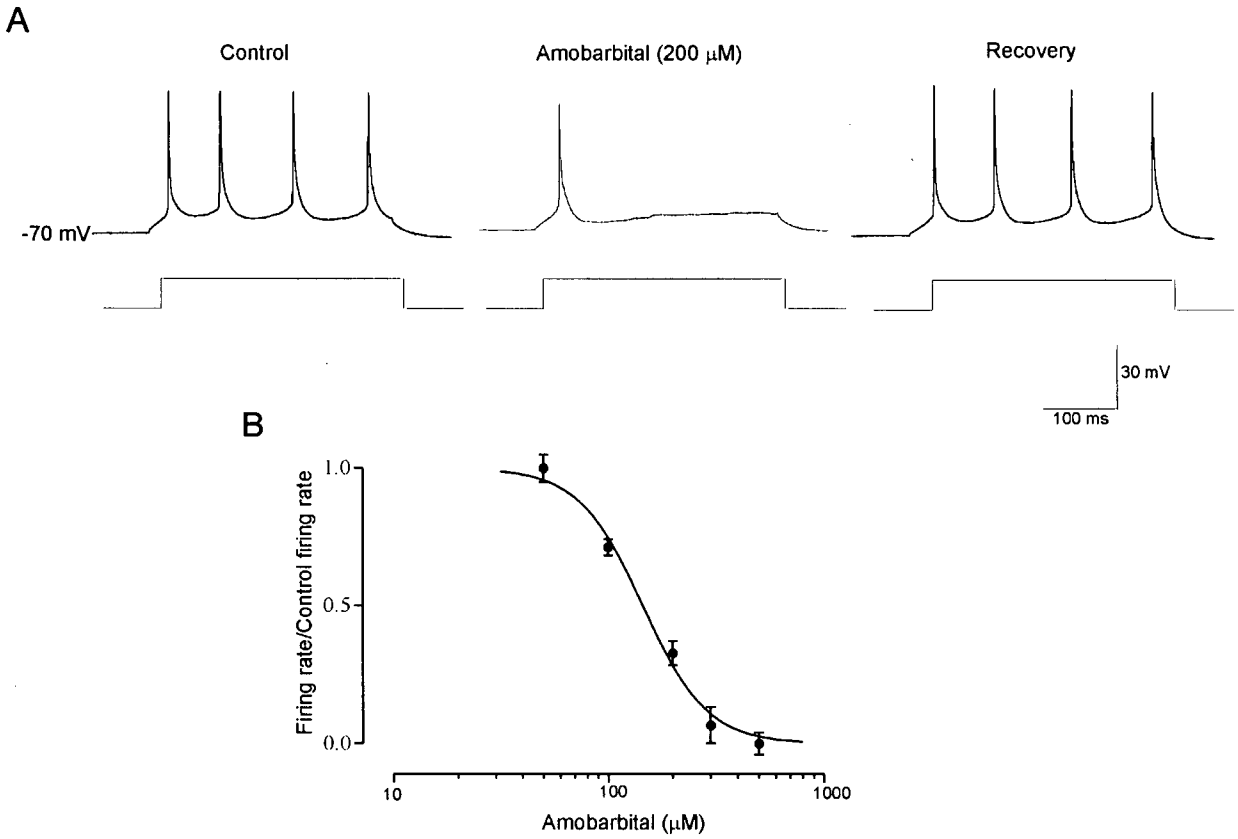

Figure 3.25. Amobarbital depressed neuronal firing in neocortical neurons. (A) Amobarbital (200 μM) reversibly depressed neuronal firing in a neocortical neuron held at –70 mV. The recovery was obtained after 15 min termination of the drug application. (B) Amobarbital depressed neuronal firing in neocortical neurons in a concentration-dependent manner with an IC_{50}=151 ± 17 μM. Each data point (mean ± SEM) represents 3 to 5 neurons.

Further clues about the mechanism of action were obtained from amobarbital-induced changes in the current-voltage (I-V) relationship obtained with voltage clamp. The I-V relationship showed that amobarbital increased the slope conductance over a 40 mV range in both neuron types. Amobarbital induced inward current (I_{Amo}) at potentials negative to -55 mV, which was evident from subtraction of the currents obtained during control and amobarbital conditions (Figure. 3.27A, B). The control and amobarbital I-V curves intersected at -54 ± 2 mV in 24 ventrobasal neurons and -55 ± 2 mV in 12 nRT neurons. These values were very close to E_{Cl} and accounted for the depolarization observed from -60 mV in current clamp recordings, indicating the increase in Cl^- conductance.

This reversal potential was consistent with our observations that picrotoxinin (50 μM), a Cl^- ionophore inhibitor, prevented amobarbital-induced depression of tonic firing of neurons in both ventrobasal nuclei (Figure. 3.24A) and nRT. Bicuculline or picrotoxinin application abolished the increases in slope conductance induced by amobarbital at 100 μM in ventrobasal neurons, and at 300 μM in nRT neurons. This blockade by picrotoxinin (50 μM) was observed in 3 ventrobasal (Figure 3.27A), and 3 nRT neurons. The blockade bicuculline (25 μM) also eliminated the increased slope conductance in 3 ventrobasal, and 3 nRT neurons (Figure. 3.27B).

Amobarbital actions on membrane properties were examined on neocortical neurons. The data were obtained from 20 layer IV neocortical neurons. Amobarbital (200-500 μM) depolarized membrane potential by 3 ± 2 mV (n = 10) in neocortical neurons. Accompanying depolarization, amobarbital (300 μM) decreased R_i from 201 ± 19 MΩ to 164 ± 17 MΩ (n =

10; $P<0.05$). I-V relationship showed that amobarbital also decreased slope resistance at the voltage range from –40 mV to –80 mV under voltage-clamp in neocortical neurons.

3.3.1.1.3. $GABA_A$ receptor mediation

The actions of amobarbital on neuronal firing and R_i in ventrobasal, nRT and neocortical neurons were summarized in Figure 3.28. There was no significant difference in pentobarbital-induced alteration of neuronal firing and R_i between nRT and neocortical neurons (n = 20, $P>0.05$). Therefore, these two types of neurons were pooled in the analysis. $GABA_A$ receptor antagonists, bicuculline (25 μM) or picrotoxinin (50 μM), eliminated the blockade of neuronal firing and decreases in R_i induced by amobarbital in three types of neurons (Figure. 3.28). Hence, it was apparent that a $GABA_A$ receptor-gated increase in Cl^- conductance accounted for amobarbital depression of tonic firing in three neuron types.

3.3.1.1.4. Actions on I_h

I_h were evoked by stepping from V_h = -50 to -80 mV with a pulse of 1 sec duration. Maximal amplitude of I_h was not significantly altered in 6 ventrobasal neurons (control, 53 ± 5 pA and 100 μM amobarbital, 55 ± 6 pA; $P> 0.05$) and 5 nRT neurons (control, 48 ± 5 pA and 300 μM amobarbital, 47 ± 4 pA; $P> 0.05$). In this voltage range, I_h largely accounts for inward rectification (McCormick and Pape, 1990). In neocortical neurons, a greater I_h was observed, which was not significantly altered by 50-500 μM amobarbital (control, 112 ± 9 pA and 300 μM amobarbital, 114 ± 12 pA; $P> 0.05$). Hence, amobarbital did not likely have significant effects on I_h in ventrobasal, nRT and neocortical neurons.

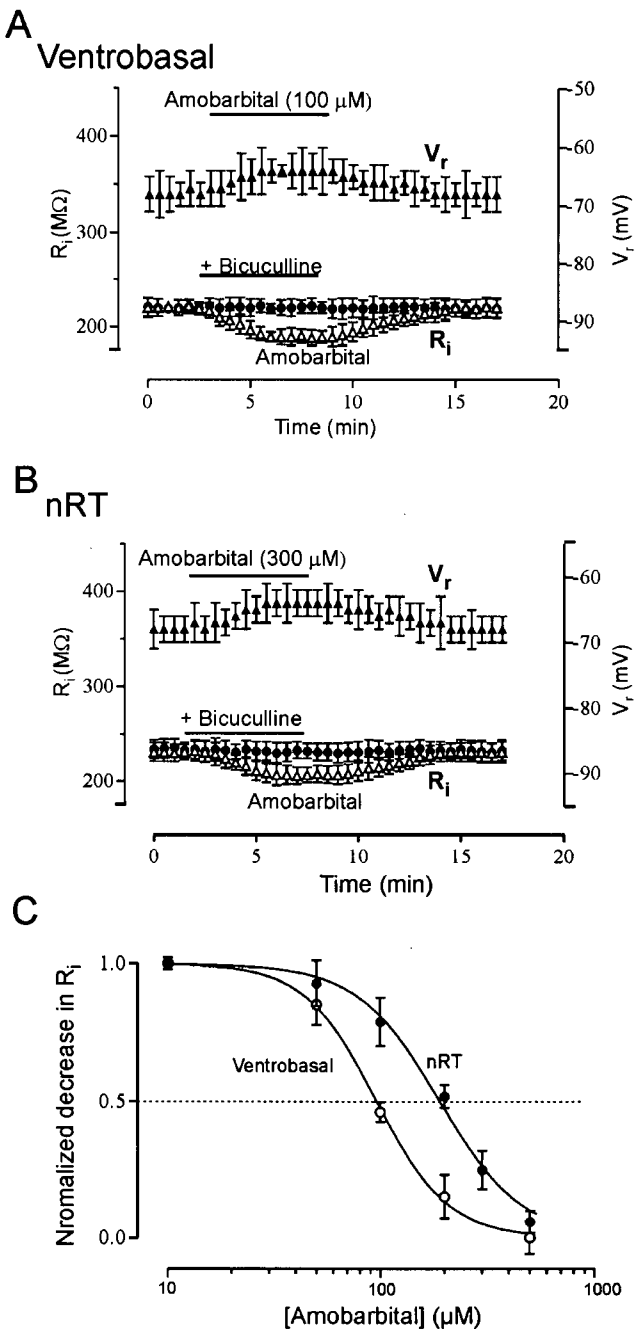

Figure. 3.26. Amobarbital reduced input resistance (R_i) and increased membrane potential (V_r) in ventrobasal and nRT neurons. (A,B) Bicuculline (25 M) completely antagonized amobarbital actions. (C) Concentration-response relationships show amobarbital-induced decrease in R_i with IC_{50}s = 96 ± 7 μM in ventrobasal, and 194 ± 9 μM in nRT neurons. Each data point (mean ± S.E.M) represents 3-5 neurons.

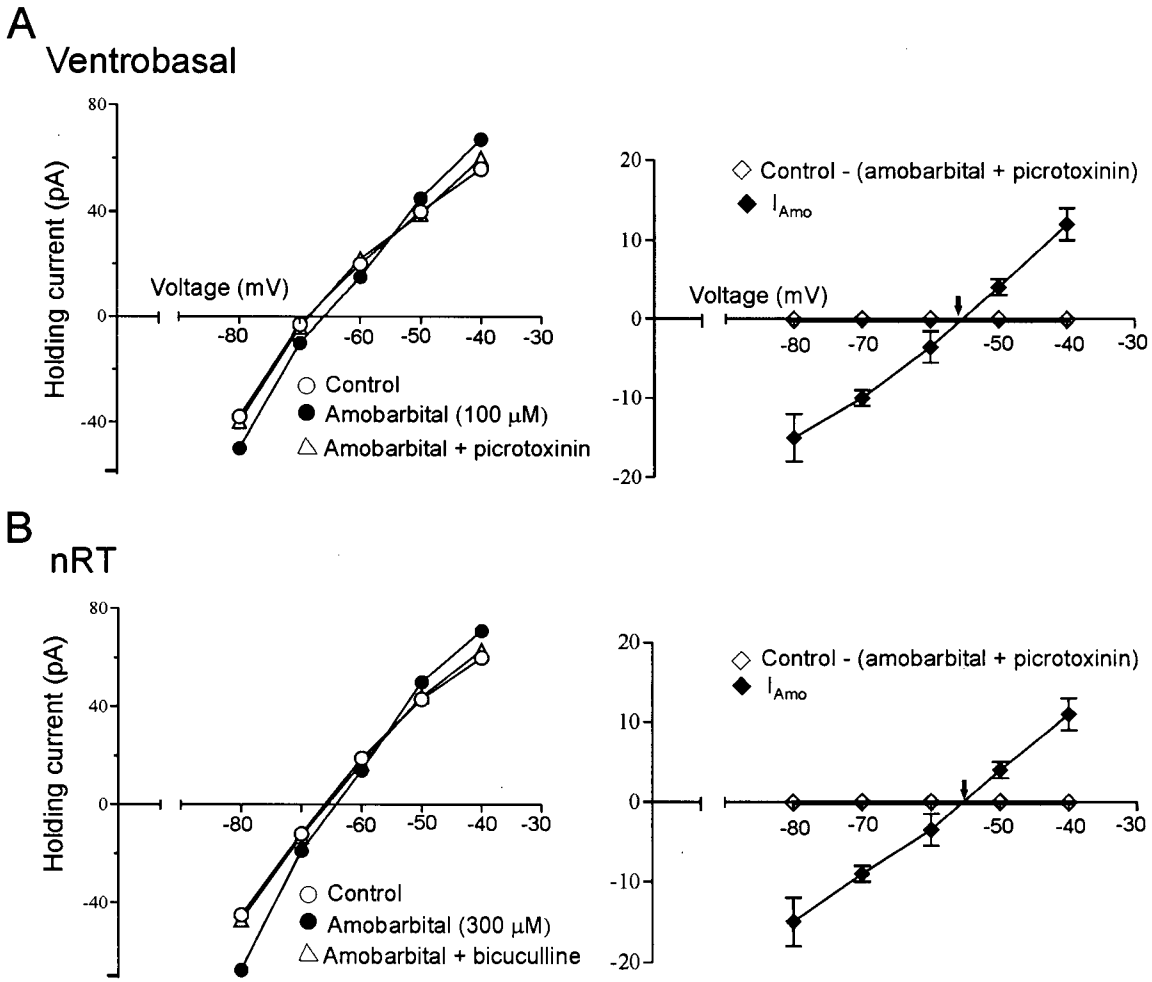

Figure. 3.27. Current-voltage (I-V) relationships for amobarbital actions in two voltage-clamped neurons. (A,B) Amobarbital increased slope of I-V curves which intersected with control curves at -55 mV (reversal potentials). Picrotoxinin (50 μM) antagonised amobarbital action on I-V relationships. In the right panel of A and B, amobarbital-induced current (I_{Amo}) obtained on subtraction of drug from control curves reversed near -55 mV (arrows). The different current between control and co-application of amobarbital and picrotoxinin was almost 0, which indicated amobarbital-induced current was picrotoxinin-sensitive (A and B, *right*).

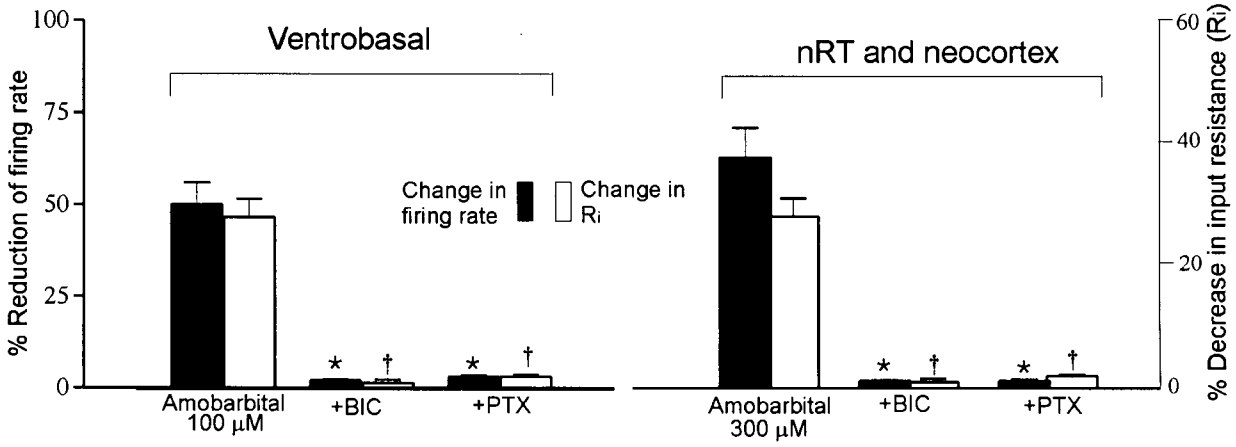

Figure 3.28. Amobarbital depressed neuronal firing and decreased input resistance (R_i) due to $GABA_A$ receptor activation in ventrobasal, nRT and neocortical neurons. The suppression of firing rate and decrease in R_i were antagonized by bicuculline (50 μM; $P<0.05$) or picrotoxinin (50 μM; $P<0.05$). The data represent 4 to 6 cells in each condition. * $P< 0.05$, firing rate significantly different from amobarbital alone. † $P< 0.05$, R_i significantly different from amobarbital alone.

3.3.1.2. Thalamocortical and neocortical IPSCs

Amobarbital actions on inhibitory neurotransmission in the thalamus and neocortex were then examined. This study includes investigation on interactions between amobarbital and thalamocortical, intra-reticular and neocortical IPSCs.

3.3.1.2.1. Actions on thalamocortical, intra-reticular and neocortical IPSCs

The effects of amobarbital on thalamocortical and intra-reticular IPSCs, which were evoked by nRT stimulation, were examined in 20 ventrobasal and 18 nRT neurons. Fast IPSCs that decayed with a single exponential time course in all neurons were observed, which was consistent with previous reports, Thalamocortical IPSCs showed a faster decay rate than intra-reticular IPSCs (Huntsman and Huguenard, 2000; Browne et al., 2001). A slow component in the outward IPSCs was present in ~25% of ventrobasal and nRT neurons held at V_h = -40 mV, but became negligible at V_h = -80 mV. The $GABA_B$ receptor antagonist, CGP 35348 (100 μM), abolished the slow component (n = 4). Amobarbital (50-300 μM) did not significantly alter the slow component (n = 4, P>0.05), which was likely mediated by K^+ permeable $GABA_B$ receptors (Wan et al., 2003).

The fast IPSCs reversed polarity at E_{Cl}, implicating Cl^- mediation. These IPSCs, evoked from V_h = -80 mV, had a significantly larger amplitude in nRT, compared to ventrobasal neurons (Figure. 3.29, Table 3.2). Amobarbital (100 μM) reversibly increased IPSC amplitude by 31 ± 5 % (Figure. 3.29) in 5 ventrobasal and 24 ± 3 % in 5 nRT neurons (Table 3.2). Application of bicuculline (50 μM) eliminated the IPSCs (Figure. 3.29C; ventrobasal neurons, n = 4 and nRT neurons, n = 4), implicating $GABA_A$ receptor mediation.

3.3.1.2.2. Concentration-response relationship

The concentration dependent actions of amobarbital on the $GABA_A$ component of IPSC amplitude had an $EC_{50} = 61 \pm 7$ μM in ventrobasal neurons (n = 14; Figure. 3.29B) and $EC_{50} = 143 \pm 18$ μM in nRT neurons (n = 15; Figure. 3.29D). The EC_{50} values were significantly different in the two types of neurons (n = 5, $P<0.05$).

The IPSCs had a significantly longer decay time constant in nRT, compared to ventrobasal neurons held at -40 and -80 mV (Figure. 3.29A,C, Table 3.2). Amobarbital (50-500 μM) prolonged the IPSC decay in both neuron types by 10% to 800% of the control values. These actions were concentration-dependent, with $EC_{50} = 94 \pm 11$ μM (n = 15) in ventrobasal neurons and $EC_{50} = 309 \pm 33$ μM (n = 16) in nRT neurons (Figure. 3.29B,D). These two EC_{50} values were significantly different (n = 5, $P<0.05$). Thus, the IPSCs in ventrobasal neurons were more susceptible than nRT neurons to prolongation by amobarbital.

3.3.1.2.3. Neocortical IPSCs

As addressed above, neocortical IPSCs were mainly composed of $GABA_A$ receptors mediated component. Amobarbital (20-800 μM) reversibly increased IPSC amplitude and prolonged IPSC decay in neocortical neurons (n = 15; Figure 3.30A). Application of bicuculline (50 μM) eliminated almost all neocortical IPSCs (n = 5), which was consistent with our previous findings.

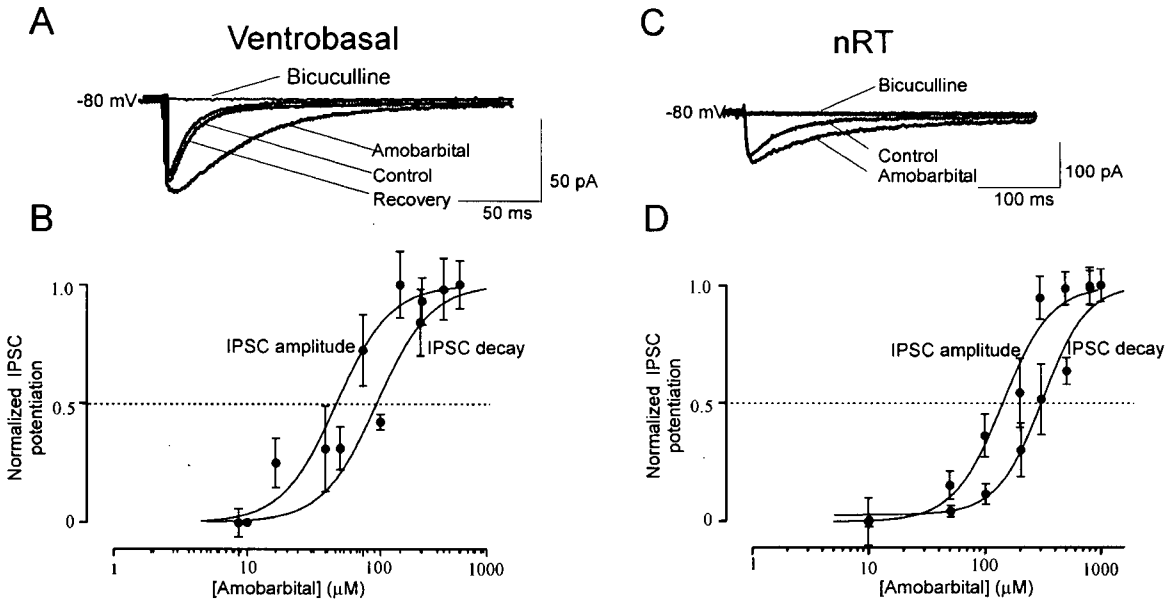

Figure 3.29 Amobarbital potentiated GABAergic IPSCs in ventrobasal and nRT neurons. (A, C) Amobarbital (100 μM in A and 200 μM in C) reversibly increased the amplitude and duration of IPSCs. Bicuculline (50 μM) abolished these effects. (B) The EC_{50} was 61.4 ± 7 μM for increasing amplitude and 94.3 ± 11 μM for prolonging the decay of IPSCs in ventrobasal neurons. (D) The EC_{50} was 142.4 ± 18 μM for increasing amplitude and 309 ± 33 μM for prolonging the decay of IPSCs in nRT neurons. Each data point (mean ± S.E.M) in B and D represents 3-6 neurons.

The amplitude of neocortical IPSCs was 59 ± 7 pA (n = 6) when neurons were held at –80 mV, which was similar with intra-reticular IPSCs (P>0.05; n = 6) and significantly larger than IPSCs recorded in ventrobasal neurons (P<0.05; n = 6). Neocortical IPSC had a decay time constant of 24 ± 4 ms (n = 6), which was significantly shorter than intra-reticular IPSCs (P<0.05; n = 6), and was slightly but not significantly longer than thalamocortical IPSCs recorded in VB neurons (P>0.05; n = 6). Amobarbital significantly increased neocortical IPSC amplitude and prolonged IPSC decay time constant (Figure 3.30A).

Amobarbital increased neocortical IPSC amplitude in a concentration-dependent manner with an EC_{50}=103 ± 7 μM (n = 12; Figure. 3.30B). The prolongation of IPSC decay time constant induced by amobarbital also depended on the applied concentration with an EC_{50}= 210 ± 22 μM (n = 12; Figure. 3.30C).

3.3.1.3. Actions on corticothalamic EPSPs in VB neurons

3.3.1.3.1. EPSP amplitude and duration

As addressed before, corticothalamic EPSPs were evoked by stimulating the internal capsule and were recorded in ventrobasal neurons. These corticothalamic EPSPs were composed of two components: non-NMDA receptors mediated component and NMDA receptors mediated component. Amobarbital (50-500 μM) suppressed corticothalamic EPSP amplitude by 5% to 50%, and did not change the decay time constant of EPSPs (Figure. 3.31A). This suppression was reversible after 15 min termination of the amobarbital application. These results indicated that amobarbital inhibited corticothalamic excitatory neurotransmission by suppressing EPSP amplitude.

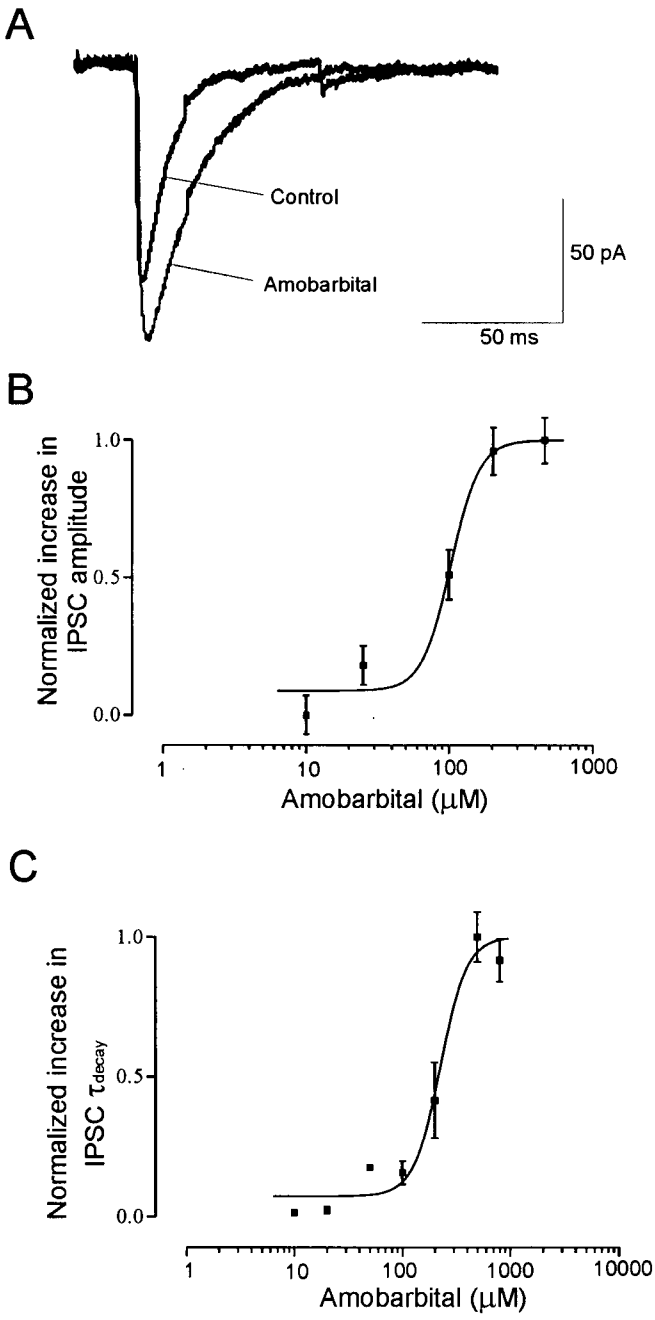

Figure 3.30. Amobarbital potentiated neocortical IPSCs. Neocortical IPSCs were isolated by co-application of APV (50 μM) and CNQX (25 μM) to block glutamatergic synaptic transmission. (A) Amobarbital increased IPSC amplitude and prolonged IPSC decay time constant in a neocortical neuron held at –80 mV. (B) Amobarbital increased neocortical IPSC amplitude in a concentration-dependent manner with an EC_{50}=103 ± 7 μM. (C) Amobarbital prolonged neocortical IPSC decay time constant in a concentration-dependent manner with an EC_{50}=210 ± 22 μM.

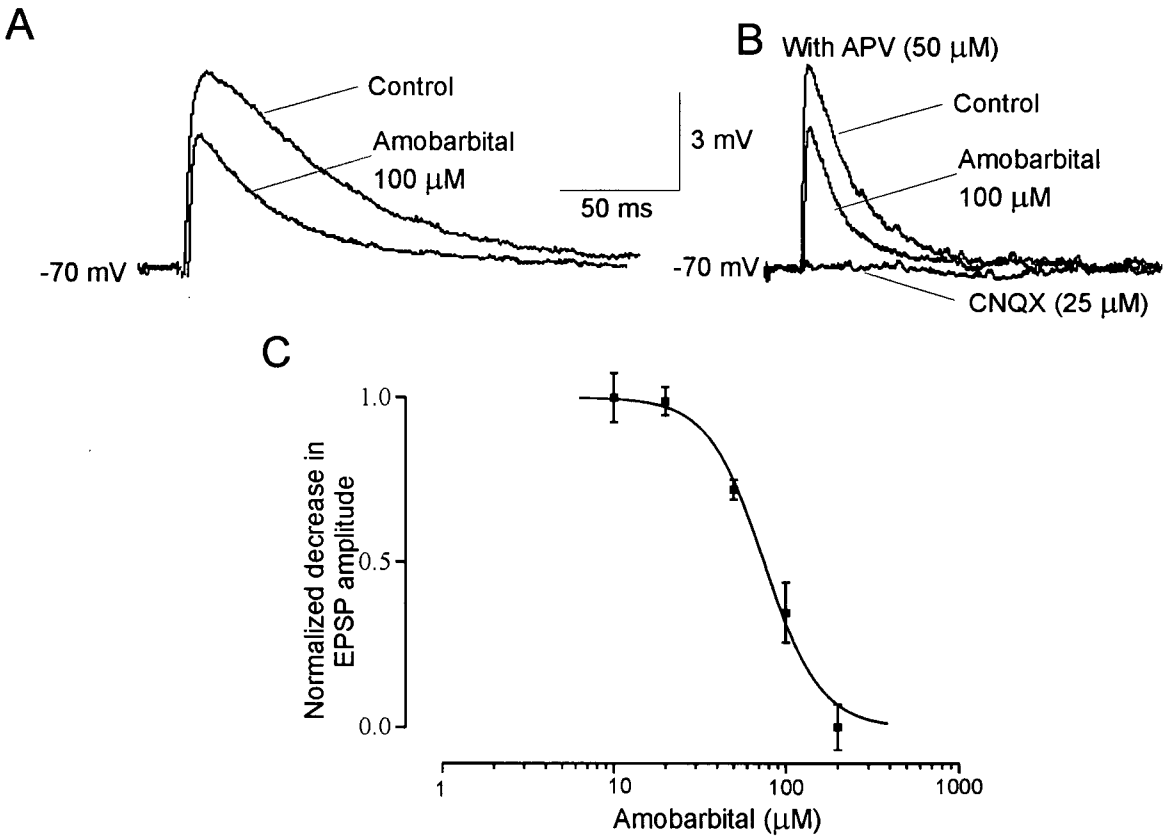

Figure 3.31. Amobarbital inhibited corticothalamic EPSPs. (A) Amobarbital (100 μM) depressed amplitude of EPSPs recorded in ventrobasal neurons by stimulating the internal capsule, which were isolated by co-application of picrotoxinin (50 μM) and CGP 35384 (100 μM). (B) With APV (50 μM) to block NMDA receptor mediated EPSPs, amobarbital (100 μM) depressed the remaining EPSPs, which was completely abolished by application of CNQX (25 μM). (C) Amobarbital depressed EPSPs in a concentration-dependent manner with an IC_{50}=81 ± 7 μM. Each data point was mean ± S.E.M of 3-6 neurons.

3.3.1.3.2. Concentration-response relationship

The decrease of corticothalamic EPSP amplitude induced by amobarbital was concentration dependent. The concentration-response of this action was fitted by sigmoidal function with an IC_{50}=81 ± 7 μM (n = 15; Figure. 3.31C). This value was significantly higher than IC_{50}, at which pentobarbital depressed EPSPs in VB neurons (n = 5; P<0.05).

3.3.1.3.3. Non-NMDA receptor mediation

To identify the receptor mechanism that mediated amobarbital-induced decrease on EPSP amplitude, APV (50 μM) were applied first, followed by co-application of APV and amobarbital (100 μM). With the blockade of NMDA receptors, amobarbital induced similar depression on the remaining non-NMDA receptor-mediated EPSPs (Figure. 3.31B). This depression was completely abolished by co-application with CNQX (25 μM; Figure. 3.31B). These data indicated that amobarbital suppressed corticothalamic EPSPs by blocking non-NMDA receptors.

3.3.1.3. *Single channel currents in VB and nRt neurons*

3.3.1.3.1. Direct activation of single $GABA_A$ channels

Amobarbital application activated single $GABA_A$ channels. Recordings in ventrobasal and nRT membrane patches held at -60 mV exhibited spontaneous inward currents at a low frequency, due to single channel openings. Amobarbital (100 μM) greatly increased channel openings in all patches, as shown for the ventrobasal patch in Figure 3.32A. Open probability did not differ in ventrobasal and nRT patches (Table 3.2).

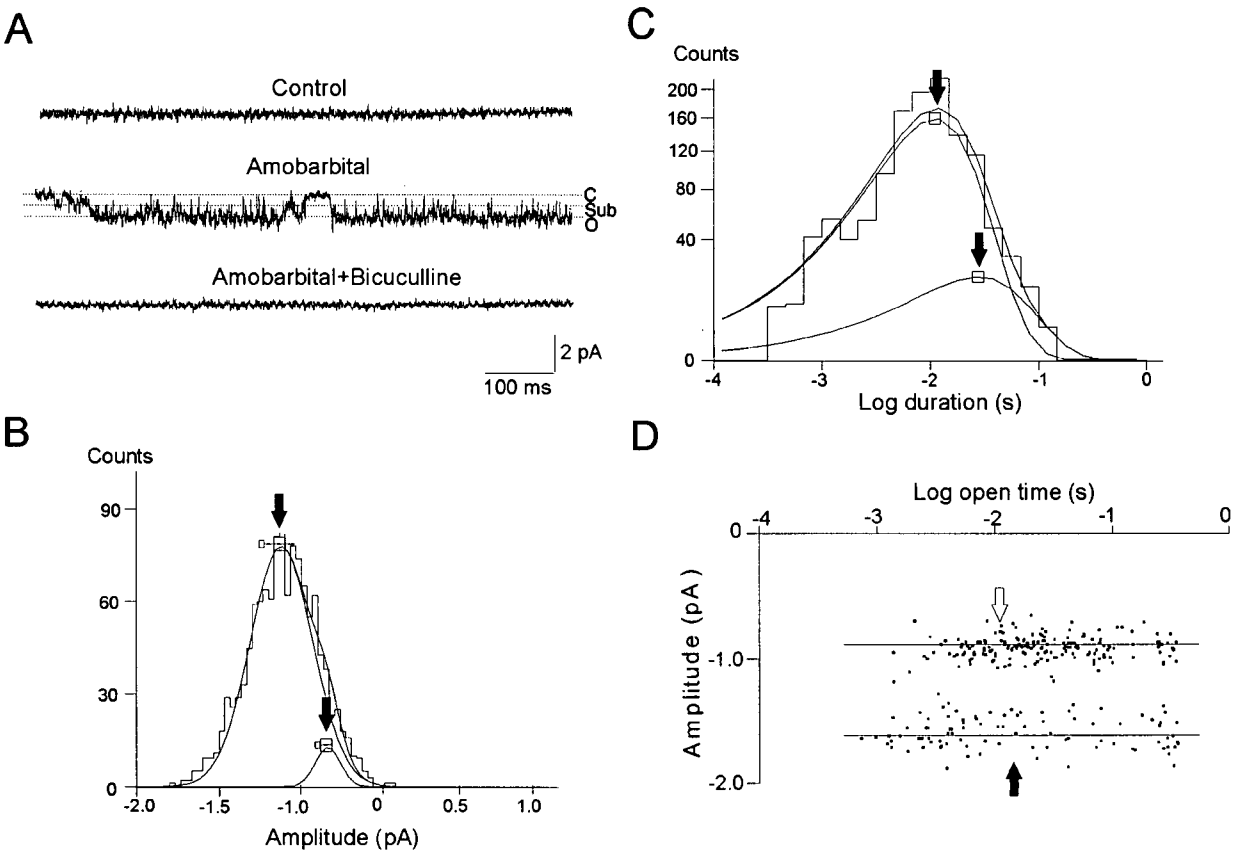

Figure. 3.32. Amobarbital activates single channels in nRT membrane patches. (A) amobarbital (100 μM) induced frequent channel openings that possessed two open state conductance levels, a main conductance (o) and a subconductance (sub) in an outside-out membrane patch held at V_H = -60 mV. Bicuculline (50 μM) blocked these channel openings. An amplitude versus duration scatter plot showed two discrete populations with mean amplitudes at -0.9 and -1.6 pA in different patch at V_H = -60 mV. The mean open times were, respectively, 10.9 and 13.1 ms, which were not significantly different. (B) shows distribution of channel amplitudes activated by amobarbital in another patch at V_H = -60 mV (number of events = 526). The distribution was fitted by the sum of two Gaussian curves representing the current levels of the main (-1.4 pA) and subconductance (-0.9 pA) states (see arrows). (C) Distribution of open times (number of events = 711) in different patch at V_H =-60 mV was well fitted by the sum of two exponential terms, $y = A_{of} \cdot e^{-t/\tau of} + A_{os} \cdot e^{-t/\tau os}$ with the following parameters (A_{of}, area of fast component; A_{os}, area of slow component; τ_{of}, time constant for fast component; τ_{os}, time constant for slow component). The fitted values were A_{of} = 0.8, τ_{of} = 8.3 ms, A_{os} = 0.2, τ_{os} = 78.0 ms (arrows indicate τ_{of} and τ_{os}).

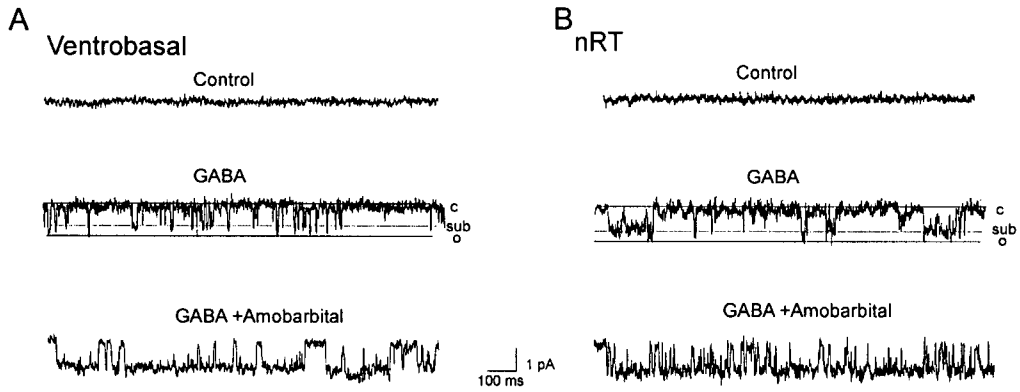

Figure 3.33. Properties of single GABA activated channels in outside-out ventrobasal (A) and nRT (B) membrane patches at V_H = -60 mV. (A, B) Application of GABA (10 μM) induced frequent channel openings showing a main conductance (o) and a subconductance (sub) state in ventrobasal (A) and nRT (B) membranes. Note that the mean channel open time in the nRT patch was longer than in the ventrobasal patch. On co-application with amobarbital (100 μM), channel open time was prolonged and most openings adopted a main conductance level in both membrane types.

Amobarbital-activated currents in membrane patches reversed polarity at 0 mV (not shown) which was the same as E_{Cl} in these experiments. Co-application with bicuculline (50 μM) eliminated the currents in all patches, as shown for the ventrobasal patch of Figure 3.32A. The reversal of the amobarbital-activated current at E_{Cl} and susceptibility to bicuculline antagonism implicated agonist actions at $GABA_A$ receptors.

In ventrobasal patches, the amplitude distributions of amobarbital-activated currents (Figure. 3.32B) showed a prominent peak that corresponded to a conductance state of 23 ± 1.1 pS (n = 5). In 2 out of 5 ventrobasal patches, the channels exhibited a subconductance state of ~16.0 pS (Figure. 3.32A,B). The channels in nRT membrane had the same main conductance (23 ± 1.7 pS, n = 5), as well as a subconductance state (~15 pS) in 2 out of 5 patches. Table 3.2 summarizes the similarities of amobarbital-activated channels in ventrobasal and nRT patches. Open time distributions for amobarbital-activated channels in ventrobasal and nRT patches were well described by the sum of two exponentials (see Figure. 3.32C). Mean open time did not differ between ventrobasal and nRT patches (Table 3.2). For both ventrobasal and nRT patches, scatter plots of current amplitude as a function of open time (see Figure. 3.32D) revealed that main conductance and subconductance states had similar mean open times.

3.3.1.4.2. Enhancement of GABA currents

In view of the potentiation of fast IPSCs by amobarbital, we examined its effects on single channel currents activated by exogenous GABA application, establishing a baseline for amobarbital's effects. GABA (10 μM) evoked inwardly directed currents in 13 patches (Figure. 3.33A,B) that were sensitive to blockade by bicuculline (50 μM) and had an extrapolated reversal potential near 0 mV, similar to E_{Cl} (Figure. 3.33C). GABA activated channels had a

main open state conductance of 16 ± 0.4 pS (n = 5) in ventrobasal, and 17 ± 0.8 pS (n = 5) in nRT patches. In a few patches, GABA activated channels showed a second, higher conductance state of 23 ± 1.0 pS (n = 4) for ventrobasal, and 24 ± 1.4 pS (n = 4) for nRT patches (Figure. 3.33, 3.34). As expected (Browne et al., 2001), the mean conductance of GABA-activated channels was not significantly different in ventrobasal and nRT patches (Table 3.2). Open time distributions of GABA channels were well fitted by the sum of two exponential terms (Figure. 3.35A,B). The mean open probability and channel open time were significantly higher in nRT, than in ventrobasal patches (Table 3.2). The mean conductance of GABA channels, and the dual conductance states, did not greatly differ from amobarbital-activated channels.

Amobarbital was co-applied with GABA (10 μM) and resultant single channel currents were recorded (Figure. 3.33). Amplitude distributions for currents seen during co-application of amobarbital and GABA to all patches displayed a single peak (Figure. 3.34), corresponding to a mean conductance of 24 ± 0.4 pS (n = 4) in ventrobasal, and 25 ± 2.1 pS (n = 4) in nRT patches (Table 3.2). This conductance state was comparable to that occasionally seen during GABA or amobarbital application. However, the mean conductance was significantly higher than that observed during application of either agonist alone (Table 3.2). This implied that amobarbital stabilized the $GABA_A$ receptor in the high conductance state.

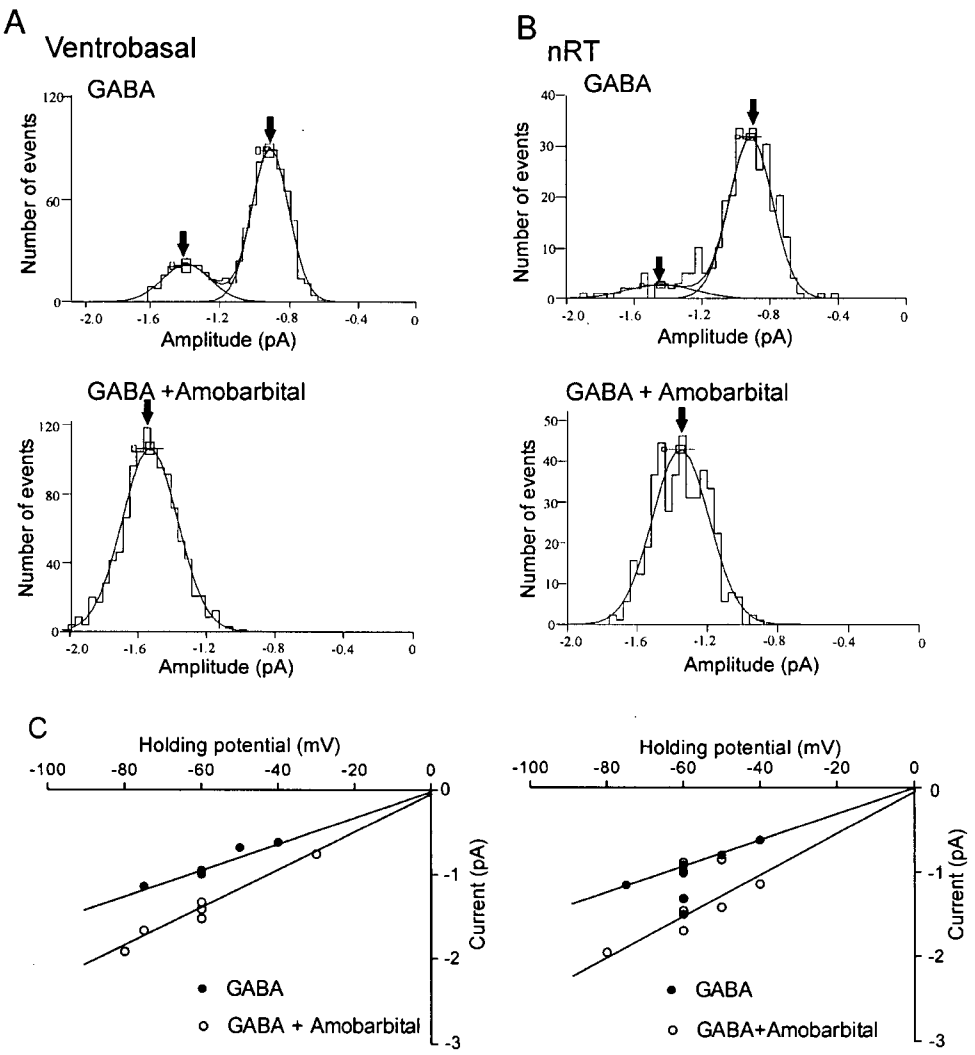

Figure 3.34. Amplitude histograms and current-voltage plots for single channels activated by GABA, alone (10 μM), or with amobarbital (100 μM) in ventrobasal and nRT patches. (A, B) Amplitude histograms of GABA activated single channel currents were well fitted by the sum of two Gaussian curves, which showed two current levels, corresponding to main conductance and subconductance states in ventrobasal and nRT patches (see arrows). In ventrobasal patch, higher amplitude was -1.4 pA and lower amplitude was -0.9 pA (n = 1240). In nRT patch, higher amplitude was -1.4 pA and lower amplitude was -0.9 pA. Amplitude histograms for currents during co-application of amobarbital and GABA were well fitted by single exponential curves in ventrobasal and nRT patches. Mean amplitudes were -1.5 pA in ventrobasal, and -1.5 pA in nRT patches (number of events = 1476 in ventrobasal, and 720 in nRT patches). (C) Current activated by GABA or GABA with amobarbital had an extrapolated reversal potential near 0 mV in both patch types. Current-voltage relationships are shown for both main and subconductance levels.

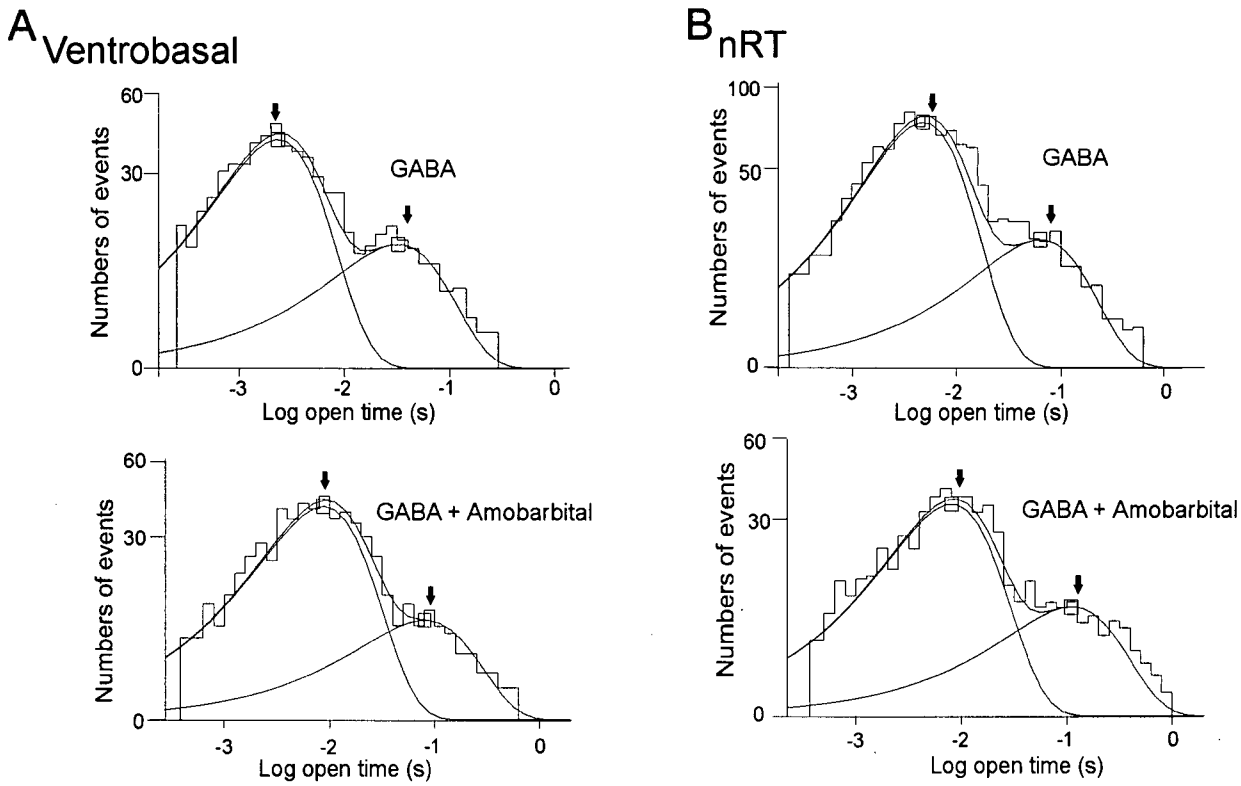

Figure 3.35. Open time histograms for single channel currents activated by GABA, alone (10 μM), or with amobarbital (100 μM) in ventrobasal and nRT patches. (A) Open time distribution in ventrobasal patch clamped at V_h = -60 mV during GABA or co-applied GABA and amobarbital. These distributions were well fitted by the sum of two exponential terms. The fit parameters in ventrobasal patch (A) were τ_{of} = 2.2 ms, A_{of} = 0.8, τ_{os} = 32.0 ms and A_{os} = 0.2 for GABA (number of events = 798), and τ_{of} = 8.8 ms, A_{of} = 0.8, τ_{os} = 80.3 ms and A_{os} = 0.18 for GABA with amobarbital (number of events = 828). The fit parameters in nRT patch (B) were τ_{of} = 4.8 ms, A_{of} = 0. 8, τ_{os} = 63.8 ms and A_{os} = 0.2 for GABA (number of events = 1512), and τ_{of} = 8.0 ms, A_{of} = 0.8, τ_{os} = 110.0 ms and A_{os} = 0.20 for GABA with amobarbital (number of events = 902).

Open time distributions for ventrobasal and nRT channels activated during co-application of GABA and amobarbital were well described by the sum of two exponential terms (Figure. 3.35). Table 3.3 shows the parameter estimates from these distributions. Co-application of GABA and amobarbital resulted in an increase in the time constant for long-, but not short-duration channel openings in ventrobasal patches. In nRT patches, the time constant for short-duration openings was also greatly enhanced (Table 3.3). This implied that amobarbital stabilized the $GABA_A$ receptor in open channel configurations. Closed time distributions for ventrobasal and nRT channels activated during co-application of GABA and amobarbital were well described by the sum of three exponential terms. Amobarbital (100 μM) co-applied with GABA (10 μM) shortened the mean closed time (Table 3.2). In both ventrobasal and nRT patches, the combined effects on channel open and closed times resulted in a significant increase in the open probability during co-application of amobarbital with GABA (Table 3.2).

3.3.1.4.3. Prolongation of $GABA_A$ channel burst duration

As seen in Table 3.2, a poor correlation existed between the mean open time of GABA activated channels and the decay time constants of fast IPSCs, recorded in ventrobasal and nRT neurons. However, the calculated mean burst durations of GABA activated channels were in accordance with fast IPSC decay time constants (Table 3.2). This agreement was retained after application of amobarbital (Table 3.2). Hence, the prolongation of fast IPSC decay by amobarbital was likely due to increased mean burst duration of $GABA_A$ channels.

Table 3.2. Effects of amobarbital (100 μM) on amplitude and decay of fast $GABA_A$ergic IPSCs and single channel currents activated by GABA (10 μM).

	Ventrobasal neurons or membrane patches			nRT neurons or membrane patches		
	Control (n = 5)	Amo (n = 5)		Control (n = 5)	Amo (n = 5)	
IPSC amplitude (pA)	42 ± 5	55 ± 6[a]		54 ± 5[h]	67 ± 5[e]	
IPSC τ_{decay}(ms)	20 ± 4	51 ± 7[a]		41 ± 5[h]	64 ± 7[e]	
Mean burst duration (ms)	17.8 ± 0.82	46.7 ± 1.7[a]		35.8 ± 1.3[h]	58.3 ± 1.6[e]	
	Amo (n = 5)	GABA (n = 6)	GABA + Amo (n = 6)	Amo (n = 5)	GABA (n = 7)	GABA + Amo (n = 7)
Open probability	0.25± 0.06[b]	0.038 ± 0.009	0.39 ± 5.1[c, d]	0.31 ± 0.005	0.15 ± 0.038[h]	0.41 ± 0.072[g]
Mean conductance (pS)	20.1 ± 1.4[b]	15.7 ± 0.4	24.1 ± 0.4[c, d]	19.2 ± 1.9	16.5 ± 0.8	24.8 ± 2.1[f, g]
Mean open time (ms)	14.3 ± 1.1[b]	8.9 ± 0.4	19.2 ± 1.9[d]	16.1 ± 2.4	17.0 ± 2.3[h]	26.7 ± 3.1[f, g, h]
Mean closed time (ms)	26.9 ± 13.3[b]	87.8 ± 16.6	22.4 ± 5.9[d]	29.9 ± 10.5	38.2 ± 8.2	28.8 ± 6.2

Parameters were defined in text. Significant differences ($P<0.05$) in ventrobasal patches or neurons are denoted as [a]Control versus amobarbital, [b]amobarbital versus GABA, [c]amobarbital versus GABA + amobarbital, [d]GABA versus GABA + amobarbital; in nRT patches or neurons, significance is denoted as [e]Control versus amobarbital, [f]amobarbital versus GABA + amobarbital, and [g]GABA versus GABA + amobarbital. Significant differences between patches or neurons are denoted as [h]ventrobasal nuclei versus nRT. Holding potential = -60 mV.

Table 3.3. Kinetic parameters derived from biexponential fits to open time distributions for channels activated by amobarbital (100 μM), GABA (10 μM) or during co-application of amobarbital and GABA.

	Ventrobasal patches			nRT patches		
	Amo (n = 5)	GABA (n = 6)	GABA + Amo (n = 6)	Amo (n = 5)	GABA (n = 7)	GABA + Amo (n = 7)
τ_{of} (ms)	3.9 ± 0.6[a]	1.3 ± 0.09	10.9 ± 0.7[b, c]	8.4 ± 1.6	4.7 ± 0.62	7.1 ± 1.0
A_{of}	0.86 ± 0.07	0.77 ± 0.09	0.86 ± 0.02	0.74 ± 0.05	0.73 ± 0.03	0.8 ± 0.02
τ_{os} (ms)	34.6 ± 5.4	35.1 ± 1.5	85.3 ± 19.1[b, c]	43.5 ± 8.5	57.2 ± 11.2	116 ± 23[d]
A_{os}	0.14 ± 0.07	0.23 ± 0.09	0.14 ± 0.03	0.26 ± 0.05	0.27 ± 0.03	0.2 ± 0.02

Parameters were defined in text. Significant differences ($P<0.05$) are denoted in ventrobasal patches as [a]amobarbital versus GABA, [b]amobarbital versus GABA + amobarbital, and [c]GABA versus GABA + amobarbital; and in nRT patches, as [d]amobarbital versus GABA + amobarbital. Holding potential = -60 mV.

3.3.*2. Phenobarbital actions on neuronal firing and synaptic transmission in thalamocortical and neocortical neurons*

Phenobarbital was the first organic, and is still one of the most effective anti-epileptic agents. Phenobarbital is very effective in relieving generalized tonic-clonic and simple partial seizures. However, it worsens or lacks efficacy in the treatment of absence seizures (Mattson, 1995). The cortico-thalamocortical system is crucial for the generation of seizures, including absence seizures (Hosford, et al., 1997). Therefore, a study of phenobarbital's action on neurons in this system will further our understanding of the mechanisms of phenobarbital's distinct effects in the treatment of epilepsy.

3.3.2.1. Neuronal firing

Phenobarbital (50-300 μM) inhibited neuronal firing in neocortical neurons. Figure 3.35A shows that phenobarbital (150 μM) inhibited multiple firing of a neocortical neuron held at –66 mV. The blockade was reversible after 15 min termination of phenobarbital application. In contrast to effects in neocortical neurons, phenobarbital (150 μM) did not inhibit neuronal firing in nRT and ventrobasal neurons (Figure. 3.36B,C), but application of a higher concentration of phenobarbital (500 μM) reversibly suppressed neuronal firing in these neurons (Figure 3.36B,C). Phenobarbital did not significantly alter the amplitude or the duration of action potentials in neocortical, nRT and ventrobasal neurons.

In summary, at clinically relevant concentrations, phenobarbital selectively inhibited repetitive neuronal firing in neocortical neurons. At higher concentrations, phenobarbital depressed neuronal firing in thalamic neurons. These results implied that different types of neurons in the CTC system reacted to phenobarbital-induced inhibition with different susceptibility.

3.3.2.2. Membrane properties

Phenobarbital (150 μM) induced 4 ± 2 mV (n = 4) depolarization of resting membrane potential in neocortical neurons. However, at this concentration, phenobarbital did not alter resting membrane potential in nRT (n = 4) and ventrobasal neurons (n = 4). At higher concentrations (500 μM), phenobarbital caused ~ 2-3 mV depolarization in resting membrane potential of ventrobasal and nRT neurons (P>0.05; n = 4). Phenobarbital (10-300 μM) did not significantly decrease R_i in neocortical (n = 8), ventrobasal (n = 6) and nRT (n = 6) neurons (P>0.05).

3.3.2.3.Concentration-response for neuronal firing suppression

Phenobarbital inhibited repetitive neuronal firing in a concentration-dependent manner in neocortical neurons in the concentration range from 50 to 500 μM. The IC_{50} of this action was 161 ± 12 μM (n = 12; Figure. 3.37A). In ventrobasal and nRT neurons, 100 μM phenobarbital did not significantly alter neuronal firing (n = 4, P>0.05 in ventrobasal neurons; and n = 5, P>0.05 in nRT neurons; Figure 37B, C). However, phenobarbital (500 μM) significantly decreased neuronal firing in ventrobasal and nRT neurons (n = 9, P<0.05; Figure 3.37B, C).

3.3.2.3. Neocortical IPSCs

Neocortical IPSCs were evoked by electrically stimulating layer III neurons and were recorded in layer IV neurons. As addressed before, neocortical IPSCs were mainly mediated by $GABA_A$ receptors. Phenobarbital (100 μM) significantly prolonged IPSC decay time constant without altering IPSC amplitude (Figure. 3.38A). The prolongation of phenobarbital was completely blocked by co-application with bicuculline (50 μM) or picrotoxinin (50 μM).

Phenobarbital prolonged neocortical IPSCs in a concentration-dependent manner. The EC_{50} of this action was 141 ± 13 μM (n = 14; Figure. 3.38C). There was no significant difference between IC_{50}, at which phenobarbital depressed neuronal firing, and EC_{50}, at which phenobarbital prolonged IPSC decay time constant in neocortical neurons (n = 5; P>0.05). These data indicated that phenobarbital prolonged the decay time constant of $GABA_A$ergic IPSCs in a concentration-dependent manner.

3.2.2.4. Thalamocortical IPSCs

Thalamocortical IPSCs were electrically evoked by stimulating nRT and were recorded in ventrobasal neurons. V_H was held at –80 mV to eliminate the K^+-related contribution. Phenobarbital (10-400 μM) did not significantly alter either the amplitude or the decay time constant of thalamocortical IPSCs. When the applied concentrations were higher than 400 μM, phenobarbital slightly increased IPSC amplitude by ~ 10 % and significantly prolonged IPSC decay time constant (Figure 3.38B). These effects were blocked by co-application with bicuculline (50 μM) or picrotoxinin (50 μM), indicating $GABA_A$ receptor mediation.

In summary, phenobarbital selectively suppressed neuronal firing and potentiated GABAergic IPSCs in neocortical neurons, in concentration-dependent manners. At clinically relevant concentrations (40-150 μM), phenobarbital did not induce depression in thalamic neurons, which may account for its lack of efficacy in the treatment of absence epilepsy.

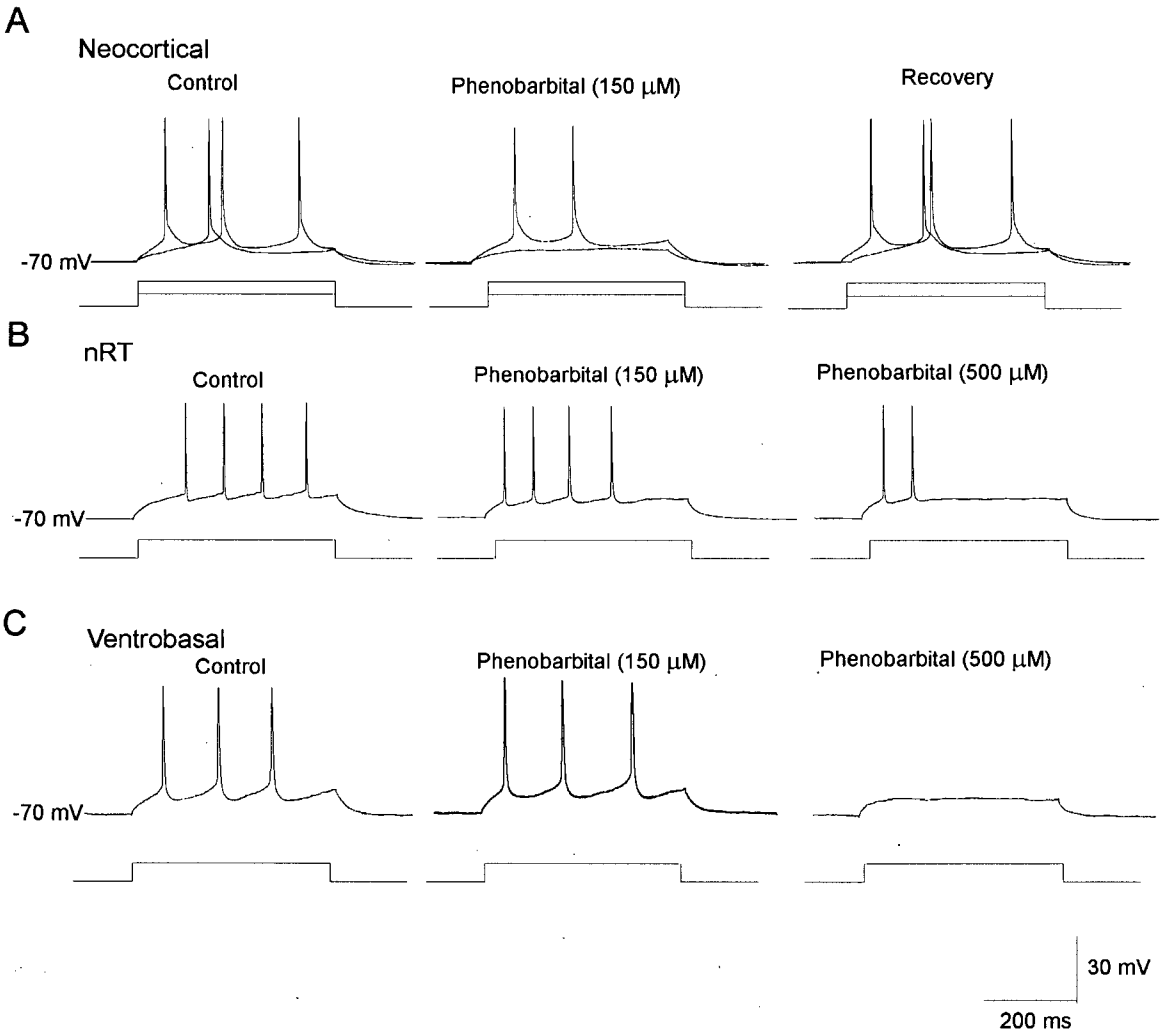

Figure 3.36. Phenobarbital selectively inhibited neuronal firing in neocortical neurons. (A) Phenobarbital (100 μM) inhibited tonic firing of neocortical neurons held at –66 mV. The recovery can be obtained after 15 min termination of phenobarbital application. (B) In a nRT neuron, phenobarbital (100 μM) did not inhibit neuronal firing, whereas a higher concentration of phenobarbital application (500 μM) depressed neuronal firing. (C) Similar to nRT neurons, phenobarbital (100 μM) did not inhibited neuronal firing in a ventrobasal neuron, whereas 500 μM phenobarbital depressed neuronal firing.

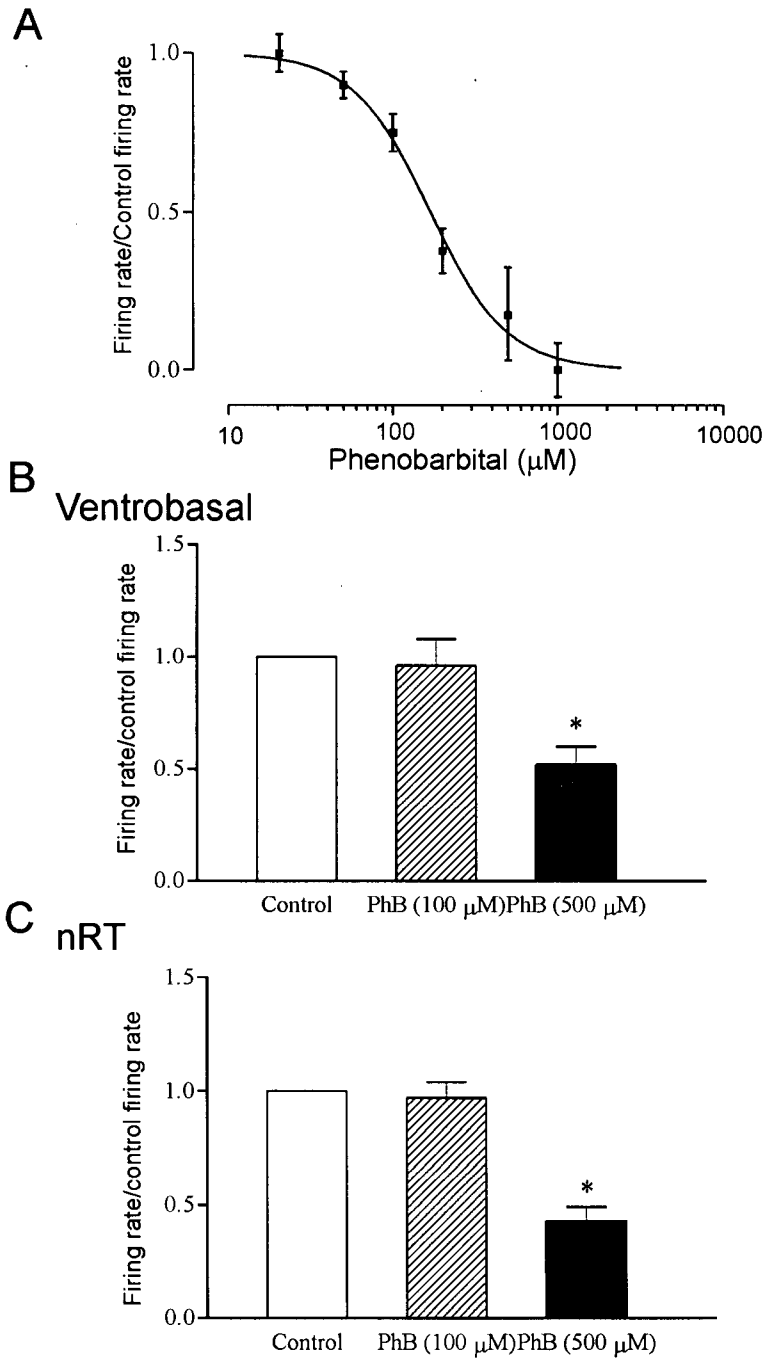

Figure 3.37. Phenobarbital selectively inhibited neuronal firing in neocortical neurons. (A) In neocortical neurons, phenobarbital depressed neuronal firing in a concentration-dependent manner with an IC_{50} = 161 ± 12 μM. (B) In ventrobasal neurons, phenobarbital (100 μM) did not significantly alter neuronal firing rate, whereas 500 μM phenobarbital induced 48% reduction of neuronal firing compared to control. (C) In nRT neurons, phenobarbital (100 μM) did not significantly alter neuronal firing rate, whereas 500 μM phenobarbital induced 54% reduction of neuronal firing compared to control. * $P< 0.05$, firing rate significantly different from control

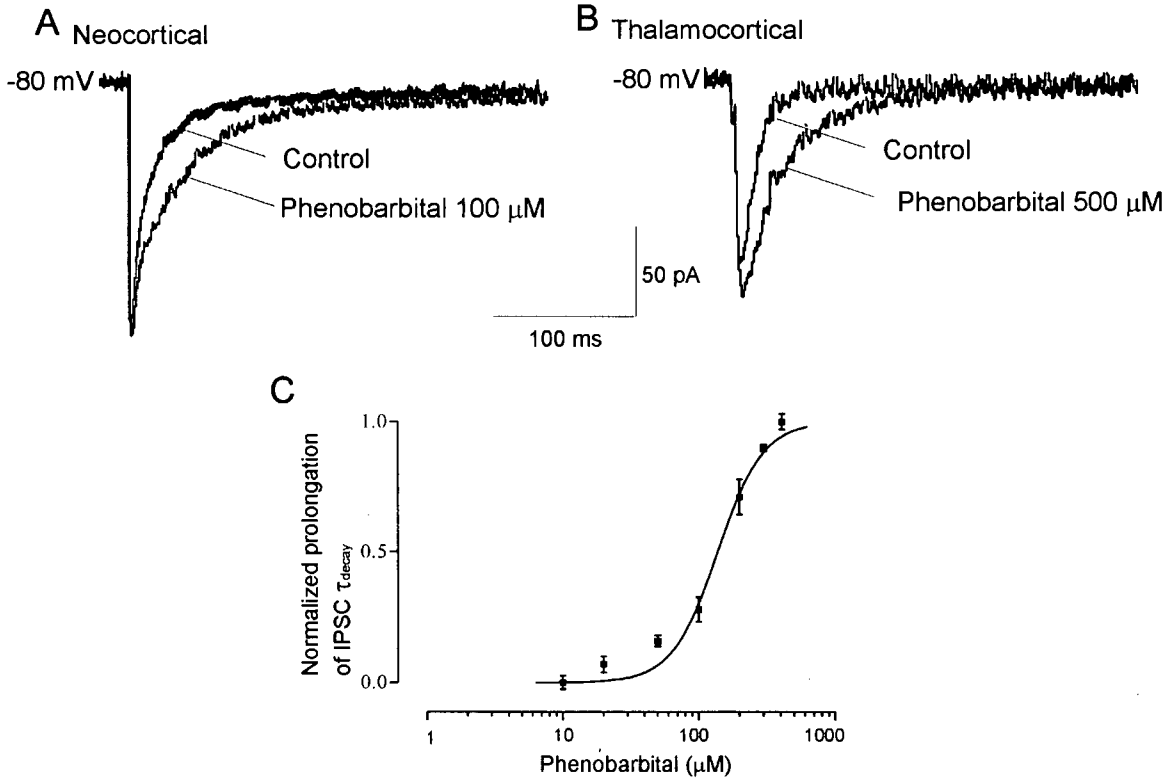

Figure 3.38. Phenobarbital selectively potentiated neocortical IPSCs. (A) While phenobarbital (100 μM) prolonged neocortical IPSC decay time constant, while it did not significantly alter IPSC amplitude. (B) 100 μM phenobarbital did not change thalamocortical IPSCs recorded in a ventrobasal neuron. 500 μM phenobarbital increased amplitude and prolonged the decay of thalamocortical IPSCs. (C) Phenobarbital prolonged neocortical IPSCs in a concentration-dependent manner with an EC_{50}=141 ± 13 μM. Each data point was mean ± S.E.M of 3-6 neurons.

Chapter 4
DISCUSSION

4.1. Summary of the results

This thesis studied the actions of three barbiturates on non-synaptic intrinsic ion channels and synaptic transmission on neurons of the CTC system based on concentration-dependence. The aim of this thesis was to determine potential mechanisms that may contribute to *in vivo* effects of barbiturates.

4.1.1. Summary of pentobarbital actions

Pentobarbital suppressed action potentials and decreased neuronal excitability in thalamocortical neurons by several mechanisms. Firstly, pentobarbital decreased non-NMDA receptor-mediated corticothalamic EPSP amplitude. This action may be attributable to the blockade of postsynaptic non-NMDA receptors by pentobarbital.

Secondly, pentobarbital prolonged GABAergic IPSCs by enhancing the open probability of single $GABA_A$ channels. The EC_{50} for this action was significantly higher than EC_{50} for the suppression of neuronal firing by pentobarbital. This implies that the potentiation of IPSCs may not be an absolute requirement for pentobarbital-induced inhibition.

Thirdly, at low micromolar concentrations (EC_{50} = 8 μM), pentobarbital increased membrane conductance, which shunted action potential spike generation. This depressant

action did not involve known types of GABA receptor interactions. However, pentobarbital increased leak and inward rectifying K^+ currents.

Fourthly, at similar low concentrations, pentobarbital decreased a hyperpolarization-activated Na^+/K^+ inward current (I_h). The decrease of I_h and activation of leak and inward rectifying K^+ currents contributed to the net outward current induced by pentobarbital. This outward current reversed at –76 mV.

In nRT and neocortical neurons, pentobarbital modulated neuronal excitability by similar mechanisms as in thalamocortical neurons, but at higher concentrations. The lower EC_{50} in thalamocortical neurons implicates that these neurons were more susceptible to pentobarbital action compared to nRT and neocortical neurons. This implies that different types of neurons in the CTC system may have different roles in pentobarbital effects *in vivo*.

4.1.2. Summary of amobarbital actions

Although amobarbital is an isomer of pentobarbital, it exerted significantly different actions on neurons of the CTC system. Amobarbital suppressed glutamatergic excitatory neurotransmission, increased the amplitude and prolonged the decay of $GABA_A$ergic IPSCs. Amobarbital did not alter intrinsic ion channels in all types of neurons that we examined. However, amobarbital exerted modulatory and agonist actions at $GABA_A$ receptors, increasing channel open probability and conductance in thalamic neurons. Hence, amobarbital decreased neuronal excitability, producing inhibition on spontaneous firing by modulating synaptic transmission.

4.1.3. Summary of phenobarbital actions

Phenobarbital, which has anti-epileptic properties, selectively decreased neuronal excitability by inhibiting repetitive neuronal firing and potentiating GABAergic synaptic transmission in neocortical neurons. However, at clinically relevant concentrations, phenobarbital did not significantly alter neuronal repetitive firing or inhibitory neurotransmission in thalamic neurons. This may provide an explanation for phenobarbital's efficacy in the treatment of generalized tonic-clonic and simple partial seizures, and a lack of efficacy in the treatment of absence seizures (Mattson, 1995).

In summary, barbiturates modulated neuronal excitability in the cortico-thalamocortical system by multiple mechanisms. These actions on synaptic transmission and non-synaptic intrinsic ion channels have different but overlapping concentration-dependence, which may contribute to varying levels of inhibition from sedative-hypnosis to general anesthesia.

4.2. Pentobarbital actions in the CTC system

4.2. 1. Blockade of neuronal firing

Pentobarbital blocked tonic and burst firing of Na^+ dependent action potentials in thalamocortical neurons through a decrease in membrane resistance, which shunted spike generation. The increase in membrane conductance would inhibit the synaptic relay of voltage transfers through the thalamus and the cortex by reducing neuronal integration in the dendrites and Na^+-spike excitabilities in the axon and then affect transmitter release at corticothalamic and thalamocortical synapses. An increase in conductance by pentobarbital would both shunt the voltage response to excitatory synaptic current inputs and reduce the time-dependent voltage responses during electronic conduction. As a result, synaptic

summation in both the spatial and temporal domain would be undermined and many passive dendritic signals would decay before propagating to the soma and axon hillock.

Pentobarbital-induced inhibition on neuronal firing may also involve in decrease in Na^+ dependent inward rectification on depolarization to threshold. Normally, thalamic neurons inwardly rectify in a range between the resting potential and threshold (~-50 mV; Jahnsen and Llinas 1984; Tennigkeit et al., 1996a), due to a persistent Na^+ current that activates at potentials as negative as –75 mV (Parri and Crunelli 1998). Tetrodotoxin (TTX) eliminated both Na^+-dependent rectification and the pentobarbital-induced decrease in membrane resistance at depolarized voltages in the majority of thalamocortical neurons. An increase in the input current evoked a return of Na^+ dependent action potentials during pentobarbital application. The rate of rise of action potentials did not decrease, substantially, during the pentobarbital blockade of Na^+ dependent rectification. This implies that pentobarbital application may produce effects similar to TTX application at low concentrations, i.e., pentobarbital may have produced a greater block of the persistent Na^+ current rather than the transient Na^+ current, which underlies the action potential (cf. Blaustein 1968; Tennigkeit et al., 1998a).

Pentobarbital inhibited neuronal firing and increased membrane conductance in neurons of the CTC system with different IC_{50}s. These IC_{50}s were the lowest in thalamocortical neurons and the highest in neocortical neurons. It is not clear why thalamocortical neurons were more sensitive to the pentobarbital-induced increase in membrane conductance. However, this may be due to a difference in leak K^+ channel distribution in the thalamus and the neocortex. For example, at P14 rats, expression of TASK-1 is higher in thalamocortical and nRT neurons

compared to neocortical neurons (Brickley et al., 2001). Pentobarbital activates leak K^+ channels to increase membrane conductance and shunt action potentials (Wan et al., 2003), which could be more prominent in thalamocortical neurons compared to neocortical neurons due to different expression levels of leak K^+ channels.

4.2.2. Depression of corticothalamic EPSPs

At intermediate concentrations, pentobarbital suppressed corticothalamic EPSPs. There was an approximately four-fold difference in the IC_{50}s for EPSP suppression and decreased R_i. This suggests that the suppression of the EPSP was not simply due to a low resistance shunt but was likely a consequence of an independent pentobarbital action. Pentobarbital depressed the fast non-NMDA component of the corticothalamic glutamatergic EPSPs. This is consistent with the observations in other CNS neurons that pentobarbital decreases EPSPs (Sawada and Yamamoto, 1985) and kainate-induced currents much more than NMDA-induced currents (Marszalec and Narahashi, 1993; Essin et al., 2002). In contrast, inhalational and intravenous non-barbiturate anesthetics selectively reduce the NMDA-receptor mediated component of EPSPs in hippocampal and spinal neurons (Orser et al., 1995; Cheng and Kendig, 2000). The postsynaptic actions of pentobarbital on EPSPs may depend on particular receptor components, such as the GluR2 receptor subunit (Essin et al., 2002) which is expressed in the thalamus (Spreafico et al., 1994). Like inhalational anesthetics (Kitamura et al., 2003), pentobarbital may also decrease glutamate release from nerve terminals (Potashner and Lake, 1981), depressing excitatory transmission. In summary, pentobarbital inhibited excitatory neurotransmission in thalamic neurons, which decreased neuronal excitability and may contribute to pentobarbital-induced anesthesia *in vivo*.

4.2.3. Increases of IPSC duration and open probability of $GABA_A$ channels

At higher concentrations, pentobarbital prolonged GABAergic IPSCs in thalamocortical neurons, nRT neurons and neocortical neurons. Pentobarbital induced potentiation of inhibitory postsynaptic responses also occurs in hippocampal neurons (Weiss and Hablitz, 1984; Zhang et al., 1993) at >5-fold concentrations than required for the effects on non-ligand gated ion channels. Pentobarbital did not greatly alter IPSC amplitude but slowed the decay of fast IPSCs mediated by $GABA_A$ receptors, and independently of $GABA_B$ receptors in thalamocortical neurons. This implies that pentobarbital had little or no pre-synaptic actions on evoked GABA release in these neurons. However, we cannot exclude presynaptic effects of pentobarbital (see Richards, 2002) on spontaneous release of GABA, as observed with inhalational anesthetics (Kitamura et al., 2003). Postsynaptically, $GABA_A$ receptors assembled from most subunit combinations are sensitive to barbiturate potentiation (Thompson et al., 1996; Greenfield et al., 2002). As reported for other CNS preparations (Mathers, 1985; Macdonald et al., 1989; Eghbali et al., 2000; Steinbach and Akk, 2001), pentobarbital enhanced the stability of activated $GABA_A$ channels in thalamocortical neurons, which was examined in this thesis by applying single channel recording.

Pentobarbital did not alter the conductance of single $GABA_A$ receptor channels in ventrobasal neurons, consistent with its lack of effect on fast IPSC amplitude in thalamocortical neurons. Similar results were reported for other native and recombinant $GABA_A$ receptors that exhibit only a few, closely spaced conductance states (Mathers, 1985; Macdonald et al., 1989; Steinbach and Akk, 2001). However, some CNS neurons have $GABA_A$ receptors that display multiple subconductance states (Guyon et al., 1999; Eghbali et al., 2000). Barbiturates preferentially stabilize these receptors in their higher conductance states (Eghbali et al.,

2000). In this study, pentobarbital application at 100 μM produced negligible activation of single $GABA_A$ channels that would signal direct receptor agonism. The $GABA_A$ receptors in our preparations were functional, as evident from $GABA_A$ receptor activation by muscimol and the elimination of the fast IPSC component by $GABA_A$ receptor antagonists. The $GABA_A$ receptor α_6 subunit, which imparts high affinity for direct receptor activation by pentobarbital (Thompson et al., 1996), is absent in ventrobasal neurons (Wisden et al., 1992; Browne et al., 2001). Barbiturates only weakly activate receptors containing the α_1 and β_2 subunits, prevalent in rat thalamocortical neurons (Thompson et al., 1996; Wisden et al., 1992). Thalamocortical neurons also express high levels of the α_4 and δ subunits (Wisden et al., 1992), which, when combined with $\beta_{2/3}$ subunits produce channels poorly activated by pentobarbital (Adkins et al., 2001). Hence, $GABA_A$ receptors in thalamocortical neurons frequently lack the receptor subunits required for efficient direct activation by pentobarbital.

Pentobarbital prolonged neocortical, intra-reticular and thalamocortical IPSC decay with different IC_{50}s. These IC_{50}s were the lowest in thalamocortical IPSCs recorded in VB neurons, and were followed by intra-reticular IPSCs and neocortical IPSCs. This divergence may be due to different subunit compositions of $GABA_A$ receptors in VB, nRT and neocortex (Wisden et al., 1992). VB neurons expressed higher levels of β_2 subunits than nRT and neocortical neurons, which enhance the ability of pentobarbital to potentiate GABA actions at $GABA_A$ receptors (Cestari et al., 1996; Harris et al., 1995). Hence, the higher potency of pentobarbital to prolong thalamocortical IPSCs may be attributable to the higher expression level of β_2 subunits of $GABA_A$ receptors.

In contrast to the actions in VB neurons, pentobarbital slightly increased IPSC amplitude in addition to prolonging IPSC decay time constant in nRT and neocortical neurons. nRT and neocortex express much lower α_4 and $\beta_{2/3}$ but higher $\alpha_{2/3}$ subunits (Wisden et al., 1992). Most importantly, instead of δ subunit, which is expressed in thalamic relay neurons, γ_2 subunit is expressed in the RT and the neocortex, which enables direct activation of $GABA_A$ receptors by pentobarbital (Wisden et al., 1992; Adkins et al., 2001). These results imply that different actions of pentobarbital on GABAergic IPSC in different neuron types of the CTC system may be attributable to different subunit combinations of $GABA_A$ receptor in these neurons.

4.2.4. Increases of membrane conductance independent of GABA receptors

Pentobarbital suppressed neuronal firing and increased membrane conductance in thalamocortical neurons that resisted pharmacological blockade of $GABA_A$, $GABA_B$ and $GABA_C$ receptors. The $GABA_A$ receptor antagonists, bicuculline and picrotoxinin, did not block pentobarbital-induced decreases in tonic and burst firing. These agents, which interact at distinct sites on the $GABA_A$ receptor complex, did not affect the accompanying increase in input conductance. This is similar to the findings in frog spinal motoneurons (Nicoll and Madison 1982). Interestingly, these antagonists do not block the pentobarbital suppression of L-type Ca^{2+} plateau potentials in turtle spinal motoneurons (Guertin and Hounsgaard 1999). In neocortical neurons of P0-P1 rats, bicuculline antagonizes the depressant effects of $GABA_A$ receptor agonists and some general anesthetics, but not pentobarbital (Antkowiak (1999). In embryonic neurons of human dorsal root ganglia, $GABA_A$ antagonists suppress the Cl^--current induced by GABA, but not alphaxalone, an anesthetic neurosteroid (Valeyev et al., 1999a; 1999b). Hence, a resistance to GABA receptor antagonists is evident from studies of the depressant effects of anesthetics on both adult and immature neurons.

A question arises from our observation that pentobarbital evoked a depression that was insensitive to blockade by $GABA_A$ antagonists is whether GABA receptors in our preparation were sensitive to pentobarbital. The neurons studied were from the ventral division of the MGB and VB nuclei of rats aged postnatal day 14 (P14). These neurons cease to show discernible development changes in their morphological and electrical membrane properties after P13 (Tennigkeit et al., 1998b). The insensitivity to $GABA_A$ antagonists is probably not due to specialization of the immature brain because auditory transmission, as evident in the behaviour of young rats after postnatal day 13, is similar to that of the adult (Rubel 1978; Ehret 1983). During development, the subunit composition and expression of GABA receptors undergo changes. However, there is high expression of thalamic GABA receptors at postnatal day 14 (Laurie et al., 1992; Okada et al., 2000). The principal $GABA_A$ subunit transcripts, α_1, α_4, β_2, and δ mRNA, reach adult levels in the thalamus of rats by P12 (Laurie et al., 1992; Wisden et al., 1992). Attempts to define a receptor subunit composition for sites of anesthetic actions have shown that GABA action requires the presence of the α subunit whereas the β_2 subunit enhances the sensitivity of $GABA_A$ receptors to pentobarbital (Cestari et al., 1996; Harris et al., 1995; Thompson et al., 1996). Hence, medial geniculate and ventrobasal neurons at the end of the second postnatal week should have functional GABA receptors and thus the sensitivity to pentobarbital.

We demonstrated that $GABA_A$ receptors were functional in our slice preparations. Application of muscimol, a $GABA_A$ receptor agonist, produced a large, reversible increase in input conductance, which was completely blocked by bicuculline. Hence, it is unlikely that the resistance of pentobarbital's effects to $GABA_A$ antagonists resides in a dysfunctional

organization of the $GABA_A$ receptor (Cherubini and Conti 2001; Thompson et al., 1996). The insensitivity to $GABA_A$ antagonism and low IC_{50} for pentobarbital's action on membrane conductance and neuronal firing distinguish the pentobarbital depression in thalamocortical neurons from the "direct or GABA-mimetic" effects. These effects were produced by at least ten-fold higher concentrations of pentobarbital in cultured neurons and in recombinant channels expressed in *Xenopus oocytes* (Barker and Ransom 1978; Nicoll and Wojtowicz 1980; cf. Thompson et al., 1996). Furthermore, $GABA_B$ and $GABA_C$ receptor antagonists, and combined application of $GABA_A$, $GABA_B$ and $GABA_C$ antagonists, did not significantly alter the depression produced by pentobarbital. The above data imply an involvement of other GABA-independent mechanisms or sites of action, which induced an increase on membrane conductance.

4.2.5. Interaction with intrinsic ion channels in thalamocortical neurons

4.2.5.1. Activation of a net outward current

Pentobarbital activated an outward membrane current (I_{PB}) at V_H = -50 mV and increased conductance, which was eliminated by Cs^+. The net current blocked by Cs^+ was inwardly rectifying between -80 and -140 mV and reversed to outward at voltages positive to -80 mV. I_{PB} reversed somewhat positive to the predicted E_K (-84 mV). This reversal potential is unexpected because in theory when one conductance increases and another decreases, the reversal potential should lie outside the reversal potentials of the two contributing ions (Werman, 1980). The observation of a reversal potential in this study may be due to simultaneous changes of two ion channels (Adams; 1980; Werman, 1980). These observations were consistent with I_{PB} comprised of voltage-dependent rectifiers, I_h and I_{Kir}, and leak current, I_{leak}. Both I_h and I_{Kir} were separable from Ba^{2+} insensitive I_{leak} by virtue of

their dependence on hyperpolarizing activation and differing pharmacological sensitivities to blockade by extracellular application of ZD-7288 and Ba^{2+}.

4.2.5.2. Decrease of an inward rectifier current, I_h

At membrane potentials between E_K and action potential threshold, pentobarbital decreased I_h in thalamocortical neurons. Application of ZD-7288 blocked I_h and left an outward current at voltages positive to -80 mV. The net current blocked by ZD-7288 was inwardly rectifying between -50 and -140 mV. In thalamocortical neurons, I_h activates at approximately -60 to -65 mV and is carried by Na^+ and K^+ ions (McCormick and Pape, 1990). The findings of an increased net outward current during ZD-7288 implicated a constitutive contribution of I_h to the resting potential. The evidence consistent with pentobarbital blockade of I_h, includes (1) pentobarbital reduced the magnitude of I_h, (2) application of ZD-7288 induced an outward current, however, co-application of ZD-7288 and pentobarbital induced a smaller extra outward currents compared to pentobarbital alone, and (3) the reversal potential for I_{PB} shifted by 9 mV towards E_K during ZD-7288 application. Physiologically, I_h contributes to the resting membrane potential and oscillogenesis in thalamocortical neurons (McCormick and Pape, 1990; Williams et al., 1997). Hence, pentobarbital interactions with I_h, as revealed in this study, may modulate excitability and rhythmic oscillations in thalamocortical neurons.

4.2.5.3. Increase of the K^+ rectifier, I_{Kir} and leak current

Pentobarbital increased the magnitude of I_{Kir} in thalamocortical neurons. I_{Kir} activated between -70 and -80 mV in this study, similar to cat thalamocortical neurons (Williams et al., 1997). Therefore, I_{Kir} unlikely greatly contribute to the resting potential, which is ~ 66 mV in thalamocortical neurons.

Pentobarbital activated Ba^{2+}-sensitive and Ba^{2+} –insensitive I_{leak} currents in thalamocortical neurons. We used extracellular Ba^{2+} blockade to identify the current as I_{Kir} (McCormick and Pape, 1990; Williams et al., 1997) and to infer its involvement in I_{PB}. During co-application with Ba^{2+}, pentobarbital produced only a net outward current over the tested voltage range, representing its effects on I_h and I_{leak}. Blockade of I_h with ZD-7288 resulted in a residual I_{PB} that reversed near E_K, consistent with I_{leak}. Alone, Ba^{2+} reduced I_{leak}, as measured by stepping from V_H = -50 to -60 mV. Hence, the actual magnitude of I_{leak} induced by pentobarbital is likely larger, as represented by adding the Ba^{2+} sensitive leak component to the residual current. There are similarities of these pentobarbital actions to inhalational anesthetics, which principally activate I_{leak} in ventrobasal neurons (Ries and Puil, 1999b) and I_{Kir} and I_{leak} in hypoglossal motoneurons (Sirois et al., 1998). Thalamic neurons express the two-pore leak K^+ channels TASK-1, TASK-3 and TREK2, which are activated by inhalational anesthetics (Lesage et al., 2000; Karschin et al., 2001). Therefore, pentobarbital may activate these leak potassium channels and I_{Kir} to increase membrane conductance, which contribute to pentobarbital induced inhibition of neuronal excitability.

In summary, pentobarbital increased I_{Kir} and I_{leak}, and decreased I_h in thalamocortical neurons. The shallow concentration-response relationship for the pentobarbital-induced increase in conductance is consistent with multiple actions of pentobarbital on intrinsic membrane currents. The alteration in I_{Kir}, I_{leak}, and I_h induced by low pentobarbital concentrations, would provide voltage-dependent and voltage-independent modulation of excitatory postsynaptic potentials and IPSPs in thalamocortical neurons. The combination of these synaptic and non-synaptic actions in the CTC system may contribute to pentobarbital-induced anesthesia *in vivo*.

4.2.6. Excitatory effects on thalamocortical neurons

In 17% of neurons, pentobarbital application enhanced firing of action potentials and LTSs. These concentration-dependent effects resulted from increases in R_i and inward rectification on depolarization in a 10 to 15 mV range, subthreshold to action potential genesis. Application of TTX eliminated this rectification, but not the pentobarbital-induced effects on the R_i measured at hyperpolarized potentials. The higher input resistance and greater inward rectification on depolarization can account for the observed excitation and increased LTSs in thalamocortical neurons.

It is unclear why pentobarbital induced opposite effects in different thalamocortical neurons. In a few neurons, we observed an excitation at low concentrations, followed by a depression at high concentrations. Neurons that were depressed by pentobarbital tended to have lower input resistances, less inward rectification on depolarization, as well as a lower rate of rise of the LTS, than neurons that were excited by pentobarbital (cf. Table 3.1). The excitatory effects induced by pentobarbital may relate to decreased inhibitory transmitter release (Collins 1981), increased excitatory transmitter release (Rohde and Harris 1983), or to the existence of distinct subpopulations of thalamocortical neurons (Turner et al., 1997).

4.2.7. Functional significance of pentobarbital modulation

This thesis demonstrated the ability of pentobarbital to modulate thalamocortical and neocortical inhibition, which may occur through interacting intrinsic and $GABA_A$ receptor currents. Following hyperpolarizing IPSPs, CTC neurons exhibit rebound excitation (McCormick and Pape, 1990). This reflects activation of I_h and inactivation removal of the low threshold calcium current, I_T (McCormick and Pape, 1990). Thus, pentobarbital induced

inhibition of I_h, and enhancement of I_{Kir} and I_{leak} accounts for the suppression of rebound excitation after hyperpolarizing inputs in thalamocortical neurons (cf. Wan and Puil, 2002).

A prediction from this study is that low pentobarbital concentrations should shunt the amplitude of IPSPs. This may account for the paradoxical excitatory effects of pentobarbital in thalamic slices (Wan and Puil, 2002). Pentobarbital increases oscillatory activity and, with rising concentration, decreases oscillations in thalamocortical neurons of *in vivo* and *in vitro* preparations (Curro Dossi et al., 1992; Jacobsen et al., 2001).

Pentobarbital (10-50 μM) increased I_h in neocortical neurons, which is in opposition to the blockade of I_h observed in thalamocortical neurons. I_h depolarizes the cells in response to hyperpolarizing inputs and contributes to the inherent rhythmicity of a number of classes of neurons (McCormick and Pape, 1990; Soltesz et al., 1991). The function of I_h in the neocortex is not clear; however, this current is subject to modulation by a number of neurotransmitters and accordingly may play a pivotal role in controlling neuronal dynamics (Banks et al., 1993; Bobker and Williams 1989; McCormick and Pape, 1990; Spain et al., 1987; Soltesz et al., 1991). I_h may also interact with synaptic processes in the CNS. The activation curve of I_h between rest and spike threshold is nearly flat, but I_h activates steeply below rest, with half-maximal activation occurring at –82 mV (Spain et al., 1987). This sigmoidal activation curve of I_h makes it possible for this current to interact with IPSPs. Membrane hyperpolarization from –65 mV to –75 mV during the rising phase of an IPSP turns on I_h. This action is to oppose hyperpolarization, as the resulting inward current will return membrane potential back to rest and shorten the IPSPs (van Brederode and Spain, 1995). In our study, pentobarbital

increased I_h and potentiated IPSCs in neocortical neurons. This action may augment the interaction between I_h and IPSPs and thus weaken and shorten hyperpolarizing inhibitory input *in vivo*.

4.2.8. Clinical implications

Pentobarbital actions on neurons of the CTC system, which depressed neuronal excitability, may have significance for anesthetic effects *in vivo*. On induction of anesthesia, successive increases in pentobarbital concentrations in cerebrospinal fluid sequentially produce sedation, hypnosis and surgical anesthesia (Sato et al., 1995). These concentrations were similar in the present studies for observed pentobarbital modulation of intrinsic and GABA receptor currents in neurons of the CTC system. Interestingly, $GABA_A$ antagonists do not reverse *in vivo* anesthesia produced by pentobarbital (Little et al., 2000). Hence, the potentiation of $GABA_A$ receptor function is not an absolute requirement for production of anesthesia. We do not know if the observed effects on intrinsic non-ligand gated channels are an additional requirement. For example, pentobarbital modulated a persistent Na^+ current (I_{NaP}), which activates on depolarization, a critical determinant of excitability in a neuron's trajectory towards threshold (cf. Krnjević and Puil, 1997). Hence, pentobarbital anesthesia may include additional mechanisms of thalamocortical inhibition, consistent with the overlapping, possibly redundant mechanisms. This study also suggested that different molecular mechanisms might underlie multidimensional phenomenon of general anesthesia.

4.3. Amobarbital action in the CTC system

4.3.1. Decreases of neuronal firing and input resistance

Amobarbital suppressed both tonic and burst firing by directly activating $GABA_A$ receptors. This suppression was due to the accompanying increase in input conductance and was surmountable by stronger depolarizing stimuli. Amobarbital suppressed burst firing more effectively than tonic firing. Both firing modes were more susceptible in ventrobasal and intralaminar neurons than in nRT neurons, not known to receive nociceptive inputs (Yen *et al.*, 1989). Antagonists of $GABA_A$ receptors abolished this shunt mechanism, and restored the normal firing modes. The selective action of amobarbital contrasts with pentobarbital, which continued to shunt firing during total blockade of GABA receptors. The reversal potential for the amobarbital-induced current was close to E_{Cl}. Therefore, amobarbital shunted firing primarily by increasing a Cl^- conductance gated by $GABA_A$ receptors.

Amobarbital inhibited burst firing more effectively than tonic firing. Antagonism of $GABA_A$ receptors still prevented amobarbital-induced decreases in R_i and the low threshold Ca^{2+} spike (LTS) during TTX-blockade of persistent and transient Na^+ channels. The selective attenuation of LTS bursts may relate to a proximal dendritic distribution of $GABA_A$ receptors (Pirker et al., 2000) which would shunt or inactivate T-type Ca^{2+} channels (cf. Zhan et al., 2000; Gutierrez et al., 2001). In summary, the depression of LTS bursts did not result in amobarbital inhibition of Ca^{2+} channels (cf. Werz and Macdonald, 1985; ffrench-Mullen et al., 1993) but from the activation of $GABA_A$ receptors.

4.3.2. Direct activation of single channel currents in thalamic neurons

Amobarbital directly activated single $GABA_A$ channel currents. The activated channels displayed susceptibility to $GABA_A$ antagonism and had similar biophysical properties, despite the presence of $GABA_A$ receptor β subunits on ventrobasal neurons, and their absence on nRT neurons (Browne et al., 2001). Amobarbital increased the open probability of $GABA_A$ channels in both types of membrane patches. Again, this agonist action contrasts with pentobarbital, which causes negligible activation of GABA receptors on thalamocortical neurons at similar concentrations (Wan et al., 2003).

4.3.3. Potentiation of GABA induced currents

Amobarbital modulated $GABA_A$ receptors, enhancing synaptic inhibition. This modulation increased the amplitude and duration of fast, $GABA_A$ IPSCs, with negligible effects on slow $GABA_B$ IPSCs. Amobarbital or GABA activated channels with two open conductance states. When co-applied with GABA, amobarbital stabilized the $GABA_A$ receptor in its higher conductance state which increased the mean conductance of the channel. This may account for the increased IPSC amplitude. Amobarbital also increased the burst duration of GABA activated channels, which likely produced the prolonged IPSCs. We cannot discount the possibility that amobarbital increased release of GABA from terminals of thalamic axons (cf. Collins, 1981; Potashner and Lake, 1981).

4.3.4. Comparison between pentobarbital and amobarbital action

Amobarbital had a higher EC_{50} for potentiating the duration than for increasing amplitude of IPSCs. Barbiturates potentiate GABA actions by interacting with amino acid residues in the M2 domains of the $GABA_A$ receptor (Birnir et al., 1997). Pentobarbital is more potent in

prolonging thalamocortical IPSCs, but does not greatly affect their amplitude (Wan et al., 2003). Amobarbital's extended 5′ side chain conformation may afford a better fit to M2 domains for amplitude modulation (cf. Krasowski and Harrison, 1999; Arias et al., 2001). This molecular distinction, and the different EC_{50}s for modulating amplitude and duration imply that amobarbital interacted at two distinct sites on the $GABA_A$ receptor.

A greater IPSC amplitude during amobarbital application would likely produce a greater IPSP amplitude. This is relevant for the hyperpolarization activation of I_h, an inward current at subthreshold potentials (McCormick and Pape, 1990). Unlike pentobarbital (Wan et al., 2003), amobarbital did not have significant effects on I_h which regulates firing patterns and oscillations (McCormick and Pape, 1990). Hence, a greater IPSP amplitude due to amobarbital would enhance I_h, producing different effects on spontaneous firing patterns, than other barbiturates (cf. Lancel, 1996).

4.3.5. Functional significance

Compared to action of pentobarbital in thalamic neurons, amobarbital had different pharmacological properties that included modulating endogenous GABA actions, as well as directly activating $GABA_A$ receptors. Amobarbital modulated fast IPSCs, increasing their amplitude and duration. We attribute these changes mainly to increases in conductance and burst duration of single $GABA_A$ channels. One of potential targets for therapeutic intervention of neuropathic pain is restoration or augmentation of GABAergic inhibition in the dorsal horn of the spinal cord (reviewed by Smith, 2004). The interaction of amobarbital with $GABA_A$ receptors in neurons of the CTC system may contribute to its analgesic effects.

Amobarbital also directly activated the receptor Cl^- channel complex, which shunted tonic and LTS burst firing. Somatosensory neurons in the human thalamus fire action potential bursts more frequently in central pain conditions (Lenz et al., 1989). Hence, the depression of burst firing by amobarbital may be of clinical importance. Amobarbital caused the depression without altering intrinsic membrane conductances that could further reduce excitability, thus producing anesthesia. Unlike pentobarbital (Wan and Puil, 2002; Wan et al., 2003), amobarbital actions at two sites on the $GABA_A$ receptor may have relevance in selectively blocking excitation during anaesthesia and analgesia.

4.4. Phenobarbital actions on neurons of the CTC system

At clinical anti-epileptic concentrations (Macdonald and Barker, 1978), phenobarbital selectively inhibited neuronal firing and potentiated GABAergic IPSC in neocortical neurons, but not in thalamic neurons. These observations implied that phenobarbital selectively inhibited neuronal excitability in the neocortex.

Phenobarbital selectively potentiated GABAergic IPSCs with an EC_{50} = 106 ± 13 μM in neocortical neurons. This concentration is similar to the concentration for enhancement of a $GABA_A$ receptor-associated ionophore ligand, [^{35}S]TBPS, binding to extensively washed rat cortical membranes by phenobarbital (Honore and Drejer, 1985). Furthermore, this concentration is in the range of the clinical doses that relieve seizures (Macdonald and Barker, 1978). Several investigators have found that phenobarbital exerts anti-seizure effect at least partly by enhancing $GABA_A$ receptor function (Tatsuoka, et al., 1984; Quilichini. 2003; Soderpalm, 2002). Hence, the potentiation of $GABA_A$ergic IPSCs by phenobarbital in neocortical neurons may contribute to its anti-epileptic effects *in vivo*.

The divergence of subunit compositions of $GABA_A$ receptors in different neurons of the CTC system may account for distinct efficacy of phenobarbital-induced inhibition in these neurons. The $GABA_A$ receptor subunits that are expressed in neocortical neurons are similar to those expressed in nRT neurons, but different from thalamocortical neurons (Wisden et al., 1992). These $GABA_A$ receptor isoforms expressed in the neocortex and nRT may have different pharmacological properties compared to those expressed in thalamocortical neurons (Hosford, 1997). The possible expression of regionally selective $GABA_A$ receptor isoforms, each with different drug sensitivities, has important implications for the treatment of epilepsy. For example, the interactions between $GABA_A$ receptors and phenobarbital in neocortical neurons may contribute to the efficacy of phenobarbital to relieve generalized tonic-clonic and simple partial seizures. On the other hand, the lower potency of phenobarbital to suppress neuronal firing and potentiate IPSCs in thalamic neurons is consistent with the clinical observation that phenobarbital does not attenuate absence seizures (Mattson, 1995). Therefore, our observation that phenobarbital selectively inhibited neuronal excitability in neocortical neurons may have clinical relevance to effects of phenobarbital in the treatment of epilepsy.

There is no significant evidence showing that phenobarbital interacted with intrinsic ion channels. However, we cannot rule out the possibility that phenobarbital may exert its anti-epileptic action by other mechanisms, such as by inhibiting neuronal resonance and network oscillations in neocortical neurons (Blumenfeld, 2003; Kitayama, 2003) and therefore modulating neuronal excitability.

4.5. Comparison of three barbiturate actions in the CTC system

In this thesis, three barbiturate actions were studied on neurons of the CTC system. Among these three barbiturates, pentobarbital and amobarbital are anesthetic barbiturates and pentobarbital is more potent than amobarbital (Richter and Holtman, 1982). As a result of their sedative effects, pentobarbital and amobarbital are not clinically effective anticonvulsants (MacDonald and McLean, 1982). However, phenobarbital, an anticonvulsant barbiturate, can induce anesthesia only at very high concentrations (Richter and Holtman, 1982).

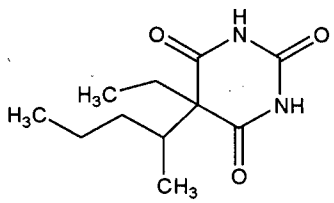

Pentobarbital

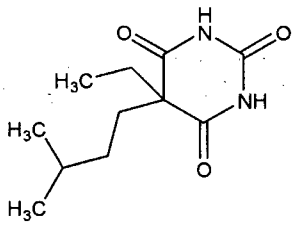

Amobarbital

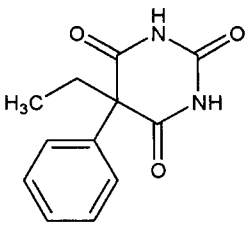

Phenobarbital

In this thesis, the major distinguishing effect of pentobarbital is that it modulated I_h, I_{kir} and leak K^+ current in neurons of the CTC system, while amobarbital and phenobarbital did not show evidence of altering these intrinsic ion channels. The actions of pentobarbital on non-synaptic intrinsic ion channels may account for its sedation effects (Wan et al., 2003). All three barbiturates potentiated GABAergic IPSCs or IPSPs with different concentration-dependence. According to the EC_{50}s of these barbiturates, pentobarbital was the most effective barbiturate in enhancing inhibitory neurotransmission, followed by amobarbital and phenobarbital. This finding is consistent with previous reports that the different efficacy of barbiturates to induce anesthesia is attributable to their different potency to activate or potentiate GABA receptors (MacDonald and Barker, 1978; 1979). These quantitative and

concentration-dependent differences in the action of three barbiturates could help to correlate to their clinical pharmacological properties (summarized in Table 4.1).

Table 4.1. Summary of three barbiturate actions in neurons of the CTC system

	In vitro actions			Clinical effects
	Neocortical neurons	nRT neurons	Thalamocortical neurons	
Pentobarbital	Inhibiting neuronal firing (IC_{50}=108 μM); Increasing IPSC amplitude (EC_{50}=45 μM) and decay (EC_{50}=101 μM); Increasing I_h	Inhibiting neuronal firing (IC_{50}=35 μM); Decreasing EPSP amplitude (IC_{50}=65 μM); Increasing of IPSC amplitude (EC_{50}=62 μM) and decay (EC_{50}=84 μM)	Inhibiting neuronal firing (IC_{50}=8 μM); Decreasing EPSP amplitude (IC_{50}=36 μM); Increasing of IPSC decay (EC_{50}=53μM); Increasing leak K^+ current and I_{Kir}; Inhibition of I_h	Sedation-hypnosis; Anesthesia
Amobarbital	Inhibiting neuronal firing (IC_{50}=151 μM); Increasing IPSC amplitude (EC_{50}=103 μM) and decay (EC_{50}=210 μM)	Inhibiting neuronal firing (IC_{50}=253 μM); Increasing of IPSC amplitude (EC_{50}=142 μM) and decay (EC_{50}=309 μM)	Inhibiting neuronal firing (IC_{50}=120 μM); Decreasing EPSP amplitude (IC_{50}=81 μM); Increasing IPSC amplitude (EC_{50}=61 μM) and decay (EC_{50}=94 μM)	Sedation-hypnosis; Anesthesia; Analgesia
Phenobarbital	Inhibiting neuronal firing (IC_{50}=161 μM); Increasing IPSC decay (EC_{50}=141 μM)	No significant effects in clinical concentrations	No significant effects in clinical concentrations	Anti-epileptic effects

4.6. Limitations and future outlook

Brain slices were used in this study to investigate drug actions on both network and cellular levels. The advantage of brain slices is that they keep local microcircuits relatively intact. This enabled us to study barbiturate actions on synaptic neurotransmission and non-synaptic intrinsic ion channels on the CTC system. One limitation of this preparation is the reduced spontaneous activity. Cutting of the brain slices may damage the neurons and networks, and hence the mechanisms of drugs effects found in brain slices represent an oversimplification of the mechanisms of drug actions *in vivo*.

Another major limitation of this work is that we did not study single channel responses of barbiturates on neocortical neurons, and therefore we were not able to determine how barbiturates differentially modulate kinetics of $GABA_A$ receptors in thalamic and neocortical neurons. This limitation is due to the difficulties in isolating layer IV neocortical neurons from slice preparation. The third limitation of this thesis is that we cannot identify the mechanisms of pentobarbital-induced excitation in MGB and ventrobasal neurons. Since the excitatory effects of pentobarbital were not commonly observed, it was not possible to study the mechanism underlying this action. The fourth limitation is that we studied barbiturate actions on corticothalamic EPSPs instead of EPSCs. EPSP amplitude may be shunted by an increase in membrane conductance; therefore, barbiturate actions in EPSPs may not necessarily reflect barbiturate actions on excitatory neurotransmission. This limitation is due to dubious space clamp in slice preparation, and the consequential inability to properly clamp EPSCs in our study.

Studies of barbiturate action in live animals are not within the scope of this thesis. Analgesic experiments on the animals treated with amobarbital, however, would clarify the recent reports showing that amobarbital may possess analgesic properties (Koyama et al., 1998), and may also further the understanding of mechanisms underlying the employment of amobarbital in the Wada test (Wada and Rasmussen, 1960). Furthermore, by comparing the actions of pentobarbital and phenobarbital with other barbiturate effects in *in vivo* experiments, we may obtain function clues about the relationships of the actions found *in vitro* slice experiments to anesthetic, anti-convulsant or analgesic effects *in vivo*.

4.7. Conclusion and significance of the study

This thesis is dedicated to the study of synaptic and non-synaptic actions of barbiturates on neurons of the CTC system. This study presented multiple mechanisms of actions of pentobarbital. The actions of amobarbital and phentobarbital, observed on the same neurons, helped to clarify the mechanisms because they had different clinical efficacies as anesthetics, anti-epileptic and analgesics.

Pentobarbital modulated synaptic and membrane excitability of CTC neurons through multiple mechanisms. At low concentrations, pentobarbital markedly decreased membrane resistance, which shunted the ability of neurons to fire action potentials in tonic patterns and to discharge low threshold Ca^{2+}-spikes when neurons were in the burst mode. These depressant actions did not involve known types of GABA receptor interactions, and were due to increased linear and voltage-dependent K^+ currents as well as a decreased Na^+/K^+ inward current. At four fold higher concentrations, pentobarbital decreased glutamatergic EPSP amplitude by inhibiting non-NMDA receptors, which decreased neuronal excitability. At

seven fold higher concentrations, pentobarbital prolonged GABAergic IPSCs by enhancing the open probability of $GABA_A$ receptor channels. Thus, the decrease in membrane resistance, which occurred with low IC_{50}, may contribute to pentobarbital-induced hypnotic-sedative action. The overlapping synaptic and non-synaptic actions of pentobarbital reduced neuronal excitability, which may account for pentobarbital-induced various levels of inhibition *in vivo*. The difference in sensitivity of neocortical, thalamocortical, and nRT neurons to pentobarbital-induced depression may relate quantitatively to different contributions of these neurons to pentobarbital-induced anesthesia.

Amobarbital, an isomer of pentobarbital, produced distinct actions on the CTC system compared with pentobarbital. Amobarbital inhibited action potential firing by activating $GABA_A$ receptors. Burst firing was more susceptible to this inhibition compared to tonic firing, which may have significance on its analgesic action *in vivo*. Amobarbital directly activated, besides potentiated, single $GABA_A$ channel activities in thalamic neurons. These actions may contribute to the enhancement of GABAergic IPSCs by amobarbital. Our results suggested that amobarbital may produce anesthesia by rather selective actions on $GABA_A$ receptors.

Phenobarbital selectively inhibited neuronal firing and potentiated GABAergic IPSCs on neocortical neurons without significantly altering either synaptic transmission or intrinsic membrane excitability in thalamic neurons at clinically relevant concentrations. Unlike pentobarbital and amobarbital, which are not anti-epileptic at subanestheic doses, phenobarbital did not decrease membrane resistance either in thalamic or neocortical neurons.

Hence, the selective inhibition on neuronal excitability in neocortical neurons by phenobarbital may account for its action as an anti-epileptic agent.

This thesis is the first study showing that synaptic and non-synaptic effects of barbiturates have different, but overlapping, concentration-dependence. Our study is also the first investigation to compare three barbiturates in all neuron types in the CTC system. The different action of these three barbiturates on neurons in this system may account for their differences in ability to cause depression in the CNS and to modulate excitability in pathophysiological concentrations. This thesis that is based on studies on brain slices and dissociated neurons provided potential targets and mechanisms for barbiturates, which may correlate to their clinical effectiveness as therapeutic agents.

Abbreviations

ACSF	Artificial cerebrospinal fluid
AMPA	alpha-amino-3-hydroxy-5-methyl-4-isoxazoleproprionate
ANOVA	Analysis of Variance
APV	2-amino-5-phosphono-valerate
ATP	Adenosine-5'-triphosphate
cAMP	Cyclic 3'5'- adenosine-monophosphate
CSF	Cerebrospinal fluid
CNQX	6-cyano-7-nitroquinoxaline
CNS	Central nervous system
E_{Cl}	Equilibrium potential for Cl^-
E_K	Equilibrium potential for K^+
EC_{50}	Concentraion of a drug that produces a half-maximal effects
EEG	Electroencephalogram
EGTA	Ethylene glycol-bis (β-aminoethyl ether) N,N,N'N'-tetraacetic acid
EPSPs	Excitatory postsynaptic potentials
EPSCs	Excitatory postsynaptic currents
GABA	γ-aminobutyric acid
h	Hour; unit for time
HEPES	N-[2-hydroxyethyl]piperazine-N'-[2-ethanesulfonic acid]
Hz	Hertz (s^{-1})
IC_{50}	Concentraion of a drug that produces a half-maximal inhibition

I_h	Hyperpolarization activated inward current
I_{Kir}	Inwardly rectifying K^+ current
I_{leak}	Voltage-independent leak current
I_{NaP}	Persistent Na^+ current
I_T	Low threshold Ca^{2+} current
IPSPs	Inhibitory postsynaptic potentials
IPSCs	Inhibitory postsynaptic currents
LTS	Low threshold spike
MAC	Minimal alveolar concentration
MGB	Medial geniculate body
Min	Minute; unit for time
NMDA	N-methyl-D-aspartate
nRT	Nucleus reticularis thalami
pH	Hydrogen ion concentration; -log $[H^+]$
pKa	Dissociation constant; pH-log[base]/[cation]
R_i	Input resistant
REM	Rapid eye movement
SEM	Standard error of mean
τ	Time constant (s); time required to reach (1-1/e) of its steady-state value
TASK	TWIK-related acid-sensing K^+ channel
TEA	Tetraethylammonium
TREK	TWIK-related K^+ channel
TTX	Tetrodotoxin

TWIK	Tandem of P domains in a weak inward rectifying K^+ channel
V_m	Membrame potential (V)
VB	Ventrobasal complex of the thalamus
VPL	Ventral posterior lateral thalamic nucleus

Bibliography

Adams WB, Parnas I, Levitan IB. Mechanism of long-lasting synaptic inhibition in Aplysia neuron R15. *J Neurophysiol* 1980, 44:1148-1160.

Adkins CE, Pillai GV, Kerby J, Bonnert TP, Haldon C, McKernan RM, Gonzalez JE, Oades K, Whiting PJ, Simpson PB. alpha4beta3delta $GABA_A$ receptors characterized by fluorescence resonance energy transfer-derived measurements of membrane potential. *J Biol Chem* 2001, 276:38934-38939.

Albrecht RF, Miletich DJ. Speculations on the molecular nature of anesthesia. *Gen Pharmacol* 1988, 19:339-346.

Alkire MT, Haier RJ, Barker SJ, Shah NK, Wu JC, Kao YJ. Cerebral metabolism during propofol anesthesia in humans studied with positron emission tomography. *Anesthesiology* 1995, 82:393-403.

Alkire MT, Haier RJ, Shah NK, Anderson CT. Positron emission tomography study of regional cerebral metabolism in humans during isoflurane anesthesia. *Anesthesiology* 1997, 86:549-557.

Alkire MT, Haier RJ, Fallon JH. Toward a unified theory of narcosis: brain imaging evidence for a thalamocortical switch as the neurophysiologic basis of anesthetic-induced unconsciousness. *Conscious Cogn* 2000, 9:370-386.

Alkire MT, Pomfrett CJ, Haier RJ, Gianzero MV, Chan CM, Jacobsen BP, Fallon JH. Functional brain imaging during anesthesia in humans: effects of halothane on global and regional cerebral glucose metabolism. *Anesthesiology* 1999, 90:701-709.

Albrecht RF, Miletich DJ. Speculations on the molecular nature of anesthesia. *Gen Pharmacol* 1988, 19:339-346.

Allan AM, Harris RA. Anesthetic and convulsant barbiturates alter gamma- aminobutyric acid-stimulated chloride flux across brain membranes. *J Pharmacol Exp Ther* 1986, 238:763-768.

Amzica F, Steriade M. Electrophysiological correlates of sleep delta waves. *Electroencephalogr Clin Neurophysio.* 1998, 107:69-83.

Angel A. Central neuronal pathways and the process of anaesthesia. *Br J Anaesth* 1993, 71:148-63.

Angel A. The G. L. Brown lecture. Adventures in anaesthesia. *Exp Physiol* 1991, 76:1-38.

Angel A, LeBeau F. A comparison of the effects of propofol with other anaesthetic agents on the centripetal transmission of sensory information. *Gen Pharmacol* 1992, 23:945-963.

Antkowiak B. Different actions of general anesthetics on the firing patterns of neocortical neurons mediated by the $GABA_A$ receptor. *Anesthesiology* 1999, 91:500-511.

Antkowiak B, Heck D. Effects of the volatile anesthetic enflurane on spontaneous discharge rate and $GABA_A$-mediated inhibition of Purkinje cells in rat cerebellar slices. *J Neurophysiol* 1997, 77:2525-2538.

Antkowiak B. How do general anaesthetics work? *Naturwissenschaften* 2001, 88:201-213.

Antognini JF, Schwartz K. Exaggerated anesthetic requirements in the preferentially anesthetized brain. *Anesthesiology* 1993, 79:1244-1249.

Archer DP, Samanani N, Roth SH. Small-dose pentobarbital enhances synaptic transmission in rat hippocampus. *Anesth Analg* 2001, 93:1521-1525.

Arias HR, McCardy EA, Gallagher MJ, Blanton MP. Interaction of barbiturate analogs with the Torpedo californica nicotinic acetylcholine receptor ion channel. *Mol Pharmacol* 2001, 60:497-506.

Avramov MN, Murayama T, Shingu K, Mori K. Electroencephalographic changes during vital capacity breath induction with halothane. *Br J Anaesth* 1991, 66:212-215.

Banks MI, Pearce RA. Dual actions of volatile anesthetics on $GABA_A$ IPSCs: dissociation of blocking and prolonging effects. *Anesthesiology*. 1999, 90:120-34.

Banks MI, Pearce RA, Smith PH. Hyperpolarization-activated cation current (Ih) in neurons of the medial nucleus of the trapezoid body: voltage-clamp analysis and enhancement by norepinephrine and cAMP suggest a modulatory mechanism in the auditory brain stem. *J Neurophysiol* 1993, 70:1420-1432.

Barker JL, Ransom BR. Pentobarbitone pharmacology of mammalian central neurones grown in tissue culture. *J Physiol* 1978, 280:355-372.

Belelli I, Pistis I, Peters JA, and Lambert JJ. General anaesthetic action at transmitter-gated inhibitory amino acid receptors. *Trends Pharmacol Sci* 1999, 20: 496-502.

Benoit E. Effects of intravenous anaesthetics on nerve axons. *Eur J Anaesthesiol* 1995, 12:59-70.

Berg-Johnsen J, Langmoen IA. Mechanisms concerned in the direct effect of isoflurane on rat hippocampal and human neocortical neurons. *Brain Res* 1990, 507:28-34.

Birnir B, Tierney ML, Dalziel JE, Cox GB, Gage PW. A structural determinant of desensitization and allosteric regulation by pentobarbitone of the $GABA_A$ receptor. *J Membr Biol* 1997, 155:157-166.

Blaustein MP. Barbiturates block sodium and potassium conductance increases in voltage-clamped lobster axons. *J Gen Physiol* 1968, 51: 293-307.

Blumenfeld H. From molecules to networks: cortical/subcortical interactions in the pathophysiology of idiopathic generalized epilepsy. *Epilepsia* 2003, 44 Suppl 2:7-15.

Bobker DH, Williams JT. Serotonin augments the cationic current I_h in central neurons. *Neuron* 1989, 2:1535-1540.

Bonhomme V, Fiset P, Meuret P, Backman S, Plourde G, Paus T, Bushnell MC, Evans AC. Propofol anesthesia and cerebral blood flow changes elicited by vibrotactile stimulation: a positron emission tomography study. *J Neurophysiol* 2001, 85:1299-1308.

Borges M, Antognini JF. Does the brain influence somatic responses to noxious stimuli during isoflurane anesthesia? *Anesthesiology* 1994, 81:1511-1555.

Brau ME, Sander F, Vogel W, Hempelmann G. Blocking mechanisms of ketamine and its enantiomers in enzymatically demyelinated peripheral nerve as revealed by single-channel experiments. *Anesthesiology* 1997, 86:394-404.

Breitinger HG, Becker CM. The inhibitory glycine receptor-simple views of a complicated channel. *Chembiochem* 2002, 3:1042-1052.

Brickley SG, Revilla V, Cull-Candy SG, Wisden W, Farrant M. Adaptive regulation of neuronal excitability by a voltage-independent potassium conductance. *Nature* 2001, 409:88-92.

Browne SH, Kang J, Akk G, Chiang LW, Schulman H, Huguenard JR, Prince DA. Kinetic and pharmacological properties of $GABA_A$ receptors in single thalamic neurons and $GABA_A$ subunit expression. *J Neurophysiol* 2001, 86:2312-2322.

Cariani P. Anesthesia, neural information processing, and conscious awareness. *Conscious Cogn* 2000, 9:387-395.

Carlen PL, Gurevich N, Davies MF, Blaxter TJ, O'Beirne M. Enhanced neuronal K^+ conductance: a possible common mechanism for sedative-hypnotic drug action. *Can J Physiol Pharmacol* 1985, 63:831-837.

Castelo-Branco M, Neuenschwander S, Singer W. Synchronization of visual responses between the cortex, lateral geniculate nucleus, and retina in the anesthetized cat. *J Neurosci* 1998, 18:6395-6410.

Charlesworth P, Jacobson I, Richards CD. Pentobarbitone modulation of NMDA receptors in neurones isolated from the rat olfactory brain. *Br J Pharmacol* 1995, 116:3005-3013.

Cheng G, Kendig JJ. Enflurane directly depresses glutamate AMPA and NMDA currents in mouse spinal cord motor neurons independent of actions on $GABA_A$ or glycine receptors. *Anesthesiology* 2000, 93:1075-1084.

Cestari IN, Uchida I, Li L, Burt D, Yang J. The agonistic action of pentobarbital on $GABA_A$ beta-subunit homomeric receptors. *Neuroreport* 1996, 7:943-947.

Catsicas M, Mobbs P. $GABA_B$ receptors regulate chick retinal calcium waves. *J Neurosci* 2001, 21:897-910.

Cheng G, Kendig JJ. Enflurane decreases glutamate neurotransmission to spinal cord motor neurons by both pre- and postsynaptic actions. *Anesth Analg* 2003, 96:1354-1359.

Cherubini E, Conti F. Generating diversity at GABAergic synapses. *Trends Neurosci* 2001, 24:155-162.

Clark DL, Rosner BS. Neurophysiologic effects of general anesthetics. I. The electroencephalogram and sensory evoked responses in man. *Anesthesiology* 1973, 38:564-582.

Collins GG. Effects of pentobarbitone on the synaptically evoked release of the amino acid neurotransmitter candidates aspartate and GABA from rat olfactory cortex. *Adv Biochem Psychopharmacol* 1981, 27:147-156.

Colquhoun D, Sakmann B. Fast events in single-channel currents activated by acetylcholine and its analogues at the frog muscle end-plate. *J Physiol* 1985, 369:501-557.

Contreras D, Steriade M. Spindle oscillation in cats: the role of corticothalamic feedback in a thalamically generated rhythm. *J Physiol* 1996, 490:159-179.

Contreras D, Steriade M. Synchronization of low-frequency rhythms in corticothalamic networks. *Neuroscience* 1997, 76:11-24.

Crick F, Koch C. Are we aware of neural activity in primary visual cortex? *Nature* 1995, 375:121-123.

Crill WE. Persistent sodium current in mammalian central neurons. *Annu Rev Physiol* 1996, 58:349-362.

Curro Dossi RC, Nunez A, Steriade M. Electrophysiology of a slow (0.5-4 Hz) intrinsic oscillation of cat thalamocortical neurones in vivo. *J Physiol* 1992, 447:215-234.

Dalley JW, Parker CA, Wulfert E, Hudson AL, Nutt DJ. Potentiation of barbiturate-induced alterations in presynaptic noradrenergic function in rat frontal cortex by imidazol(in)e alpha2-adrenoceptor agonists. *Br J Pharmacol* 1998, 125:441-446.

Debarbieux F, Brunton J, Charpak S. Effect of bicuculline on thalamic activity: a direct blockade of IAHP in reticularis neurons. *J Neurophysiol* 1998, 79:2911-2918.

Dilger JP. The effects of general anaesthetics on ligand-gated ion channels. *Br J Anaesth* 2002, 89:41-51.

Dutton RC, Smith WD, Smith NT. EEG Predicts movement response to surgical stimuli during general anesthesia with combinations of isoflurane, 70% N2O, and fentanyl. *J Clin Monit* 1996, 12:127-139.

Eghbali M, Birnir B, Gage PW. Conductance of $GABA_A$ channels activated by pentobarbitone in hippocampal neurons from newborn rats. *J Physiol (Lond)* 2003, 552:13-22.

Eghbali M, Gage PW, Birnir B. Pentobarbital modulates gamma-aminobutyric acid-activated single-channel conductance in rat cultured hippocampal neurons. *Mol Pharmacol* 2000, 58:463-469.

Ehret G. Development of hearing and response behavior to sound stimuli. In: Romand R (ed) *Development of Auditory and Vestibular Systems.* Academic Press, New York, 1983, p. 211-237.

el-Beheiry H, Puil E. Anaesthetic depression of excitatory synaptic transmission in neocortex. *Exp Brain Res* 1989, 77:87-93.

Essin K, Nistri A, Magazanik L. Evaluation of GluR2 subunit involvement in AMPA receptor function of neonatal rat hypoglossal motoneurons. *Eur J Neurosci* 2002, 15:1899-1906.

Evans BM. Sleep, consciousness and the spontaneous and evoked electrical activity of the brain. Is there a cortical integrating mechanism? *Neurophysiol Clin* 2003, 33:1-10.

Ezure K, Oshima T. Excitation of slow pyramidal tract cells and their family neurones during phasic and tonic phases of EEG arousal. *Jpn J Physiol* 1981, 31:737-748.

ffrench-Mullen JMH, Barker JL, and Rogawski MA. Calcium current block by (-)-pentobarbital, phenobarbital, and CHEB but not (+)-pentobarbital in acutely isolated hippocampal CA1 neurons: comparison with effects on GABA-activated Cl^- current. *J Neurosci* 1993, 13: 3211-3221.

Fiset P, Paus T, Daloze T, Plourde G, Meuret P, Bonhomme V, Hajj-Ali N, Backman SB, Evans AC. Brain mechanisms of propofol-induced loss of consciousness in humans: a positron emission tomographic study. *J Neurosci* 1999, 19:5506-5513.

Foote SL, Morrison JH. Extrathalamic modulation of cortical function. *Annu Rev Neurosci* 1987, 10:67-95.

Franks NP, Lieb WR. Molecular and cellular mechanisms of general anaesthesia. *Nature* 1994, 367:607-614.

Frenkel C, Duch DS, Recio-Pinto E, Urban BW. Pentobarbital suppresses human brain sodium channels. *Brain Res Mol Brain Res* 1989,6:211-216.

Frenkel C, Duch DS, Urban BW. Molecular actions of pentobarbital isomers on sodium channels from human brain cortex. *Anesthesiology* 1990, 72:640-649.

Frenkel C, Urban BW. Human brain sodium channels as one of the molecular target sites for the new intravenous anaesthetic propofol (2,6-diisopropylphenol). *Eur J Pharmacol* 1991, 208:75-79.

Frenkel C, Urban BW. Molecular actions of racemic ketamine on human CNS sodium channels. *Br J Anaesth* 1992, 69:292-297.

Friederich P, Urban BW. Interaction of intravenous anesthetics with human neuronal potassium currents in relation to clinical concentrations. *Anesthesiology* 1999,91:1853-60.

Fujiwara N, Higashi H, Nishi S, Shimoji K, Sugita S, and Yoshimura M. Changes in spontaneous firing patterns of rat hippocampal neurones induced by volatile anaesthetics. *J Physiol (Lond)* 1988, 402: 155-175, 1988.

Gasic GP, Hollmann M. Molecular neurobiology of glutamate receptors. *Annu Rev Physiol.* 1992,54:507-536.

Giuffrida R, Rustioni A. Glutamate and aspartate immunoreactivity in cortico-cortical neurons of the sensorimotor cortex of rats. *Exp Brain Res* 1989, 74:41-46.

Goldman-Rakic PS. Topography of cognition: parallel distributed networks in primate association cortex. *Annu Rev Neurosci* 1988, 11:137-156.

Greenfield LJ Jr, Zaman SH, Sutherland ML, Lummis SC, Niemeyer MI, Barnard EA, Macdonald RL. Mutation of the $GABA_A$ receptor M1 transmembrane proline increases GABA affinity and reduces barbiturate enhancement. *Neuropharmacology* 2002, 42:502-521.

Grossberg S. Neural dynamics of motion perception, recognition learning, and spatial attention. In: Port RF, Gelder TV (eds). *Mind as motion: Explorations in dynamics of Cognition*. MIT Press: Cambridge, MA. 1995, pp 449-490.

Guertin PA, Hounsgaard J. Non-volatile general anaesthetics reduce spinal activity by suppressing plateau potentials. *Neuroscience* 1999, 88:353-358.

Gutierrez C, Cox CL, Rinzel J, Sherman SM. Dynamics of low-threshold spike activation in relay neurons of the cat lateral geniculate nucleus. *J. Neurosci* 2001, 21: 1022-1032.

Guyon A, Laurent S, Paupardin-Tritsch D, Rossier J, Eugene D. Incremental conductance levels of $GABA_A$ receptors in dopaminergic neurones of the rat substantia nigra pars compacta. *J Physiol* 1999, 516:719-737.

Harris BD, Wong G, Moody EJ, Skolnick P. Different subunit requirements for volatile and nonvolatile anesthetics at gamma-aminobutyric acid type A receptors. *Mol Pharmacol* 1995, 47:363-367.

Haydon DA, Urban BW. The effects of some inhalation anaesthetics on the sodium current of the squid giant axon. *J Physiol* 1983, 341:429-439.

Heinke W, Schwarzbauer C. In vivo imaging of anaesthetic action in humans: approaches with positron emission tomography (PET) and functional magnetic resonance imaging (fMRI). *Br J Anaesth* 2002, 89:112-122.

Henry CE, Scoville WB. Suppression-burst activity from isolated cerebral cortex in man. *Electroencephalogr Clin Neurophysiol* 1952, 4:1-22.

Honore T, Drejer J. Phenobarbitone enhances [^{35}S] TBPS binding to extensively washed rat cortical membranes. *J Pharm Pharmacol* 1985, 37:928-929.

Hosford DA, Wang Y, Cao Z. Differential effects mediated by $GABA_A$ receptors in thalamic nuclei in lh/lh model of absence seizures. *Epilepsy Res* 1997, 27:55-65.

Huntsman MM, Huguenard JR. Nucleus-specific differences in $GABA_A$-receptor-mediated inhibition are enhanced during thalamic development. *J Neurophysiol* 2000, 83:350-358.

Ichinose F, Mi WD, Miyazaki M, Onouchi T, Goto T, Morita S. Lack of correlation between the reduction of sevoflurane MAC and the cerebellar cyclic GMP concentrations in mice treated with 7-nitroindazole. *Anesthesiology* 1998, 89:143-148.

Jackson MF, Joo DT, Al-Mahrouki AA, Orser BA, Macdonald JF. Desensitization of alpha-amino-3-hydroxy-5-methyl-4-isoxazolepropionic acid (AMPA) receptors facilitates use-dependent inhibition by pentobarbital. *Mol Pharmacol* 2003, 64:395-406.

Jacobsen RB, Ulrich D, Huguenard JR. $GABA_B$ and NMDA receptors contribute to spindle-like oscillations in rat thalamus in vitro. *J Neurophysiol* 2001, 86:1365-1375.

Jahnsen H, Llinas R. Ionic basis for the electro-responsiveness and oscillatory properties of guinea-pig thalamic neurones in vitro. *J Physiol* 1984, 349:227-247.

Jefferys JG, Traub RD, Whittington MA. Neuronal networks for induced '40 Hz' rhythms. *Trends Neurosci* 1996, 19:202-208.

Jones EG. A new view of specific and nonspecific thalamocortical connections. *Adv Neurol* 1998, 77:49-71

Jones EG. Chemically defined parallel pathways in the monkey auditory system. *Ann N Y Acad Sc.* 2003, 999:218-233.

Johns RA, Moscicki JC, DiFazio CA. Nitric oxide synthase inhibitor dose-dependently and reversibly reduces the threshold for halothane anesthesia. A role for nitric oxide in mediating consciousness? *Anesthesiology* 1992, 77:779-784.

Kaisti KK, Metsahonkala L, Teras M, Oikonen V, Aalto S, Jaaskelainen S, Hinkka S, Scheinin H. Effects of surgical levels of propofol and sevoflurane anesthesia on cerebral blood flow in healthy subjects studied with positron emission tomography. *Anesthesiology* 2002, 96:1358-1370.

Kao CQ, Coulter DA. Physiology and pharmacology of corticothalamic stimulation-evoked responses in rat somatosensory thalamic neurons in vitro. *J Neurophysiol* 1997, 77:2661-2676.

Karschin C, Wischmeyer E, Preisig-Muller R, Rajan S, Derst C, Grzeschik KH, Daut J, Karschin A. Expression pattern in brain of TASK-1, TASK-3, and a tandem pore domain K^+ channel subunit, TASK-5, associated with the central auditory nervous system. *Mol Cell Neurosci* 2001, 18:632-648.

Keifer JC, Baghdoyan HA, Becker L, Lydic R. Halothane decreases pontine acetylcholine release and increases EEG spindles. *Neuroreport* 1994, 5:577-580.

Kinney HC, Korein J, Panigrahy A, Dikkes P, Goode R. Neuropathological findings in the brain of Karen Ann Quinlan. The role of the thalamus in the persistent vegetative state. *N Engl J Med* 1994, 330:1469-1475.

Kissen B. Functional organization of the consciousness system. In: Conscious and unconscious programs in the brain. ed. Kissin B. Plenum Medical Book, New York, 1986, pp 81-89.

Kitamura A, Marszalec W, Yeh JZ, Narahashi T. Effects of halothane and propofol on excitatory and inhibitory synaptic transmission in rat cortical neurons. *J Pharmacol Exp Ther* 2003, 304:162-171.

Kitayama M, Miyata H, Yano M, Saito N, Matsuda Y, Yamauchi T, Kogure S. Ih blockers have a potential of antiepileptic effects. *Epilepsia* 2003, 44:20-24.

Koyama T, Arakawa Y, Shibata M, Mashimo T, Yoshiya I. Effect of barbiturate on central pain: difference between intravenous administration and oral administration. *Clin J Pain* 1998, 14:86-88.

Krasowski MD, Harrison NL. General anaesthetic actions on ligand-gated ion channels. *Cell Mol Life Sci* 1999, 55:1278-303.

Krnjević K and Puil E. Cellular mechanisms of general anesthesia. In: Bittar EE, and Bittar N (eds). *Principles of Medical Biology*. JAI Press: Greenwich, 1997, p. 811-828.

Kulkarni RS, Zorn LJ, Anantharam V, Bayley H, Treistman SN. Inhibitory effects of ketamine and halothane on recombinant potassium channels from mammalian brain. *Anesthesiology* 1996, 84:900-909.

Lancel M. Role of $GABA_A$ receptors in the regulation of sleep: initial sleep responses to peripherally administered modulators and agonists. *Sleep* 1996, **22**:33-42.

Larkman PM, Kelly JS. Modulation of the hyperpolarisation-activated current, Ih, in rat facial motoneurones in vitro by ZD-7288. *Neuropharmacology* 2001, 40:1058-1072.

Laurie DJ, Wisden W, and Seeburg PH. The distribution of thirteen $GABA_A$ receptor subunit mRNAs in the rat brain. III. Embryonic and postnatal development. *J Neurosci* 1992, 12:4151-4172.

Lenz FA, Kwan HC, Dostrovsky JO, Tasker RR. Characteristics of the bursting pattern of action potentials that occurs in the thalamus of patients with central pain. Brain Res 1989, 496:357-360.

Lesage F, Terrenoire C, Romey G, Lazdunski M. Human TREK2, a 2P domain mechano-sensitive K^+ channel with multiple regulations by polyunsaturated fatty acids, lysophospholipids, and Gs, Gi, and Gq protein-coupled receptors. *J Biol Chem* 2000, 275:28398-28405.

Little HJ, Clark A, Watson WP. Investigations into pharmacological antagonism of general anaesthesia. *Br J Pharmacol* 2000, 129:1755-1763.

Llinas R, Pare D. Of dreaming and wakefulness. *Neuroscience* 1991, 44:521-535.

Llinas R, Ribary U, Contreras D, Pedroarena C. The neuronal basis for consciousness. *Philos Trans R Soc Lond B Biol Sci* 1998, 353:1841-1849.

Lukatch HS, MacIver MB. Synaptic mechanisms of thiopental-induced alterations in synchronized cortical activity. *Anesthesiology* 1996, 84:1425-1434.

Macdonald RL, Barker JL. Anticonvulsant and anesthetic barbiturates: different postsynaptic actions in cultured mammalian neurons. *Neurology* 1979, 29:432-447.

Macdonald RL, Barker JL. Different actions of anticonvulsant and anesthetic barbiturates revealed by use of cultured mammalian neurons. *Science* 1978, 200:775-777.

Macdonald RL, McLean MJ. Cellular bases of barbiturate and phenytoin anticonvulsant drug action. *Epilepsia* 1982, 23 Suppl 1:S7-18.

Macdonald RL, Olsen RW. $GABA_A$ receptor channels. *Annu Rev Neurosci.* 1994, 17:569-602.

MacDonald RL, Rogers CJ, Twyman RE. Barbiturate regulation of kinetic properties of the $GABA_A$ receptor channel of mouse spinal neurones in culture. *J Physiol (Lond)* 1989, 417:483-500.

MacIver MB, Amagasu SM, Mikulec AA, Monroe FA. Riluzole anesthesia: use-dependent block of presynaptic glutamate fibers. *Anesthesiology* 1996a, 85:626-634.

MacIver MB, Mandema JW, Stanski DR, Bland BH. Thiopental uncouples hippocampal and cortical synchronized electroencephalographic activity. *Anesthesiology* 1996b, 84:1411-1424.

MacIver MB, Roth SH. Inhalation anaesthetics exhibit pathway-specific and differential actions on hippocampal synaptic responses in vitro. *Br J Anaesth* 1988, 60:680-691.

Mailis A, Plapler P, Ashby P, Shoichet R, Roe S. Effect of intravenous sodium amytal on cutaneous limb temperatures and sympathetic skin responses in normal subjects and pain patients with and without Complex Regional Pain Syndromes (type I and II). I. *Pain* 1997, 70:59-68.

Maingret F, Patel AJ, Lazdunski M, Honore E. The endocannabinoid anandamide is a direct and selective blocker of the background K^+ channel TASK-1. *EMBO J* 2001, 20:47-54.

Mantz J, Varlet C, Lecharny JB, Henzel D, Lenot P, Desmonts JM. Effects of volatile anesthetics, thiopental, and ketamine on spontaneous and depolarization-evoked dopamine release from striatal synaptosomes in the rat. *Anesthesiology* 1994, 80:352-363.

Marrocco RT, Witte EA, Davidson MC. Arousal systems. *Curr Opin Neurobiol* 1994, 4:166-170.

Marszalec W, Narahashi T. Use-dependent pentobarbital block of kainate and quisqualate currents. *Brain Res* 1993, 608:7-15.

Mathers DA. Pentobarbital promotes bursts of gamma-aminobutyric acid-activated single channel currents in cultured mouse central neurons. *Neurosci Lett* 1985, 60:121-126.

Mathers DA, Barker JL. (-)Pentobarbital opens ion channels of long duration in cultured mouse spinal neurons. *Science* 1980, 209:507-509.

Matsumura M, Cope T, Fetz EE. Sustained excitatory synaptic input to motor cortex neurons in awake animals revealed by intracellular recording of membrane potentials. *Exp Brain Res* 1988, 70:463-469.

Mattson RH. Efficacy and adverse effects of established and new antiepileptic drugs. *Epilepsia* 1995, 36:S13-26.

McCormick DA. Neurotransmitter actions in the thalamus and cerebral cortex. *J Clin Neurophysiol* 1992, 9:212-223.

McCormick DA, Bal T. Sleep and arousal: thalamocortical mechanisms. *Annu Rev Neurosci* 1997, 20:185-215.

McCormick DA, Pape HC. Properties of a hyperpolarization-activated cation current and its role in rhythmic oscillation in thalamic relay neurones. *J Physiol* 1990, 431:291-318.

McCormick DA, von Krosigk M. Corticothalamic activation modulates thalamic firing through glutamate "metabotropic" receptors. *Proc Natl Acad Sci U S A* 1992, 89:2774-2778.

Mehta AK, Ticku MK. An update on $GABA_A$ receptors. *Brain Res Brain Res Rev* 1999, 29:196-217.

Mesulam MM. A cortical network for directed attention and unilateral neglect. *Ann Neurol* 1981, 10:309-325.

Meyer H. Zur Theorie der Alkolnarkose. Der Einfluss wechselnder Temperatur auf Wirkungsstäke und Theilungscoefficient der Narkotika. *Arch Exp Pathol Pharmakol (Naunyn-Schmiedebergs)* 1901, 46: 338-346.

Mihic SJ, McQuilkin SJ, Eger EI 2nd, Ionescu P, Harris RA. Potentiation of gamma-aminobutyric acid type A receptor-mediated chloride currents by novel halogenated compounds correlates with their abilities to induce general anesthesia. *Mol Pharmacol* 1994, 46:851-857.

Motzko D, Glade U, Tober C, Flohr H. 7-Nitro indazole enhances methohexital anesthesia. *Brain Res* 1998, 788:353-355.

Mountcastle VB, Lynch JC, Georgopoulos A, Sakata H, Acuna C. Posterior parietal association cortex of the monkey: command functions for operations within extrapersonal space. *J Neurophysiol* 1975, 38:871-908.

Murthy VN, Fetz EE. Synchronization of neurons during local field potential oscillations in sensorimotor cortex of awake monkeys. *J Neurophysiol* 1996, 76:3968-3982.

Nash HA. In vivo genetics of anaesthetic action. *Br J Anaesth* 2002, 89:143-155.

Nelson LE, Guo TZ, Lu J, Saper CB, Franks NP, Maze M. The sedative component of anesthesia is mediated by $GABA_A$ receptors in an endogenous sleep pathway. *Nat Neurosci* 2002, 5:979-984.

Nicoll RA, Madison DV. General anesthetics hyperpolarize neurons in the vertebrate central nervous system. *Science* 1982, 217:1055-1057.

Nicoll RA, Wojtowicz JM. The effects of pentobarbital and related compounds on frog motoneurons. *Brain Res* 1980, 191:225-237.

Nishikawa K, MacIver MB. Membrane and synaptic actions of halothane on rat hippocampal pyramidal neurons and inhibitory interneurons. *J Neurosci* 2000, 20:5915-5923.

O'Beirne M, Gurevich N, Carlen PL. Pentobarbital inhibits hippocampal neurons by increasing potassium conductance. *Can J Physiol Pharmacol* 1987, 65:36-41.

Okada M, Onodera K, Van Renterghem C, Sieghart W, and Takahashi T. Functional correlation of $GABA_A$ receptor alpha subunits expression with the properties of IPSCs in the developing thalamus. *J Neurosci* 2000, 20:2202-2208.

Olsen RW, Bureau MH, Endo S, Smith G. The $GABA_A$ receptor family in the mammalian brain. Neurochem Res. 1991, 16:317-325.

Orser BA, Bertlik M, Wang LY, MacDonald JF. Inhibition by propofol (2,6 di-isopropylphenol) of the N-methyl-D-aspartate subtype of glutamate receptor in cultured hippocampal neurones. *Br J Pharmacol* 1995, 116:1761-1768.

Orser BA, Wang LY, Pennefather PS, MacDonald JF. Propofol modulates activation and desensitization of $GABA_A$ receptors in cultured murine hippocampal neurons. *J Neurosci* 1994, 14:7747-7760.

Pape HC. Queer current and pacemaker: the hyperpolarization-activated cation current in neurons. *Annu Rev Physiol* 1996, 58:299-327.

Parri HR, Crunelli V. Sodium current in rat and cat thalamocortical neurons: role of a non-inactivating component in tonic and burst firing. *J Neurosci* 1998, 18:854-867.

Patel AJ, Honore E, Lesage F, Fink M, Romey G, Lazdunski M. Inhalational anesthetics activate two-pore-domain background K^+ channels. *Nat Neurosci* 1999, 2:422-426.

Peruzzi D, Bartlett E, Smith PH, Oliver DL. A monosynaptic GABAergic input from the inferior colliculus to the medial geniculate body in rat. *J Neurosci* 1997, 17:3766-3777.

Pirker S, Schwarzer C, Wieselthaler A, Sieghart W, Sperk G. $GABA_A$ receptors: immocytochemical distribution of 13 subunits in the adult rat brain. *Neuroscience* 2000, 101, 815-850.

Pocock G, Richards CD. Excitatory and inhibitory synaptic mechanisms in anaesthesia. *Br J Anaesth* 1993, 71:134-147.

Potashner SJ, Lake N. Action of baclofen and pentobarbital on amino acid release. *Adv Biochem Psychopharmacol* 1981, 27:139-145.

Prevett MC, Duncan JS, Jones T, Fish DR, Brooks DJ. Demonstration of thalamic activation during typical absence seizures using H2(15)O and PET. *Neurology* 1995, 45:1396-1402.

Puil E and El-Beheiry H. Anaesthetic suppression of transmitter actions in neocortex. *Br J Pharmacol* 1990,101: 61-66.

Puil E, Gimbarzevsky B. Modifications in membrane properties of trigeminal sensory neurons during general anesthesia. *J Neurophysiol* 1987, 58:87-104.

Puil E, Ries CR, Schwarz DWF, Tennigkeit T, Yarom Y. Sleep induced and anesthetic actions of drugs on neurons of auditory thalamus. International Symposium: Acoustical Signal Processing in the Central Nervous System. Prague, Czech Republic, September 1996.

Quilichini PP, Diabira D, Chiron C, Milh M, Ben-Ari Y, Gozlan H. Effects of antiepileptic drugs on refractory seizures in the intact immature corticohippocampal formation in vitro. *Epilepsia* 2003, 44:1365-1374.

Ragozzino D, Woodward RM, Murata Y, Eusebi F, Overman LE, Miledi R. Design and in vitro pharmacology of a selective gamma-aminobutyric acid C receptor antagonist. *Mol Pharmacol* 1996, 50:1024-1030.

Rampil IJ, Laster MJ. No correlation between quantitative electroencephalographic measurements and movement response to noxious stimuli during isoflurane anesthesia in rats. *Anesthesiology* 1992, 77:920-925.

Rampil IJ, Mason P, Singh H. Anesthetic potency (MAC) is independent of forebrain structures in the rat. *Anesthesiology* 1993, 78:707-712.

Rampil IJ. Anesthetic potency is not altered after hypothermic spinal cord transection in rats. *Anesthesiology* 1994, 80:606-610.

Ratnakumari L, Hemmings HC Jr. Inhibition by propofol of [^{3}H]-batrachotoxinin-A 20-alpha-benzoate binding to voltage-dependent sodium channels in rat cortical synaptosomes. *Br J Pharmacol* 1996, 119:1498-1504.

Rehberg B, Bennett E, Xiao YH, Levinson SR, Duch DS. Voltage- and frequency-dependent pentobarbital suppression of brain and muscle sodium channels expressed in a mammalian cell line. *Mol Pharmacol* 1995, 48:89-97.

Rehberg B, Xiao YH, Duch DS. Central nervous system sodium channels are significantly suppressed at clinical concentrations of volatile anesthetics. *Anesthesiology* 1996, 84:1223-1233.

Richards CD. Anaesthetic modulation of synaptic transmission in the mammalian CNS. *Br J Anaesth* 2002, 89:79-90.

Richards CD. The selective depression of evoked cortical EPSPs by pentobarbitone. *J Physiol* 1971, 217:41P-43P.

Richter JA, Holtman JR Jr. Barbiturates: their in vivo effects and potential biochemical mechanisms. *Prog Neurobiol* 1982, 18:275-319.

Ries CR, Puil E. Ionic mechanism of isoflurane's actions on thalamocortical neurons. *J Neurophysiol* 1999a, 81:1802-1809.

Ries CR, Puil E. Mechanism of anesthesia revealed by shunting actions of isoflurane on thalamocortical neurons. *J Neurophysiol* 1999b, 81:1795-1801.

Rohde BH, Harris RA. Effects of barbiturates and ethanol on muscimol-induced release of [^{3}H]-D-aspartate from rodent cerebellum. *Neuropharmacology* 1983, 22:721-727.

Rubel EW. Ontogeny of structure and function in the vertebrate auditory system. In: Jacobson M (ed) *Handbook of Sensory Physiology*, Vol. IX, Springer Verlag, Berlin, 1978, p. 135-237.

Sato S, Koshiro A, Kakemi M, Fukasawa Y, Katayama K, and Koizumi T. Pharmacokinetic and pharmacodynamic studies of centrally acting drugs in rat: effect of pentobarbital and chlorpromazine on electroencephalogram in rat. *Biol Pharm Bull* 1995, 18: 1094-1103.

Sawada S, Yamamoto C. Blocking action of pentobarbital on receptors for excitatory amino acids in the guinea pig hippocampus. *Exp Brain Res* 1985, 59:226-231.

Schlame M, Hemmings HC Jr. Inhibition by volatile anesthetics of endogenous glutamate release from synaptosomes by a presynaptic mechanism. *Anesthesiology* 1995, 82:1406-1416.

Seeman P. The membrane actions of anesthetics and tranquilizers. *Pharmacol Rev* 1972, 24:583-655.

Selemon LD, Goldman-Rakic PS. Common cortical and subcortical targets of the dorsolateral prefrontal and posterior parietal cortices in the rhesus monkey: evidence for a

distributed neural network subserving spatially guided behavior. *J Neurosci* 1988, 8:4049-4068.

Shin WJ, Winegar BD. Modulation of noninactivating K^+ channels in rat cerebellar granule neurons by halothane, isoflurane, and sevoflurane. *Anesth Analg* 2003, 96:1340-1344.

Siegelbaum SA, Camardo JS, Kandel ER. Serotonin and cyclic AMP close single K^+ channels in Aplysia sensory neurones. *Nature* 1982, 299:413-417.

Singer W. Development and plasticity of cortical processing architectures. *Science* 1995, 270:758-764.

Sirois JE, Lei Q, Talley EM, Lynch C 3rd, Bayliss DA. The TASK-1 two-pore domain K^+ channel is a molecular substrate for neuronal effects of inhalation anesthetics. *J Neurosci* 2000, 20:6347-6354.

Sirois JE, Pancrazio JJ, III CL, Bayliss DA. Multiple ionic mechanisms mediate inhibition of rat motoneurones by inhalation anaesthetics. *J Physiol* 1998, 512:851-862.

Smith PA. Neuropathic pain: drug targets for current and future interventions. *Drug News Perspect* 2004, 17:5-17.

Snead OC 3rd. Basic mechanisms of generalized absence seizures. *Ann Neurol* 1995, 37:146-157.

Soderpalm B. Anticonvulsants: aspects of their mechanisms of action. *Eur J Pain* 2002, 6 Suppl A:3-9.

Soltesz I, Lightowler S, Leresche N, Jassik-Gerschenfeld D, Pollard CE, Crunelli V. Two inward currents and the transformation of low-frequency oscillations of rat and cat thalamocortical cells. *J Physiol* 1991, 441:175-197.

Spain WJ, Schwindt PC, Crill WE. Anomalous rectification in neurons from cat sensorimotor cortex in vitro. *J Neurophysiol* 1987, 57:1555-1576.

Spreafico R, Frassoni C, Arcelli P, Battaglia G, Wenthold RJ, De Biasi S. Distribution of AMPA selective glutamate receptors in the thalamus of adult rats and during postnatal development. A light and ultrastructural immunocytochemical study. *Brain Res Dev Brain Res* 1994, 82:231-244.

Squire LR, Moore RY. Dorsal thalamic lesion in a noted case of human memory dysfunction. *Ann Neurol* 1979, 6:503-506.

Stafstrom CE, Schwindt PC, Crill WE. Negative slope conductance due to a persistent subthreshold sodium current in cat neocortical neurons in vitro. *Brain Res* 1982, 236:221-226.

Steinbach JH, Akk G. Modulation of $GABA_A$ receptor channel gating by pentobarbital. *J Physiol (Lond)* 2001, 537:715-733.

Steriade M. Corticothalamic resonance, states of vigilance and mentation. *Neuroscience* 2000, 101:243-276.

Steriade M. Impact of network activities on neuronal properties in corticothalamic systems. *J Neurophysiol* 2001, 86:1-39.

Steriade M. Sleep oscillations in corticothalamic neuronal networks and their development into self-sustained paroxysmal activity. *Rom J Neurol Psychiatry* 1993, 31:151-161.

Steriade M. Sleep oscillations and their blockage by activating systems. *J Psychiatry Neurosci* 1994, 19:354-358.

Steriade M, McCormick DA, Sejnowski TJ. Thalamocortical oscillations in the sleeping and aroused brain. Science 1993, 262:679-685.

Stucke AG, Zuperku EJ, Tonkovic-Capin V, Tonkovic-Capin M, Hopp FA, Kampine JP, Stuth EA. Halothane depresses glutamatergic neurotransmission to brain stem inspiratory premotor neurons in a decerebrate dog model. *Anesthesiology* 2003, 98:897-905.

Sugiyama K, Muteki T, Shimoji K. Halothane-induced hyperpolarization and depression of postsynaptic potentials of guinea pig thalamic neurons in vitro. *Brain Res* 1992, 576:97-103.

Tatsuoka Y, Kato Y, Yoshida K, Imura H. In vivo effects of phenytoin and phenobarbital on GABA receptors in rat cerebral cortex and cerebellum. *Neurosci Lett* 1984, 46:255-260.

Tennigkeit F, Schwarz DW, Puil E. Modulation of bursts and high-threshold calcium spikes in neurons of rat auditory thalamus. *Neuroscience* 1998a, 83:1063-1073.

Tennigkeit F, Schwarz DW, Puil E. Postnatal development of signal generation in auditory thalamic neurons. *Brain Res Dev Brain Res* 1998b, 109:255-263.

Thompson SA, Whiting PJ, Wafford KA. Barbiturate interactions at the human $GABA_A$ receptor: dependence on receptor subunit combination. *Br J Pharmacol* 1996 ,117:521-527.

Todorovic SM, Lingle CJ. Pharmacological properties of T-type Ca^{2+} current in adult rat sensory neurons: effects of anticonvulsant and anesthetic agents. *J Neurophysiol* 1998, 79:240-252.

Tomlin SL, Jenkins A, Lieb WR, Franks NP. Stereoselective effects of etomidate optical isomers on gamma-aminobutyric acid type A receptors and animals. *Anesthesiology* 1998, 88:708-717.

Tononi G, Edelman GM. Consciousness and complexity. *Science* 1998, 282:1846-1851.

Turner JP, Anderson CM, Williams SR, Crunelli V. Morphology and membrane properties of neurones in the cat ventrobasal thalamus in vitro. *J Physiol* 1997, 505:707-726.

Uchida S, Nakayama H, Maehara T, Hirai N, Arakaki H, Nakamura M, Nakabayashi T, Shimizu H. Suppression of gamma activity in the human medial temporal lobe by sevoflurane anesthesia. *Neuroreport* 2000, 11:39-42.

Urban BW. Differential effects of gaseous and volatile anaesthetics on sodium and potassium channels. *Br J Anaesth* 1993, 71:25-38.

Valeyev AY, Hackman JC, Holohean AM, Wood PM, Katz JL, and Davidoff RA. Alphaxalone activates a Cl^- conductance independent of $GABA_A$ receptors in cultured embryonic human dorsal root ganglion neurons. *J Neurophysiol* 1999a, 82: 10-15.

Valeyev AY, Hackman JC, Holohean AM, Wood PM, Katz JL, and Davidoff RA. GABA-induced Cl^- current in cultured embryonic human dorsal root ganglion neurons. *J Neurophysiol* 1999b, 82: 1-9.

van Brederode JF, Spain WJ. Differences in inhibitory synaptic input between layer II-III and layer V neurons of the cat neocortex. *J Neurophysiol* 1995, 74:1149-1166.

Wade J, Rasmussen T. Intracarotid injection of sodium amytal for the lateralization of cerebral speech dominance: experimental and clinical observations. *J Neurosurg* 1960, 17: 266-282.

Wan X, Mathers DA, Puil E. Pentobarbital modulates intrinsic and GABA-receptor conductances in thalamocortical inhibition. *Neuroscience* 2003, 121:947-958.

Wan X, Puil E. Pentobarbital depressant effects are independent of GABA receptors in auditory thalamic neurons. *J Neurophysiol* 2002, 88:3067-3077.

Watson RT, Valenstein E, Heilman KM. Thalamic neglect. Possible role of the medial thalamus and nucleus reticularis in behavior. *Arch Neurol* 1981, 38:501-506.

Weakly JN. Effect of barbiturates on 'quantal' synaptic transmission in spinal motoneurones. *J Physiol (Lond)* 1969, 204: 63-77.

Weiss DS, Hablitz JJ. Interaction of penicillin and pentobarbital with inhibitory synaptic mechanisms in neocortex. *Cell Mol Neurobiol* 1984, 4:301-317.

Werman R. The reversal potential as a diagnostic tool in transmitter identification. *Adv Biochem Psychopharmacol* 1980, 21:21-31.

Werz MA and Macdonald RL. Barbiturates decrease voltage-dependent calcium conductance of mouse neurons in dissociated cell culture. *Mol Pharmacol* 1985, 28: 269-277.

Williams SR, Turner JP, Hughes SW, Crunelli V. On the nature of anomalous rectification in thalamocortical neurones of the cat ventrobasal thalamus in vitro. *J Physiol* 1997, 505:727-747.

Wisden W, Laurie DJ, Monyer H, and Seeburg PH. The distribution of 13 $GABA_A$ receptor subunit mRNAs in the rat brain. I. Telencephalon, diencephalon, mesencephalon. *J Neurosci* 1992, 12:1040-1062.

Yang J, Uchida I. Mechanisms of etomidate potentiation of $GABA_A$ receptor-gated currents in cultured postnatal hippocampal neurons. *Neuroscience* 1996, 73:69-78.

Yoshimura M, Higashi H, Fujita S, Shimoji K. Selective depression of hippocampal inhibitory postsynaptic potentials and spontaneous firing by volatile anesthetics. *Brain Res* 1985, 340:363-368.

Zhan XJ, Cox CL, Sherman SM. Dendritic depolarization efficiently attenuates low-threshold calcium spikes in thalamic relay cells. *J Neurosci* 2000, 20:3909-3914.

Zhang L, Weiner JL, Carlen PL. Potentiation of gamma-aminobutyric acid type A receptor-mediated synaptic currents by pentobarbital and diazepam in immature hippocampal CA1 neurons. *J Pharmacol Exp Ther* 1993, 266:1227-1235.